Etude de traitement par plasma froid de surfaces contaminés par biofilms

Zuzana Šipoldová

NNT : 2016SACLC054

Thèse de doctorat

de

Comenius University in Bratislava

et de

l'Université Paris-Saclay

préparée à CentraleSupélec

École doctorale n°575
Electrical, Optical, Bio-physics and Engineering
Spécialité de doctorat : Physique

par

Mrs. Zuzana Kovalova

Etude de traitement par plasma froid de surfaces contaminés par biofilms

Thèse présentée et soutenue à Gif-sur-Yvette, le 30 août 2016.

Composition du Jury :

M. Michael DuBow	Professeur, Université Paris-Sud	Président du jury
M. Jean-Michel Pouvesle	Directeur de recherche, Université d'Orléans	Rapporteur
M. Lluis Mir	Directeur de recherche, Institute Gustave-Roussy	Rapporteur
M. David Graves	Professeur, University of California Berkeley	Rapporteur
M. Martin Kopáni	Professeur associé, Comenius University	Examinateur
M. Emmanuel Odic	Professeur, CentraleSupélec	Directeur de thèse
M. Zdenko Machala	Professeur associé, Comenius University	Directeur de thèse
M. Michael Kirkpatrick	Docteur, CentraleSupélec	CoDirecteur de thèse

Acknowledgments

My deepest thanks go to my supervisors for making this thesis possible. Thank you Zdenko Machala for contacting Emmanuel Odic and giving a good recommendation for me and supporting and believing in my work even when I was in doubts. Thank you Emmanuel for making my doctorate in France possible, for helping me with all the paperwork and finding an accommodation for me. I acknowledge with gratitude the help I have received from both of you during the last four years and for time you found to read this thesis before publication and valuable suggestions. I also wish to warmly thank Mike Kirkpatrick for all your help in laboratory, for English corrections in our publications and for all cool experiments, especially cloud chamber and plasma speaker, you showed me. I am indebted for a knowledge of bacterial bioflms and their cultivation to Magali Leroy, who spent with us at Supelec only one year, but it was a very fruitful and intense year. I would like to thank Carolyn Jacobos for the set up of the spectrometer at Supelec and all the help with time resolved spectroscopy. I also wish to thank Karol Hensel, you were practically my supervisor during the first year of my PhD, without you we would be lost during our trip in Japan, also thank you for all the help with FTIR measurements. Thanks to Mário Janda for building us the fluorescence spectrometer and all funny stories about your sons. Special thanks go to Dana Lajdová and Ľubomír Tomáška from The Department of Genetics of Faculty of Natural Sciences at Comenius University in Bratislava for CSLM analysis. I am grateful to Micheal DuBow, Christophe Laux and Filipa Lopes, who were at the beginning of this thesis and gave it direction. Many thanks to Baša, Katka, Braňo, both Florents, Alex, Dany and others, I had a great time and lots of fun with you during my PhD, and even before with some of you. Lastly I would like to thank my husband Michal for your patience and support during long months of my stay in France, my parents, brother and grandparents that you supported my decision to go study in France and were always happy to see me during our Skype calls on Sundays.

Abstract

In this PhD thesis, biomedical applications of low-temperature plasmas at atmospheric pressure are investigated. In particular, bio-decontamination of planktonic bacteria and bacterial biofilms on both flat and complex surfaces by direct current (DC) air corona discharges and by pulsed discharges in argon is considered. We first provide a theoretical overview of biofilms, plasmas, and the current state of knowledge on bio-decontamination by low-temperature plasma, as well as methods presently used for biofilm decontamination in the plasma medicine domain.

We characterize three plasma sources for the decontamination of *Escherichia coli* bacteria and biofilm. DC corona discharges in air - positive streamer corona and negative Trichel pulses were used for decontamination of planktonic bacteria and bacterial biofilms. In some experiments water was electrosprayed onto samples from a high voltage (HV) electrode. Stable reactive species were identified in the gas phase by Fourier transform infrared spectroscopy (FTIR) and the concentration of reactive oxygen and nitrogen species was measured in the electrosprayed water. Bio-decontamination of bacterial biofilms was carried out on glass cover slides. Within 15 min of the plasma treatment, most of the bacteria were rendered uncultivable. Some of the uncultivable bacteria remained viable, only bacteria in the top layers of the biofilm were killed, as demonstrated by a confocal laser scanning microscopy (CLSM) of biofilms stained by live/dead viability kit. Water electrospray through the corona discharges significantly improves the biofilm inactivation and disintegrates the polymeric protective matrix of the biofilm.

The second plasma source investigated was the pulsed corona discharge propagated inside long narrow quartz tubes, in which dry argon or argon with water vapor were flowing at atmospheric pressure. This type of discharge has a potential application in decontamination of inner surfaces of catheters or other long tubular devices, and could be able to deliver low-temperature plasma over longer distances inside the human body. This pulsed corona discharge was characterized by its electrical parameters, such as the discharge propagation velocity and the mean electric field in the plasma channel. Optical emission spectroscopy of such plasma identified UV B emission form excited hydroxyl radicals, especially with humid argon working gas. The effect of this UV B was tested on planktonic bacteria sensitive to UV damage (*recA*-), and was found to cause a substantial damage even to bacteria placed far downstream in the tube or on the outer surface of the tube.

The third plasma source tested was an argon jet based on cylindrical dielectric barrier discharge with dry, humid or water saturated argon as a working gases. This discharge was used for biofilm decontamination, where we obtained similar results as with DC corona discharges – strong inactivation of biofilm bacteria determined from the cultivability tests and biofilm thickness shrinkage shown by CLSM. We used this discharge to test the effect

of vacuum UV on bacterial survival, but the effect was neither confirmed nor disproved.

Keywords: Corona discharges, argon plasma jet, *Escherichia coli*, planktonic bacteria, bacterial biofilm

Abstrakt

V predkladanej dizertačnej práci sú rozoberané aplikácie nízkoteplotnej plazmy pri atmosférickom tlaku na bio-dekontamináciu planktonických baktérií a bakteriálnych biofilmov na rovných a zložitých povrchoch pomocou korónových výbojov vo vzduchu napájaných jednosmerným napätím, pulzných korónových výbojov v argóne a pomocou argónovej trysky. V práci sú zhrnuté teoretické poznatky o biofilmoch, plazme a súčasný stav vedomostí o biologickej dekontaminácii nízkoteplotnou plazmou a metódach, ktoré sú používané v štúdiách dekontaminácie biofilmov a v plazmovej medicíne.

V práci sú charakterizované tri zdroje plazmy, ktoré sú použité na dekontamináciu baktérií a biofilmov *Escherichia coli*. Korónové výboje vo vzduchu – pozitívna streamerová koróna a negatívne Trichelove pulzy boli použité pre dekontamináciu planktonických baktérií a bakteriálnych biofilmov. V niektorých experimentoch bola voda rozprašovaná na vzorky z vysokonapäťovej (VN) elektródy. Stabilné reaktívne častice boli identifikované v plynnej fáze pomocou infračervenej spektroskopie (FTIR) a koncentrácia aktívnych zložiek bola meraná v rozprašovanej vode. Bio-dekontaminácia bakteriálnych biofilmov bola vykonaná na sklenených krycích sklíčkach. Po 15 minútach plazmového opracovania bola väčšina baktérií nekultivovateľná. Časť z týchto nekultivovateľných baktérií zostalo životaschopných, pričom boli zabité iba baktérie z vrchných vrstiev biofilmu, čo bolo preukázané pomocou konfokálnej laserovej skenovacie mikroskopie (CLSM) biofilmov farbených live/dead viability kitom. Rozprašovanie vody v korónovom výboji výrazne zlepšuje inaktiváciu biofilmu a rozkladá polymérový ochranný matrix biofilmu.

Druhým zdrojom plazmy bol pulzný korónový výboj v dlhej úzkej kremennej trubici, v ktorej prúdil suchý argón alebo argón s vodnou parou pri atmosférickom tlaku. Tento typ výboja má potenciálne uplatnenie pri dekontaminácii vnútorných povrchov katétrov alebo iných dlhých rúrkovitých zariadení. Tiež by mohol umožniť prevod nízkoteplotnej plazmy na väčšie vzdialenosti do vnútra ľudského tela. Najskôr bol tento zdroj nízkoteplotnej plazmy charakterizovaný jeho elektrickými parametrami, ako je rýchlosť šírenia výboja a stredné elektrické pole v plazmovom kanáli. Potom bola pomocou optickej emisnej spektroskopie plazmy identifikovaná UV B emisia z excitovaných hydroxylových radikálov, najmä vo výboji vo vlhkom argóne. Účinok UV B bol testovaný na planktonických baktériách citlivých na poškodenie UV žiarením (*recA*-), pričom bolo zistené podstatné poškodenie baktérií aj vo vzdialenej časti trubice.

Tretím zdrojom plazmy bola argónová tryska, založená na princípe valcového dielektrického bariérového výboja so suchým, vlhkým alebo vodou nasýteným argónom ako pracovným plynom. Tento výboj bol použitý najmä na dekontamináciu biofilmov. Dosiahnuté výsledky sú porovnateľné s dekontamináciou pomocou jednosmerných korónových výbojov, výrazná inaktivácia baktérií v biofilme bola zistená použitím kultivačných testov a mer-

aním hrúbky biofilmov pomocou CLSM. Argónová tryska bola tiež použitá na identifikáciu možného účinku vákuového UV žiarenia na bakteriálnu dekontamináciu. Tento efekt UV žiarenia nebol výsledkami práce potvrdený, ani vyvrátený.

Kľúčové slová: korónové výboje, plazmová argónová tryska, *Escherichia coli*, planktonické baktérie, bakteriálny biofilm

Résumé

Ces travaux de thèse portent sur les applications biomédicales des plasmas froids (hors équilibre thermodynamique) obtenus à pression atmosphérique. En particulier, la bio-décontamination de surfaces planes et complexes, portant des bactéries planctoniques ou des biofilms bactériens, est étudiée en utilisant des sources plasma de type décharge couronne dans l'air et décharge pulsée ou décharge à barrière diélectrique dans l'argon. En premier lieu, est proposé un état de l'art portant sur les biofilms d'une part et les plasmas de décharge d'autre part. Puis, nous présentons l'état actuel des connaissances sur la bio-décontamination par plasma froid, et en particulier sur les méthodes mises en œuvre dans le domaine de la « plasma-médecine » pour le traitement des biofilms.

Dans ce travail, nous avons caractérisé trois sources plasma qui ont été utilisées pour la décontamination de surfaces. Le modèle bactérien est *Escherichia coli*. Les bactéries étaient soit déposées sous forme planctonique sur lame de verre, soit cultivées préalablement sur lame de verre pour produire un biofilm (48h). Une décharge couronne produite dans l'air en géométrie pointe-plan par alimentation haute tension continue de la pointe a été utilisée pour le traitement de bactéries sous forme planctonique ou organisées en biofilm. Selon la polarité, deux régimes ont été explorés : la décharge couronne positive en régime de streamer et la décharge couronne négative en régime de Trichels. Dans certaines expériences, de l'eau a été électro-pulvérisée sur les surfaces contaminées. Les espèces réactives stables ont été identifiées dans la phase gazeuse par spectroscopie d'absorption infrarouge à transformée de Fourier (IRTF) et dans la phase aqueuse (électro-pulvérisée) par des techniques colorimétriques. Dans ces conditions de traitement, une exposition de 15 minutes du biofilm à la décharge couronne a conduit à une réduction de $6{,}7\log_{10}$ de la population bactérienne cultivable. Un examen du biofilm par microscopie confocale laser à balayage (MCLB) a révélé la présence de bactéries viables mais non-cultivables dans les couches inférieures du biofilm alors que celles présentes en surfaces étaient mortes.

La deuxième source de plasma était une décharge couronne pulsée propagée à pression atmosphérique sur les parois internes d'un tube de quartz long et étroit balayé par de l'argon sec ou chargé en vapeur d'eau. Ce type de dispositifs peut trouver une application potentielle dans la décontamination des surfaces internes de cathéters ou d'autres dispositifs invasifs tels les endoscopes, ou encore permettre de transférer en extrémité de tubes longs souples un plasma froid pouvant alors être introduits dans des cavités du corps humain. Tout d'abord, cette source plasma a été étudiée. Le champ électrique moyen dans la colonne a été calculé, le mécanisme de propagation a été mis en évidence et sa vitesse mesurée. La spectroscopie d'émission optique a permis de caractériser l'émission UV-B issue de la désexcitation radiative du radical hydroxyle, en particulier en présence de vapeur d'eau. Cette décharge, testée sur des bactéries planctoniques sensibles aux UV (*recA*-), a permis

d'obtenir des chutes substantielles de population bactérienne cultivable sur toute la longueur du tube.

Enfin, une troisième source plasma constituée par une décharge à barrière diélectrique alimentée en argon (sec ou humide) a été utilisée pour le traitement de biofilm cultivé sur lame de verre. Des résultats similaires à ceux obtenus avec la décharge couronne dans l'air ont été obtenus, c'est-à-dire une chute drastique de la population bactérienne cultivable et une réduction significative de l'épaisseur du biofilm (mesurée par MCLB). Ce dispositif a également été utilisé pour tenter de mettre en évidence l'effet du rayonnement UV lointain sur les bactéries, sans toutefois permettre de trancher sur cette question.

Mots clés: décharge couronne, jet de plasma d'argon, *Escherichia coli*, bactéries planctoniques, biofilm bactérien

List of Abbreviations

CFU	Colony-forming unit
CLSM	Confocal laser scanning microscope/microscopy
CV	Crystal violet
DAPI	4',6-diamidino-2-phenylindole
DBD	Dielectric barrier discharge
DC	Direct current
EPS	Extracellular polymeric substance
FTIR	Fourier transform infrared spectroscopy
HV	High voltage
LB	Lysogeny broth
NC	Negative corona
OES	Optical emission spectroscopy
PAM	Plasma activated medium
PBS	Phosphate buffered saline
PC	Positive (streamer) corona
PI	Propidium iodide
PLIF	Planar laser induced fluorescence
ppm	Parts per million
QS	Quorum sensing
RNS	Reactive nitrogen species
RONS	Reactive oxygen and nitrogen species
ROS	Reactive oxygen species
slm	Standard liter per minute
UV	Ultra violet
VBNC	Viable but non-culturable
VUV	Vacuum ultra violet
Vis	Visible

Contents

List of Figures

List of Tables

Introduction

Bacteria on surfaces exist mostly in the form of biofilms, which are populations of microorganisms concentrated at an interface and encased in a hydrated matrix of exopolymeric substances (EPS), polysaccharides, and proteins that are produced by the resident microorganisms [1]. EPS protects cells from the harsh outer environment (high temperature, low pH, ultraviolet radiation, dehydration ...) and facilitates cell-to-cell communication (so called quorum sensing) [2]. The quorum sensing is required for biofilm differentiation [3], it coordinates gene expression and regulates the diverse array of physiological activities [4]. Bacteria in the biofilm are more resistant than their planktonic (suspended cells) counterparts [2]. Biofilms may be present on almost every biological surface of our body, for instance teeth, skin, altered endothelial surface, and they may also appear on non-biological surfaces and interfaces introduced in human body - prosthetic heart valves, intravenous catheters, cardiac pacemakers, and others. Biofilms that contain pathogenic bacteria can act as the nodes of relapsing infections or the causes of chronic infections such as infectious endocarditis and cystic fibrosis, etc. [2, 3, 5, 6].

Bacterial contamination of surfaces is a common problem in hospitals, food industry, water distribution systems (also referred to as biofouling), etc. According to Bryers [7], nosocomial infections (NI), or so-called hospital acquired infections are the fourth leading cause of death in the U.S. with 2 million cases per year with biofilms as a contributing factor. In European Union (EU) these infections are responsible for infecting 2-11% of the patients admitted to the hospital and approximately 37 000 deaths/year are caused directly by NI in EU 27 and contribute to additional 111 000 deaths/year. *Escherichia coli* is one of the most frequently isolated strains from all infection sites in health care facilities [8]. Eradication of bacteria in biofilms by common antibiotics or chemotherapy is difficult due to the higher resistance of biofilm bacterial cells in comparison with their planktonic counterparts. Cells in biofilms are protected by EPS and have acquired new genetic traits and metabolic adaptations to the biofilm mode of growth [2, 9, 10]. In order to avoid using toxic chemicals or high concentration of antibiotics to achieve desired decontamination efficiency in biofilms, a search for new alternative methods of decontamination is required, one of them represented by low-temperature plasma.

Low-temperature (cold) plasmas can be generated at atmospheric pressure [11, 12] and they are usually done by electrical discharges in helium [13] or argon [14, 15] with admixtures of reactive gases such as oxygen or water vapor [16, 17] or they are directly generated in air [18–21]. In cold non-thermal atmospheric pressure plasma sources, main reactive components comprise reactive neutral species (reactive oxygen and nitrogen species, RONS, when plasma is produced in air), UV-Vis radiation, and charged species (electrons and ions) with the corresponding electromagnetic fields [22]. Low-temperature plasmas have been suc-

cessfully tested for bio-decontamination of various surfaces from microorganisms, without causing severe damage to sensitive materials such as polymers [23, 24] and tissues (bovine dentine [25]). Over the course of the last decade, non-thermal plasma technologies have been investigated for medical purposes and surface decontamination [26,27] using different plasma sources and operating pressures. Both early [28–30] and more recent works [31,32] have been conducted in reduced pressure conditions, but the current trend is to work at atmospheric pressure [27], mainly due to operational constraints and the demand for medical applications. In the field of surface treatment of thermally sensitive materials, decontamination of small diameter tubes (catheters, endoscopes) is an important issue. In previous studies, the inner walls of tubes were exposed to different plasma processes at atmospheric pressure in direct [33] or remote exposure mode [34, 35]. There are many studies which used single bacterial species to form biofilms, although real biofilms contain multiple microbial species.

In this thesis, we investigate the impact of three low-temperature plasma sources in argon or in ambient air on *Escherichia coli* biofilms. It is follow-up of my Master's thesis which was focused on decontamination of *Streptococci* biofilms on extracted human teeth [36]. We apply DC corona discharges in both positive and negative polarities, pulsed corona in argon-filled long tubes and Ar plasma jet.

This thesis starts with introduction and then continues with two main parts - the first is Theoretical background and the second Experimental part. The first part contains three chapters with basic theoretical knowledge to plasma physics, bacterial biofilms and the current state of knowledge for biofilm decontamination by low-temperature plasma. The second part is divided into five chapters. In the first one we define aims of our work. The second chapter contains bio-decontamination of *E. coli* planktonic and in the biofilm by DC corona discharges in air with or without water electrospray. In the third chapter HV pulsed corona discharge is propagated inside a long quartz tube in which argon gas is flowing. Physical characteristics of the discharge are measured and effect of UV B on bacteria from this discharge is evaluated. The fourth chapter presents the argon plasma jet in argon atmosphere for decontamination of *E. coli* biofilms. After this chapter there is a common discussion for last three chapters and conclusion. After the conclusions, the thesis contains list of used literature and appendices.

Part I

Theoretical background

1 Biofilms

A **biofilm** is a microbially derived sessile community characterized by cells that are irreversibly attached to a substratum or interface or to each other, are embedded in a matrix of extracellular polymeric substances (EPS) that they produce, and exhibit an altered phenotype with respect to the growth rate and gene transcription. Aggregates of cells not attached to a surface but matrix-enclosed fragments that have broken off from a biofilm on a colonized surface are sometimes termed flocs and have all the resistance characteristics of the parent community. Nonbiofilm populations include colonies of bacteria growing on the surface of agar, behave like **planktonic** cells stranded on a surface and exhibit none of the inherent resistance characteristics of true biofilms [37].

1.1 Formation of a biofilm and its dispersal strategies

Presently, there are several hypotheses why is biofilm formation and bacterial surface adhesion such a widespread phenomenon among bacteria. How might the biofilm mode of growth get a reproductive advantage when one considers that bacteria in biofilm have a reduced rate of growth relative to bacteria growing planktonically in broth culture? However, outside of the laboratory, bacteria rarely find themselves in an environment as nutrient rich as culture media, and in these less-than-ideal conditions, there are a number of advantages in the biofilm mode of growth. Four proposed advantages are illustrated and presented in Figure 1.1.

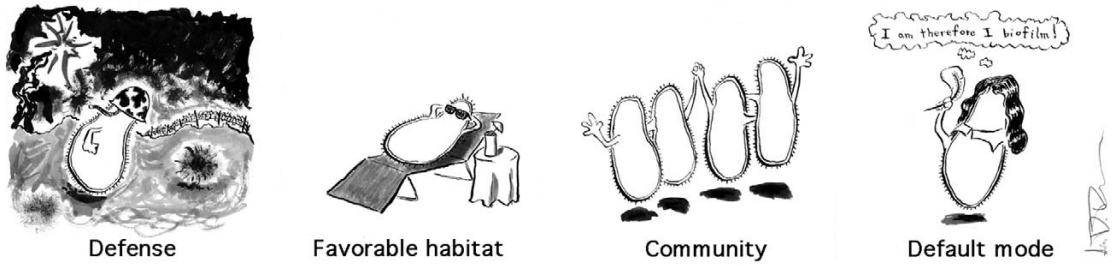

Figure 1.1: Dr. Sean D. Taverna's artistic interpretation of the four driving forces behind bacterial biofilm formation [38].

One is that the biofilm formation allows protection from a wide range of environmental challenges. Biofilms are resistant to shear forces of blood flow or the washing by saliva, and to phagocytosis. EPS shields cells from the exposure to UV, dehydration, osmotic stress, acid exposure, metal toxicity, and diverse antibiotics and antimicrobial agents.

The second hypothesis is that biofilm formation is a mechanism for microorganisms to stay in a favorable environment of the human host with glucose or another readily utilizable carbon sources in abundant. When nutrient sources are depleted, the bacteria detach and become planktonic, suggesting that nutrient deprivation is a trigger to move on, in search of a better habitat.

Another hypothesis is that biofilms should be regarded as multicellular organisms and that biofilm bacteria exhibit cooperative, unselfish behavior. Although bacteria can sense their surroundings, and they are able to adjust their metabolic processes, they do not premanently differentiate. The cell close proximity in the biofilm allows for horizontal gene transfer of e.g. antibiotic resistance determinants. The evidence of unselfish behavior was found in a process similar to apoptosis.

The biofilm mode of growth may be the default mode of growth for at least some bacterial species. One example might be the oral bacteria, the planktonic growth would cause them to be quickly washed away by saliva, swallowed and destroyed within the acidic juices of the stomach. These bacteria likely spend the majority of their natural existence growing as a biofilm. And yet they are often grown planktonically in the laboratory. This hypothesis suggests that we should be questioning what triggers the planktonic mode of growth rather than what motivates the biofilm mode of growth. [2, 38]

1.1.1 Formation of biofilm

The biofilm formation is a regulated sequence of development occurring in multiple steps, five stages have been recently proposed (Figure 1.2): Stage *one* is when the bacterium approaches the surface so closely that its motility is slowed. The bacterium may then form a transient association with the surface and/or other microbes previously attached to the surface, although the adherent cells might not yet go through differentiation process leading to biofilm formation, and many may actually leave the surface to resume the planktonic lifestyle. After association with the surface, stage *two* follows by robust adhesion. The cells that have committed to adhesion upregulate specific adhesion genes like *algC* and *D*, responsible for alginate production (beginning of EPS production) and downregulate the synthesis of flagellum (that might destabilize the biofilm) within a few minutes of their attachment to the surface. Stages *three* and *four* involve the aggregation of cells into microcolonies and subsequent growth and maturation. Cells alter their physiological processes (e.g., grow anaerobically) in response to conditions in their particular niches. This results in the generation of complex architecture, like: channels, pores, and redistribution of bacteria away from the substratum. Biofilm structures can be flat or mushroom-shaped depending on the nutrient source. Individual microcolonies may detach from the surface or may give rise to planktonic revertants that swim or float away from these matrix-enclosed structures. Additionally, whole microcolonies may naturally break away from the biofilm without any

obvious perturbation to the system, although the mechanisms behind this phenomenon are yet unclear. Stage *five* is characterized by a return to transient motility where biofilm cells are sloughed or shed. It is interesting that the stages of biofilm development seem to be conserved among a remarkable range of prokaryotes. [2, 5, 39, 40]

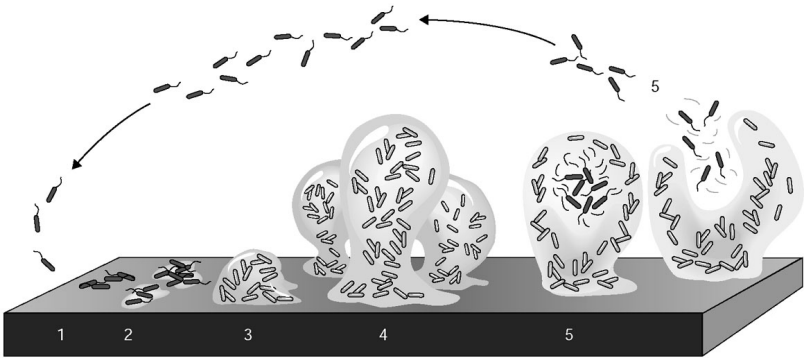

Figure 1.2: The stages of bacterial biofilm development. At stage 1, the bacterial cells attach reversibly to the surface. Then, at stage 2, the cells attach irreversibly, a step mediated mainly by exopolymeric substances, and the cells lose their flagella-driven motility. At the next stage (3), the first maturation phase is reached, as indicated by early development of biofilm architecture. The second maturation phase is reached at stage 4 with fully mature biofilms, as indicated by the complex biofilm architecture. At the dispersion stage (5), single motile cells (dark cells on the figure) disperse from the microcolonies. [1]

Bacteria detachment can be caused by external perturbations, such as increased fluid shear, by internal biofilm processes, such as endogenous enzymatic degradation, or by the release of EPS or surface-binding proteins. In some species, dispersal from biofilms seems to be an active process, presumably adapted to allow colonization of new niches. Three distinct biofilm dispersal strategies can be identified: *swarming/seeding dispersal* in which individual cells are released from a microcolony into the surrounding fluid; *sclumping dispersal*, in which aggregates of cells are shed as clumps or emboli; and *surface dispersal*, in which biofilm structures move across surfaces. [2]

1.1.2 Architecture of the biofilm

The basic structural unit of the biofilm is the microcolony – discrete matrix-enclosed community of bacterial cells that may include cells of one or of many species. Depending on the species involved, the microcolony may be composed of 10 – 25% cells and 75 - 90% EPS matrix, the material of matrix is often the most dense in the core area of the microcolony. Microcolonies in thin biofilms are often arranged in a horizontal array, but in very thick sessile communities they may also form vertical arrays shape like mushroom, in which most of colonies are in the “crown” of the mushroom and very few in the “stalk”. In most biofilms,

the microorganisms account for less than 10% of the dry weight, whereas the matrix can account for over 90%.

The EPS polymers produced by different species of bacteria are different, therefore even within adjacent microcolonies, the composition of immediate surrounding of different cells might be very different [5]. Interestingly, biofilms formed from single species *in vitro* and those produced in nature by mixed species consortia exhibit similar overall structural features. Most biofilms have been found to display some level of heterogeneity in which patches of cells and aggregates, not monolayers, are interspersed throughout an exopolysaccharide matrix that varies in density, creating open areas where water channels are formed. [10]

1.2 Biofilm resistance to antimicrobial agents

Biofilms demonstrate unusual resistances to nearly all forms of decontamination techniques. These mechanisms can vary from non-genetic antibiotic resistance to phenotypic changes into persistent cells.

Eradication of infection by antibiotic treatment requires elimination of all the bacteria. Otherwise, infection recurs and chronicity is established. In other words, a biofilm resistance can be determined by the susceptibility of the most resistant cell. The most resistant members of a biofilm population are typically orders of magnitude more resistant than similar members of a planktonic population (yet a subculture rarely shows the existence of resistant mutants). Hence, the biofilm resistance is characteristically phenotypic. [41]

Three mechanisms have been proposed to explain the general resistance of biofilms to biocidal agents. **The first** is the barrier properties of the slime matrix. Reactive (bleach or superoxides), charged (metals) or large (immunoglobulin) antimicrobial agents are neutralized or bound by the EPS and effectively diluted to sublethal concentrations before they can reach all of the individual bacterial cells within the biofilm. The barrier properties of the EPS hydrogel might also protect against UV light and dehydration, and might localize enzymatic activity [2].

The second protective mechanism could involve the physiological state of biofilm organisms. Although many antibiotics can freely penetrate the EPS, cells within the biofilm are often still protected. The creation of starved, stationary phase dormant zones in biofilms seems to be a significant factor in the resistance of biofilm populations to antimicrobials. All antibiotics require at least some degree of cellular activity to be effective, because the mechanism of action of most antibiotics involves disruption of a microbial process. Therefore, regions of biofilm where cells are in stationary phase dormancy might represent a general mechanism of antibiotic resistance. The cell dormancy can be induced by *quorum-sensing*[1] as

[1]Quorum sensing is a sophisticated intercellular communication mechanism through which bacteria are capable to coordinate theirs activities. Many species of bacteria use quorum sensing to coordinate gene

a response to stresses. In biology, dormancy is a widespread survival response to stress. [2,41]

The third mechanism of protection could be the existence of subpopulations of resistant phenotypes in the biofilm, which have been referred to as *persisters*. Persisters comprise a small fraction of the entire biomass, whether in planktonic or biofilm culture, but as distinct phenotypes have yet to be cultured.

Although the relative contribution of each of these mechanisms (and possibly others) varies with the type of biofilm and the nature of the environmental stress, the result is a general protection. [2]

1.3 Risk of biofilm infections

The infections caused by bacterial biofilms share clinical characteristics. Intravenous catheters, prosthetic heart valves, joint prostheses, peritoneal dialysis catheters, cardiac pacemakers, cerebrospinal fluid shunts and endotracheal tubes save millions of lives, but all have an intrinsic risk of surface-associated infections. Biofilms develop preferentially on inert surfaces, or on dead tissue, and occur commonly on medical devices and fragments of dead tissue such as sequestra of dead bone. They can also form on living tissues, as in the case of endocarditis. The bacterial endocarditis shows how microorganisms on the skin or in the oral cavity that transiently enter the bloodstream can colonize implanted valves, or altered endothelial surfaces in the heart. Bacterial attachment within the body occurs as a result of interactions between microbial cells and host inflammatory response products. Biofilms grow slowly, in one or more locations, and biofilm infections are often slow to produce overt symptoms. Sessile bacterial cells release antigens and stimulate the production of antibodies, but the antibodies are not effective in killing bacteria within biofilm and may cause immune complex damage to surrounding tissues, thus facilitate further bacterial adhesion.

For individuals with excellent cellular and humoral immune reactions, biofilm infections are rarely resolved by the host defense mechanisms. Antibiotic therapy typically reverses the symptoms caused by planktonic cells released from the biofilm, but fails to kill the biofilm. For this reason biofilm infections typically show recurring symptoms, after cycles of antibiotic therapy, until the sessile population is surgically removed from the body. Therefore, biofilms can act as nodes of acute infection if the mobilized host defenses cannot eliminate the planktonic cells that are released at any time during the infection. [2,3]

expression according to the density of their local population.

2 Low-temperature plasma

Plasma is often called as the fourth state of matter and defined as a microscopically neutral ionised gas. It is constituted by particles in permanent interaction: the particles include photons and electrons ("light" species), positive and negative ions, atoms, free radicals and excited or non-excited molecules ("heavy" species). In order to study plasma in laboratory conditions one needs to generate it. In general, there are two ways of plasma generation. The first is to heat the gas to high temperature. Such a thermal plasma is characterized by an almost local thermodynamic equilibrium between the electrons and the heavy species; the gas temperature is nearly the same for all the components of the plasma and can be very high (5 to 20×10^3 K). The second method uses strong electric field between electrodes and less power, and typically generates non-thermal plasmas. These types of plasmas are usually generated by electrical discharges in low pressure gases. The electron temperature in non-thermal plasmas is much higher than that of the gas (heavy species), and consequently the plasma is not in a local thermodynamic equilibrium.

An intermediate category between these two others without clearly defined limits, is a non-thermal plasma generated in near atmospheric pressure and ambient temperature. This type of plasma is especially interesting for applications in industry, medicine and research because it does not require extreme conditions. Typical example of such plasmas are the corona discharge, dielectric barrier discharges, plasma jets, and gliding arc discharge. [11, 42]

2.1 Discharge generation

Plasma generation by electrical discharges uses transition of an electric current through the gas by imposing the electric field. When two electrodes at the ends of a discharge chamber are supplied with the low voltage from DC voltage generator, low current can be detected (10^{-15} A). It is carried by the *primary electrons*, which are generated by cosmic radiation, radioactivity, etc. The primary electrons accelerated by the increasing electric field are able to ionize atoms or molecules of the present gas and form other electrons. This process is repetitive, and the number of electrons is doubled in every ionization collision. An *electron avalanche* is thus generated. This creates an ionized gas between the electrodes, which is externally reflected by the increase in electric conductivity of the gas. [42, 43]

2.1.1 Discharges in gases

The electric discharge develops after reaching the breakdown between electrodes. The discharge characteristics depend on the gas pressure and composition, the shape of the electrodes and properties of the power supply. The breakdown voltage (U_z) of a gas is according to the Paschen's law in homogeneous electric field a function of the pressure (p_0) multiplied by the distance between electrodes. Self sustained conditions are reached when secondary emission supply mechanisms seed electrons from cathode. We distinguish several basics types of discharges: corona, arc, glow, dielectric barrier, and high frequency (radio or microwave) discharges. [42]

2.2 Corona discharge

The corona discharge is a low-current gas discharge in which the geometry confines the ionization and the high electric field in the vicinity of electrode. A non-uniform high electric fields are formed when a radius of curvature at least one of the electrodes is far less than a length of the inter-electrode gap. One of typical corona configurations is point-to-plate geometry. According to the applied voltage shape, corona discharges can be direct current (DC), alternating current (AC), high frequency (HF) or pulsed corona discharges, or their combination. Coronas are divided according to the polarity of the active electrode, into negative, positive or bipolar corona. [44, 45]

Positive corona starts with a *glow corona* regime (unipolar conduction corona), with the ionization region concentrated very close to the high field electrode. At a fixed voltage it operates quietly, with steady microampere and above currents carried by positive ions flowing through the drift region[1]. The glow corona sometimes transits to the *burst corona*. This regime seldom exhibits and non-regular current pulses accompanied with a short and faint streamers originate from the high field electrode. By increasing the voltage the burst regime proceeds to the audio noisy *streamer corona*. In this regime, the ionization region produces a conducting plasma faster than it can be absorbed by the point electrode. A cloud of many accumulated positive ions induces a space charge and the electric field between its own front and the cathode, which is superior to the original electric field. This further enhances ionizations in front of the space charge. Consequently a conductive plasma filament grows out from the point towards the plane electrode, carrying the plasma producing ionization region ahead with a velocity around 10^6 m/s (values typical for air at atmospheric pressure). When the streamer hits the plane electrode, a cathode spot is produced, the gap electric

[1] Low field region connecting the ionization region with the low field, passive electrode. In the drift region, ions and electrons drift and react with neutrals, but have too low energy to ionize and too low density to react with other ionized particles. [44]

field is redistributed along the plasma channel, and this channel either dies out by electron attachment or later converts to a thermally ionized *spark* channel. The streamer corona discharge is electrically characterized by positive current pulses, around 10 mA amplitude, 100 ns duration, and ∼10 kHz repetition rate with DC applied voltage in air at atmospheric pressure. [44, 45]

Negative corona, similarly to the positive corona starts with the ionization region concentrated near the high field electrode (cathode in this case). This regime is called *Trichel pulse corona* (unipolar conduction corona) after *G. W. Trichel* [46] who first studied this phenomenon. It is characterized by regular short (100–200 ns duration) current pulses (∼1 mA amplitude) with high repetition rate, a luminosity around the tip of the active electrode and a dark inter-electrode gap (drift region). The repetition rate of current pulses increases linearly with the applied voltage and ranges over 1–1000 kHz. Only the part of the drift region current is carried by electrons (below 10-20 μA total current), because of electron attachment (in electronegative gases). At higher currents, the space charges make the electric field distribution more uniform. This, and the higher applied voltage, sharply increase the drift region field, increasing the electron/negative ion ratio. The Trichel pulse corona is followed by a *pulse-less negative glow corona* as the applied voltage increases. In static air, if the voltage is progressively increased, this steady pulse-less corona transforms directly into a *spark* discharge. [44, 45]

2.3 Electrostatic spraying

The application of high voltage (several thousands volts) to a spray nozzle (capillary) can atomize various liquids into fine droplets. This process is called electrospray or EHD (electrohydrodynamic) spray. Fine droplet formation in an EHD spray is often explained by the balance between the repulsive electrostatic force and the restoring forces of the surface tension. Surface tension of liquids decreases under the influence of electrical potential. This is explained by the increased orientation of the water molecule dipoles in the surface layer, these dipoles repel one another, thus causing a reduction in surface energy. When the electrostatic force overcomes the surface tension of the liquid, electrically charged fine droplets are ejected from the cone (Taylor cone). However, the real process is greatly influenced by many parameters and these two forces cannot explain all the phenomena encountered in an electro-spray. According to the published literature, the parameters investigated in the electro-spray process include the type of liquid (its surface tension, conductivity, viscosity, density, relative permitivity), the nozzle diameter, the liquid flow rate, the applied voltage and its polarity, and so on. The size of liquid droplets varies from the millimeter to the submicrometre range according to the mode of electro-spray. [47, 48]

The electro-spray has been used in various applications such as generation of highly dispersed micro-and nanoparticles, ink-jet printing, paint spraying, fuel atomization, ion sources in mass spectrometry, agricultural treatment, surface coating, dust removal, drug inhalation etc. EHD sprays of polymer solutions can produce nanofibers, a process often referred to as electrospinning. Several different spray modes are observed, such as dripping, spindle, oscillating cone-jet, multi-jet, and stable cone-jet. [47, 48]

The elecro-spray was also studied together with electrical discharges, especially with corona discharges [47–51] and glow discharge [52, 53]. Electro-spraying tap water (conductivity 0.6 mS.cm^{-1}) through the discharge can affect the space charge distribution in the discharge zone and electric field intensities at a liquid surface [53]. In more conductive liquids, the discharge could more likely take place from the liquid surface, which has almost the same potential as the electrode. In more insulating low-conductivity liquids, the discharge occurs more likely at the metal electrode tip [49]. Electrical discharges such as gliding arc [54], positive and negative corona discharges [18, 24], and transient spark [20, 55] together with electro-spray were used for bio-decontamination of surfaces and liquids. The electro-spray combined with corona discharges will be employed in this thesis as well.

2.4 Plasma jets

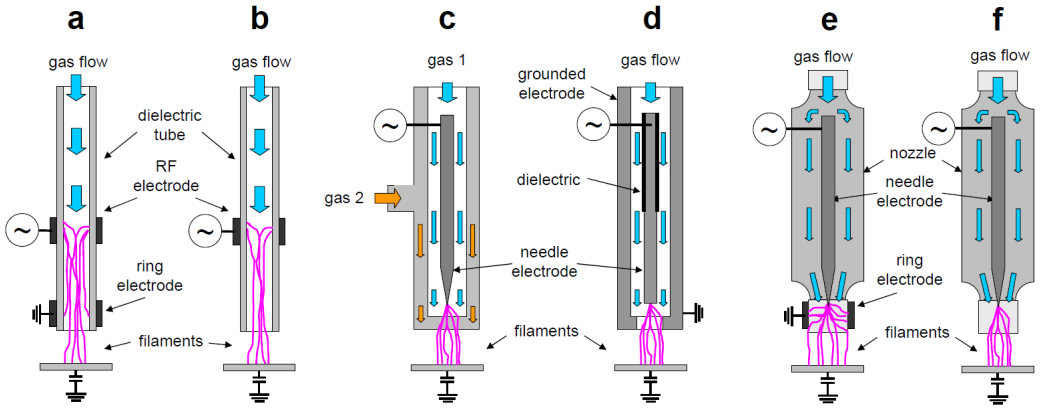

Figure 2.1: Principal designs for atmospheric pressure plasma jets a) using 1 powered and 1 grounded ring electrode, b) without grounded ring electrode, c) as combination of 2 tubes whereas the inner tube is streamed with a noble gas for discharge ignition and the outer tube with a precursor gas, d) composed of two coaxial electrodes with a dielectric in between e) consisting of an inner RF driven needle electrode and a grounded ring electrode, f) without grounded ring electrode ignition. In b) and f) the target has to be grounded. [56]

The atmospheric pressure plasma jets are the most commonly used plasma sources for decontamination and bio-medical applications. Plasmas in jets are generated between electrodes in noble gases (He, Ne, Ar) and pushed to an open space rather than being confined within its inter-electrode gap, which represents an advantage because they can be used di-

rectly for the bio-medical treatments and there is no limitation on size of the object to be treated. These plasma sources typically operate in the radio frequency or kilohertz range. In general, they consist of 2 electrodes in different arrangements (Figure 2.1). Plasma jets can be distinguished between remote plasmas, where the plasma is potential free and consists of relaxing and recombining active species from inside the nozzle, and active plasma jets where the expanding plasma contains free and high energetic electrons. In the latter case, the targeted substrate forms the second or the third electrode. The distance of the electrodes is in the range of some mm, whereas the exposure distance to the contaminated surface is rather in the cm range. Due to the use of noble gases even VUV radiation can be applied on the substrate under atmospheric conditions. Although noble gas plasma jets are relatively easy to generate and propagate (when air is used, the required electric field is about 30 kV cm^{-1}, due to the presence of electronegative oxygen, O_2), they are not as reactive as air plasma jets. That is the reason why a small percentage of reactive gases are usually added to a noble gas when the plasma jets are used for various applications. The noble gas is used to serve as the carrier gas to generate the plasma. For biomedical applications, O_2, H_2O or H_2O_2 is usually added. [22, 56, 57]

2.5 Propagation of discharges on surfaces

Propagation of discharges inside long tubes or on surfaces is an interesting problem with several practical applications, e.g. for the surface decontamination. One of them is sterilization of biopsy channels or catheters in medical practice. *Polak et al.* [33] designed their device for inner tubing decontamination by twisting the HV and grounded insulated electrodes around decontaminated tube with argon flowing inside, to form a uniform discharge inside a 5 meter long flexible tube. Also by placing the HV and grounded electrodes on the outer surface *Wang et al.* [58] were able to propagate discharge inside a 40 cm long quartz tube with helium with oxygen gas admixture flowing inside.

These previously mentioned devices consisted of modified DBD, but there exists an other option, which does not require placing electrodes around the decontaminated tube. It is propagation of streamers on dielectric surfaces. *Allen and Ghaffar* [59] measured properties of a streamer propagated over a surface in a uniform field in air. They found out that streamers usually propagate in two modes, a fast component on the surface and a slower one in ambient air. Production of secondary electrons occurs by photo emission from insulating material surface and by photoionization in gas. The energy costs are lower for photo emission. This means then that more electrons are released due to photon bombardment of the dielectric surface compared to air, resulting in a higher measured streamer current [60]. The high streamer velocities along the insulating surface are due to a combination of the effect of permittivity of the dielectric and accumulated negative charge on the surface, which gives rise

to an increase in the ionization rate [60, 61]. The net positive charge of the streamer along an insulating surface seems to spread along the streamer channel rather than be localized in the front part of the channel as is the case for the streamer in air alone [60]. Because it is easier to propagate discharge near the dielectric surface rather than in gas, in the dielectric tube, the plasma on the tube cross section has the annular shape [57].

A guided ionization wave moving inside a thin capillary is often called **plasma bullet**. In contrast to streamers in a free (unbounded) space that propagate in a stochastic manner and often branch, guided ionization waves are repetitive and highly-reproducible and propagate along the same path. In most studies this regime is achieved with a pulsed voltage or a high-frequency sinusoidal voltage. The bullet propagation (highly luminous front) was shown to be governed by a streamer mechanism and its typical velocities are in the range of $10^5 - 10^9$ cm.s^{-1} [13, 62]. The plasma bullet is connected with HV electrode through an ionization channel, which emits light of much weaker intensity compared to the head of the plasma bullet [62]. After their propagation in the capillary, such discharges are able to propagate further than the capillary's exit, into the open air, far away from the electrodes. These characteristics are suitable for applications such as processing of thermally sensitive materials or biomedical applications. That is why most of the studies were focused on the plume of plasma where the capillary exits: the so-called plasma jets or plasma plumes. [13]

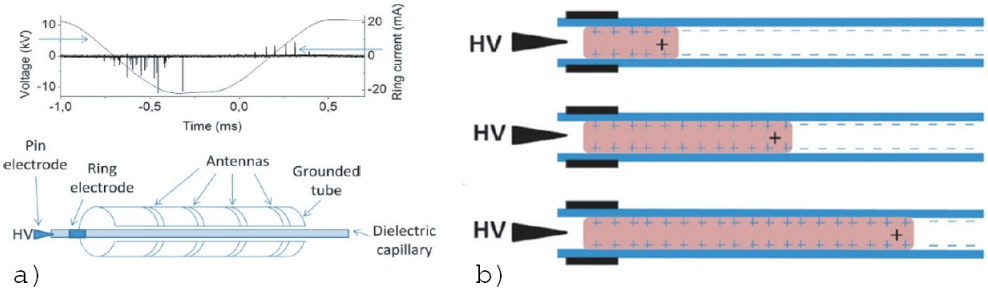

Figure 2.2: Plasma bullet propagation in a capillary; taken from [13]: a) The corresponding waveforms of voltage and current (measured on the ring electrode) during the negative and the positive cycle; b) The propagation of consecutive positive bullets in a capillary which is pre-charged negatively

To better explain how plasma bullets propagate in narrow tubes we can take the case from [13]. When we apply sinusoidal high voltage on source electrode, a large number of discharges occur during the negative half-cycle as well as during the positive one (Figure 2.2 a). The first discharge of the half-cycle does not propagate, but the following ones propagate further each time, which is also valid for the negative cycle. This suggests that the discharge propagation is separated in two distinct phases: the first one is a streamer crossing the inter-electrode space, which sometimes provides enough charges to create a bullet able to propagate in the capillary (second phase of the discharge). At the beginning of the positive cycle, the surface of the capillary is charged negatively or is neutral (if charges from the negative cycle have been lost). Positive discharges propagating within the dielectric capillary result in a

neutralization of the negative charges and/or deposition of positive charges on the surfaces. Consequently, the region where bullets have already propagated will have higher potential than downstream, so the next discharge will have to propagate further in order to reach the lower potential zone and so on, as illustrated by Figure 2.2 b. [13]

2.6 Active components of low-temperature atmospheric pressure plasmas

The complex physical and chemical processes inside a low temperature plasma give arise to a multiplicity of different biologically active agents. Their production depends on parameters such as gas composition, flow rate, moisture, temperature and high voltage signal shape. The main reactive components of the cold plasmas might comprise of reactive neutral species, UV-radiation, and electric current. In some cases charged particles are present in sufficient amounts and electric fields may play a role. [22, 56, 63]

It is difficult for vast plethora of types of plasma sources to identify, which plasma components are the most effective ones for specific bio-medical effects. The relevant agents are not identical for different kinds of plasma sources, they need to be identified and their possible synergistic effects examined.

Reactive oxygen and nitrogen species (RONS) such as atomic oxygen ($O^{\cdot}$), superoxide ($O_2^{\cdot-}$), ozone (O_3), hydroxyl radicals ($OH^{\cdot}$), nitric oxide (NO), nitrogen dioxide (NO_2) are key components of atmospheric pressure plasmas in air. With cold plasmas, at ambient temperatures, oxygen chemistry typically dominates with the one major long living reactive product - ozone. Ozone germicidal effects are caused by its interference with cellular respiration [63]. Ozone in plasma can be produced via electron impact dissociation of O_2 to form O atoms (Eq. 2.1), followed by a three-body recombination of O and O_2 to make O_3 (Eq. 2.2) [64].

$$e^- + O_2 \rightarrow e^- + O^* + O \quad , \quad e^- + O_2 \rightarrow e^- + O + O \tag{2.1}$$

$$O + O_2 + M \rightarrow \boxed{O_3} + M \tag{2.2}$$

The bacterial membrane lipid bilayers have as important components unsaturated fatty acids, which are susceptible to the attack by hydroxyl radical ($OH^{\cdot}$). OH radicals are mainly formed due to the electron-impact dissociation of H_2O molecules in cold plasmas in humid gases (Eq. 2.3). Protein molecules are susceptible to oxidation by atomic oxygen or metastable oxygen molecules [65].

$$H_2O + e^- \rightarrow H^{\cdot} + \boxed{OH^{\cdot}} + e^- \quad , \quad H_2O + e^- \rightarrow H^{\cdot} + \boxed{O^{\cdot}} + H^{\cdot} + e^- \tag{2.3}$$

Another reactive oxygen species produced in plasma is hydrogen peroxide (H_2O_2) formed by $OH^{\cdot}$ recombination [66]:

$$OH^{\cdot} + OH^{\cdot} \rightarrow \boxed{H_2O_2} \tag{2.4}$$

In hotter plasmas, even transiently for a very short time (∼ns to μs), and plasmas with initial temperatures higher than 200°C, reactive nitrogen species dominate the chemistry. NO radical is formed by Zeldovich mechanism through vibrationally excited nitrogen (N_2^*) by two steps, a limiting endothermic reaction (Eq. 2.5) and exothermic reaction (Eq. 2.6) [66]:

$$O^{\cdot} + N_2^* \rightarrow \boxed{NO} + N^{\cdot} \qquad \Delta H = 289\,\mathrm{kJ.mol^{-1}} \tag{2.5}$$

$$N^{\cdot} + O_2 \rightarrow \boxed{NO} + O^{\cdot} \tag{2.6}$$

NO quickly reacts with molecular or atomic oxygen (Eq. 2.7) as a three body collision or is oxidized with ozone (Eq. 2.8) and gives rise to nitrogen dioxide (NO_2) [67]:

$$NO + O + M \rightarrow \boxed{NO_2} + M \tag{2.7}$$

$$NO + O_3 \rightarrow \boxed{NO_2} + O_2 \tag{2.8}$$

NO_2 rapidly reacts with itself to dimerize into N_2O_4 (depending on the gas temperature, the colder tho more dimerization). Addition of water vapor to the gas leads to formation of hydroxyl radicals through water dissociation (Eq. 2.3) and other reactions. A wide variety of reactions (Eq. 2.9) with nitrogen oxides and hydroxyl and hydroperoxyl radicals lead to the formation of nitrite (NO_2^-) and nitrate (NO_3^-) [22, 66, 67]:

$$\begin{aligned} NO + OH^{\cdot} &\rightarrow \boxed{HNO_2} \\ HNO_2 + OH^{\cdot} &\rightarrow NO_2 + H_2O \\ NO_2 + OH^{\cdot} &\rightarrow \boxed{HNO_3} \\ NO + HO_2^{\cdot} &\rightarrow NO_2 + OH^{\cdot} \end{aligned} \tag{2.9}$$

Plasma generated ROS and RNS will then diffuse into the liquid which is present on the sample or into the liquid sample.

Charged particles and the electric field imposed by them can play a very significant role in the rupture of the outer membrane of bacterial cells [68, 69] as well as eukaryotic cells. The electrostatic force caused by charge accumulation on the outer surface of the cell membrane could overcome the tensile strength of the membrane and cause its rupture [65].

A temporary loss of the semipermeability of cell membranes (increased permeability), thus leading to ion leakage, escape of metabolites, and increased drugs uptake by cells, molecular probes, and DNA can be transiently achieved by electric field pulses of intensity in kilovolts per centimeter and of duration in micro to milliseconds. Under suitable conditions depending mainly on the pulse parameters (field strength, pulse duration, number of

pulses), the viability of the cell can be preserved. A generally accepted term describing this phenomenon is "electroporation". At low electric field strengths the membranes of the cells become polarized. When the changes in electric-field-induced membrane potential reach a critical value in the range 200–400 mV, areas of reversible local disorganization and transient breakdown occur making the membrane permeable to molecules and macromolecules [70]. Other effects of a high-intensity electric field on cell membranes might include irreversible changes like: membrane fusions, bleb formation, cell lysis, etc. Electroporation has found applications in: introduction of plasmids or foreign DNA into living cells for gene transfections, fusion of cells, insertion of proteins into cell membranes, improving drug delivery, activation of membrane transporters and enzymes, and alteration of genetic expression in living cells [71, 72]. Recent developments by use of nanosecond pulses of electric field showed that a cytosolic targeting was possible [73].

Electric current flows in most plasma discharges, most dominantly in direct type discharges, but also in some types of plasma jets, where the biological sample acts as an electrode and draws the most of the electric current through the sample [12]. This current has to be limited to a harmless level. International Commission On Non-Ionizing Radiation Protection has determined the touch perception limit of current flowing through the human body to 25 mA at 100 kHz as well as at 1 MHz. However, the use of electricity in medicine has a long history and many therapeutic effects also in wound healing are reported and applied today [22]. The effect of electric current on microorganisms in liquids is usually associated with production of toxic products, where hydrogen peroxide is refereed to as a primary bactericidal agent and chloride plays only minor role [74, 75]. This chemical effect might be enhanced by electrophoretic forces that allow the antimicrobial agents to overcome diffusion barriers that would otherwise limit their access to their targets within bacterial and fungal cells [76].

Thermal radiation As low-temperature plasmas do not produce high temperatures, heat should not be an important factor in the inactivation process of bacterial cells. Indeed, temperature measurements in various cold plasma sources showed that the temperature of the biological samples exposed to the plasma did not rise substantially [65]. This is the case even for transiently very hot reactive plasmas, such as air transient spark, where a high temperature is reached in the discharge for very shot time period ($\sim$10 ns) but the averaged temperature is low and the target is not heated. [20, 77]

UV radiation has been known to be germicidal for quite a long time. Various kinds of UV lamps are routinely used in biology laboratories to sterilize the surfaces of tools and instruments, and entire lab spaces. UV radiation in the 200—300 nm wavelength range with doses of several mW.s.cm^{-2} is known to cause lethal damage to cells (inhibition of the bacterial cell

ability to replicate by the dimerization of thymine bases in their DNA). Depending on the operating gas, plasmas generate UV radiation in several wavelength ranges including vacuum UV. Although they produce energetic photons, wavelengths below 200 nm are dominantly absorbed in ambient air at atmospheric pressure, therefore this kind of radiation plays a minor role when the plasma treated microorganisms are surrounded by air. However, when the air around the microorganisms is replaced by the process gases (e.g. noble gases) VUV radiation can reach and inactivate the microorganisms. [56, 65]

3 Biofilm decontamination by low-temperature plasma

Bio-decontamination of planktonic bacteria and spores on various surfaces, in different liquids and under various conditions has been successfully studied worldwide. Therefore the focus of plasma medicine moved to biofilms that are more complex and more commonly occurring. In this chapter we present an overview of results from other research groups that will allow the reader to make a picture about possibilities of the plasma bio-decontamination of biofilms and obstacles that were encountered in this field.

Biofilms are present almost everywhere, the presence of biofilms can lead to diseases, prostheses colonization, product contamination, biofouling, equipment damage, contamination of water resources, pipe plugging and others. According to the National institute of Health (NIH) and The Center of Disease Control and Prevention (CDC), 90% of infections in humans and 65% of nosocomial infections are due to biofilms. Biofilms have been considered responsible for plaque formation on teeth, gum diseases, ear infections in children, and a play role in cystic fibrosis and Legionnaire disease, among other health problems. [2, 3, 78]

Conventional methods of controlling free-living bacteria by chemical, physical or biological ways are often ineffective on biofilms. The use of moist heat and elevated pressure in autoclave is still an convenient method for many applications, but thermosensitive materials cannot withstand a high temperature. Sterilizing chemicals such as ethylen oxide is both mutagenic and carcinogenic. Other chemicals, such as chlorine, are also not suitable for many applications and pose an environmental hazard and risks to human health. Radiation can be used in some but not all cases. Current procedures to treat biofilms include catalytic generation of biocidal species at the biofilm-substratum interface. Catalysis increase the rate of free radical generation by hydrogen peroxide and potassium monopersulphate and have been shown to be useful in destruction of thick *Pseudomonas aeruginosa* biofilms [78, 79]. This methodology, however, generates hazardous compounds. The use of polychromatic light to irradiate biofilms grown on glass slides coated with TiO_2 has also been tested [78, 80].

A different approach to inactivate bacterial biofilms is by means of low-temperature plasma of electrical discharges. Plasma offers a good alternative to conventional sterilization methods since in contains reactive agents, such as radicals, charged particles, UV photons, electric field, etc.

3.1 Biofilms in dentistry

Dentistry is one of the fields where biofilms are abundant, especially in form of the dental plaque which is a complex community consisting of oral bacteria [78, 81] known to form cavities and inflammations in soft oral tissues. Therefore many scientists are interested in decontaminating the relevant bacterial biofilms for this field [82, 83].

Plasma applications in dentistry were tested for various purposes such as disinfection of pathogen bacteria characteristic for the location [84]: tooth root canal disinfection from *Streptococcus mutans*, *Enterococcus faecalis* [25, 85–89] and multispecies biofilms [90], disinfection of *Streptococcus mutans*, *S. sanguinis*, *Candida albicans* biofilms, and plaque biofilms on titanium implants or dentine [91–96], blood coagulation [97, 98], and wound healing [99]. Low temperature plasmas can also find their applications in dental aesthetics for tooth whitening [100–102]. Because of this vast range of potential low-temperature plasma applications in dentistry, it is important to investigate plasma-induced changes on teeth and tooth surface modification [102–104].

Results of biofilm decontamination of bacterial species relevant for dentistry were compared to antiseptics typically used in dentistry: chlorhexidine (CHX), sodium hypochlorite (NaOCl) calcium hydroxide ($Ca(OH)_2$) and 70 % ethanol. Various plasma sources resulted in the same bactericidal efficiency as these chemicals at the same exposure time, or even faster by synergy with plasma [25, 87, 92, 95, 105, 106]. For saliva biofilms grown *in situ* on titanium implants in [94], complete removal of the biofilm was achieved. *Enterococcus faecalis* on dentine or in root canal distinct zone without biofilm were observed after plasma treatment [25]. This is in agreement with other publication [107] where efficient plasma etching of *Candida albicans* 7 day old biofilms was reported. The report of *Schaudinn at al.* [90] on root canal disinfection of multispecies biofilm isolated from patients with irreversible pulpitis showed only 1 $\log_{10}$ decontamination efficiency after 30 min treatment with plasma needle compared to 4 $\log_{10}$ achieved with NaOCl. Also in recent publication of *Liang et al.* [89] treatment of 7 day old biofilm of *E. faecalis* with "plasma thrones" source was less efficient than the treatment with $Ca(OH)_2$ of same duration (5 min), although doubling the time of plasma treatment exceeded the efficiency of the chemical.

The use of low-temperature plasma is promising decontamination method because of negative side effects linked to use of chemicals (irritation, pain, redness, etc.).

3.2 Treatment skin and wounds pathogens in biofilms

Thanks to a relatively easy access of plasmas to the treated surfaces, dermatology and dentistry are the best fields for the first plasma medicine applications. In dermatology plasma is usually applied for wound healing, which is connected with decreasing of pathogen

bacteria population enough to suppress inflammation. Usual skin pathogens *Pseudomonas aeruginosa* and *Staphylococcus epidermis* in biofilm on skin or artificial surfaces were treated. Interestingly, in most cases argon plasma jets were used for this purpose. In all recent studies, effective elimination of bacteria and also improved wound healing without causing damage to skin was achieved [15, 19, 108–112]. The chemical treatment by CHX and polychexadine was compared with the plasma treatment, too. In some cases chemicals were more efficient than plasma [109].

Additional bacterial *Burkholderia cenocepacia* and *Staphylococcus aureus* species appeared in the study of plasma treatment by MicroPlaSter β device on rat wounds [15]. *B. cenocepacia* was easily decontaminated within 5 minutes. The same treatment period was not sufficient for decontamination of *S. aureus* and caused a delay in the wound closure. Finally, in a study on glass surface by the same author [111], a complete disinfection of *S. aureus* within 10 min was achieved.

3.3 Biofilms in food industry

Conventional postharvest washing and sanitizing treatments usually by chlorine are not highly effective for food produce, often resulting in less than $2\log_{10}$ reduction of pathogens [113–117]. In most cases of food treatment, plasma has been applied to planktonic bacteria such as *Escherichia coli* O157:H7 [118], *Listeria monocytogenes*, *Salmonella*, and *Staphylococcus aureus* on food and high decontamination efficiency of $5\log_{10}$ was obtained [113]. There are some but not many reports about the use of plasma to treat biofilms on fresh products.

In paper *Vleugels et al.* [114] the atmospheric pressure glow discharge with He/O_2 gas flowing through the interelectrode gap was used to decontaminate *Pantoea agglomerans* biofilms on bell peppers (*Capsicum annuum*). The pepper surface was mimicked by synthetic membrane and a decontamination efficiency of 2 and $1.25\log_{10}$ was achieved on 12- and 24-hour-old biofilms within 10 min.

The *Salmonella* biofilms, which are present on food processing conveyor belts, knives, containers, etc. and can contaminate food, were treated in *Niemira et al.* by air plasma jet based on glidarc [119]. The age of the biofilm (24-, 48- or 72-hour-old) did not play a role and $2.13\log_{10}$ reduction was achieved within 15 s.

3.4 Other applications of biofilm treatment

Plasma source	Targeted microorganism (surface)	Methods	Results	Ref.
Jet He/N_2	*Chromobacterium violaceum* 4 day old biofilm (polystyrene)	CFU counting	reduction of 2.75 $\log_{10}$ (10 min), 4 $\log_{10}$ (60 min)	[120]
Microwave-induced Ar plasma	*Escherichia coli* ATCC 8739, *Staphylococcus epidermidis* ATCC 12228, MRSA 24 hour old biofilm (glass)	Crystal violet assay, SEM	reduction of $\sim$8 $\log_{10}$ on planktonic forms after 5 s and biofilms after 20 s	[121]
Jet He/N_2	*Chromobacterium violaceum* CV026 4 and 7 day old biofilms (polystyrene)	CFU counting, BacTiter-Glo microbial cell viability assay, LIVE/DEAD Viability assay, AFM	4 d-old 99.61% efficiency and 7 d-old 99.94% in 5 min, total disinfection of 7-d biofilm in 60 min	[122]
Microdischarges in air like gas	*Escherichia coli* DH10B 48-hour old biofilm (glass)	CFU counting, DAPI and propidium iodide fluorescence	Indirect exposure for 40 min: planktonic form was totally reduced (6.6 $\log_{10}$), biofilm 50% reduction	[123]
Floating-electrode DBD ambient air	*Escerichia coli*, *Staphylococcus aureus*, MRSA95, MRSA -USA300 and -USA400 24-hour old biofilms (glass and polystyrene)	CFU counting, LIVE/DEAD Viability assay, Safranin assay, XTT assay	60% of MRSA were killed within 15 s, total disinfection in 120 s. Results correspond to XTT assay.	[124]
Jet He (Atomflo 300 reactor)	*Pseudomonas aeruginosa* 1, 3, and 7-day old biofilms (glass)	CFU counting, AFM	No culturable cells after 5 min, reduction of thickness and adhesion of biofilm	[125]
Jet He/O_2	*Neisseria gonorrhoeae* 4-day old biofilm (glass)	CFU count, TEM, LIVE/DEAD Viability assay	Total decontamination (7 $\log_{10}$) in 20 min, after 12 min no live bacteria detected by fluorescence	[126]
Jet N_2 or O_2	*Escherichia coli*, *Bacillus subtilis*, 3–14-day old biofilm (steel and polypropylene)	CFU count	Total disinfection of*E. coli* in 1–3 min and *B. subtilis* in 2–5 min	[127]
Jet in air	*Weissella confusa* LBAEC39.2 24-hour-old biofilm (membrane)	CFU count, LIVE/DEAD Viability assay	Reduction in 20 min was 2.63 $\log_{10}$ and 2.63 $\log_{10}$ when supplemented with sucrose	[128]
Jet in air	*Enterococcus faecalis* 7-day-old biofilm (glass)	LIVE/DEAD Viability assay	25.5 μm thick biofilm was inactivated	[129]

Jet He/O_2	*Bacillus cereus*, *Staphylococcus aureus*, *Escherichia coli*, *Pseudomonas aeruginosa* 48-hour-old biofilms (peg lid)	CFU count	Total eradication of: *B. cereus* (7 $\log_{10}$) in 45 s and *S. aureus* (6 $\log_{10}$) in 2 min; 8 and 10 min for *E. coli* and *P. aeruginosa*	[130]
Jet He/O_2	*Pseudomonas aeruginosa* 48 h biofilm (peg lid and polycarbonate)	CFU count, XTT assay, LIVE/DEAD Viability assay	Complete eradication (7 $\log_{10}$) after 4 min, supported by XTT and Live/Dead kit	[131]
Jet He/O_2	*Pseudomonas fluorescens*, *Staphylococcus saprophyticus*, *Vibrio alginolyticus*, and *Vibrio proteolyticus* 48-hour-old biofilms (peg lid and stainless steel)	CFU count, LIVE/DEAD Viability assay	Complete decontamination: *V. alginolyticus* in 60 s, *V. proteolyticus* and *S. saprophyticus* in 90 s, and *P. fluorescens* in 120 s	[132]
Jet He/N_2 (Atomflo 300 reactor)	*Pseudomonas aeruginosa* 24-hour-old biofilm (glass)	CFU count, AFM, virulence test	Reduction of 8 $\log_{10}$ in 15 min, and thickness, cell with undamaged membranes, preserved virulence	[133]
Jet Ar/O_2	*Candida albicans* 48-hour-old biofilm (dentine based resin)	CFU counting, LIVE/DEAD Viability assay, XTT assay, SEM	Reduction of 6 $\log_{10}$ in 8 min, confirmed by Live/Dead kit and SEM, increased antifungal sensitivity	[58]
Jet Ar/O_2	*Staphylococcus aureus*, *Pseudomonas aeruginosa*, *C. albicans* 24-hour-old biofilms (polystyrene)	Resazurin assay	Reduction in 3 min: *S. aureus* 73%, *C. albicans* 61%, *P. aeruginosa* 65%	[134]
Jet He	*Staphylococcus aureus* 12-hour-old biofilm (glass)	CFU count, LIVE/DEAD Viability assay, intracellular ROS	Reduction of 3 $\log_{10}$ in 10 min, only top layers had damaged membranes	[135]
Jet Ar	*Candida albicans* 48-hour-old biofilm (polyurethane)	CFU count, SEM, Trypan blue viability test, optical profilometry	85 and 99% reduction in CFU/mL within 10 min Ar and Ar/air plasma treatment	[136]
RF O_2/N_2 plasma in sealed bag	*Pseudomonas aeruginosa* 21-hour-old biofilm (glass and titanium)	CFU count, SEM	Reduction of 5.9 $\log_{10}$ in 60 min, SEM showed undamaged bacteria	[137]

Table 3.1: Summary of plasma treatment of biofilms, the table contains information about used plasma sources, bacterial strains to form biofilms, methods used to evaluate plasma bactericidal/fungicidal efficiency, results and references to original articles

Many other articles on bio-decontamination of biofilms were published. This section and Table 3.1 contains a summary of articles, which did not fall into previously mentioned categories (dentistry, wound healing, and food) or are different in other specific ways.

The study of *Mai-Prochnow et al.* [138] showed that low doses of low-temperature plasma may lead to the emergence of resistant bacteria and formation of persister cells. The study was performed on *Pseudomonas aeruginosa* in planktonic and biofilm form using kINPen med (RF argon plasma jet). No viable cells were detected after 5 min treatment and no attached biofilm cells were visible with confocal microscopy after 10 min plasma treatment. However, short plasma treatment (3 min) lead to a small number of surviving cells which exhibited enhanced resistance to subsequent plasma exposure, and also a higher degree of resistance to hydrogen peroxide. The genome comparison between surviving and control cells revealed 10 distinct polymorphic regions, with four belonging to the redox active, antibiotic pigment phenazine. *P. aeruginosa* biofilms of transposon mutants $\Delta phzD$ and $\Delta phzE$ were more sensitive to plasma treatment (3.5 and $3\log_{10}$ reduction in 3 min compared to $1.5\log_{10}$ reduction of wild type) suggesting that phenazine plays a role in protecting *P. aeruginosa* from argon plasma.

Short conference paper of *Gilmore* [139] shows the importance of biofilm matrix in attenuating the plasma bactericidal activity. Bacterial biofilms of mucoid and non-mucoid phenotypes of *Pseudomonas aeruginosa* were subjected to plasma treatment with He/O_2 jet. Results showed that mucoid strains were less susceptible to plasma inactivation in comparison with non-mucoid strain.

The report of *Flynn et al.* [140] considers different "anti-virulence" effect of plasma treatment by attacking quorum sensing (QS) as well as reducing the bacterial load. Gram negative bacteria typically use autoinducer molecules called acyl homeoserine lactones (AHL) as part of their QS. QS systems are critical in control of virulence in many clinically important Gram-negative human pathogens. Plasma treatment of AHL molecules and their subsequent interaction with three clinically relevant bacterial strains showed decrease and total attenuation of QS.

3.5 Quantitative evaluation of plasma effect on biofilms

Very important part of plasma biofilm decontamination studies is the evaluation of bactericidal effects on the biofilm. One can use multiple approaches to quantitatively evaluate this effect, each approach giving different information about bacterial survival.

In this section, the list of techniques used to measure bactericidal/fungicidal efficiency of electrical discharge low-temperature plasmas are presented.

3.5.1 Disruption and thermostatic cultivation of bacterial cells from biofilm

Traditionally, the effectiveness of plasma as a bacterial killing agent is measured by counting CFUs of the plasma-treated sample compared to the control and calculating the amount of surviving cells. The method is to scrape the biofilm from the support medium to a solution and to vortex or directly sonicate biofilm with its support in order to release individual bacteria into a solution. As a result, the method of cultivation shows only cultivable/culturable bacteria which undergo a sufficient number of times cell division to form a visible colony on an agar surface. The method has proved to be very effective and reproducible with planktonic bacteria. This approach relies only on the presence of culturable cells but does not take into account that cells might still be alive, although non-culturable, after plasma treatment. This may have catastrophic consequences if microorganisms that are assumed dead, are pathogenic ones that may retain virulence even when they are non-culturable [133, 141]. Plasma-mediated biofilm inactivation may proceed through the first step, in which bacterial cells induce enzyme synthesis and adjustments of metabolic pathways and might enter a Viable-But-Non-Culturable (VBNC) state [142]. Bacteria enter into this dormant, VBNC state in response to one or more environmental stresses, which might otherwise be ultimately lethal to the cell. This survival mechanism has been reported for many gram-negative organisms [78, 122, 143]. Another reason why cultivation of cells from biofilm can skew results is that bacteria in biofilms are embedded in polymeric substance. It protects them from the environment, thus disruption of this net can be really difficult, not all bacteria are released into a liquid medium and some cells could be disrupted by shock waves during sonication.

3.5.2 Fluorescence microscopy on intact biofilm

Another method very often used for biofilm observation is a fluorescent staining with *LIVE/-DEAD BacLight Bacterial Viability Kit* (Invitrogen) [144]. It provides a two-color fluorescence assay for assessment of bacterial viability, based on membrane integrity and utilizes the mixture of two nucleic acid stains: Syto9 and propidium iodide (PI). These stains differ both in their spectral characteristics and in their ability to penetrate healthy bacterial cells. When used alone, Syto9 stain generally labels all bacteria in a population. In contrast, PI penetrates only bacteria with damaged membranes, causing a reduction in the Syto9 stain fluorescence when both dyes are present. Thus, with their appropriate mixture, bacteria with intact cell membranes (live) are stained fluorescent green, whereas bacteria with damaged membranes (dead) stained fluorescent red.

This method was mostly used for qualitative microscopic observation, although it might also be used for quantification. However, the plasma treatment can destroy cell parts or even whole cells, therefore there is not enough membrane preserved to concentrate PI to label the cells as dead. As a consequence, the live/dead fluorescence ratio can be shifted

towards live. On the other hand, PI can in some cases penetrate into living cells with small membrane punctures which can be easily repaired, but LIVE/DEAD stain may mark these cells as dead.

3.5.3 Other methods

Morphology. Atomic force microscopy (*AFM*) and Scanning electron microscopy (*SEM*) can be used to determine morphological changes in biofilm after plasma treatment.

Biofilm developements. To monitor biofilm formation and its developed biomass the *Crystal violet assay* (CV) was used. CV is a basic dye, which binds to negatively charged surface molecules and polysaccharides in the extracellular matrix of biofilm. Because cells (both living and dead), as well as the matrix are stained by CV, it is poorly suited to evaluate killing of biofilm cells [145]. Similar method is the *Safranine assay* which is used for semiquantification of biofilms and is often used as test for the detection of biofilms in clinical isolates.

Viability tests. To distinguish between living and dead cells, quantification techniques based on the metabolic activity of viable cells are available. Various viability stains involve the use of tetrazolium salts, including CTC and XTT assays. The *XTT assay* is based on the reduction of the XTT dye to a water-soluble formazan [146]. The absorbance of the cell supernatant is proportional to the number of metabolically active microbial cells. The XTT assay has been extensively used for the quantification of viable cells in planktonic cultures and for the quantification of bacterial and yeast biofilms. Despite its popularity, problems regarding intra- and interspecies variability have been reported [145].

Another viability assay is based on the reduction of *resazurin* by metabolically active cells. Resazurin is a blue compound that can be reduced to pink fluorescent resorufin [147, 148]. Although this dye, also known as Alamar Blue, is mainly used in viability assays for mammalian cells, it has also been extensively applied in susceptibility testing of fungi and bacteria. [145]

The BacTiter-Glo^{TM} Microbial Cell Viability Assay provides a method for determining the number of viable microbial cells in a culture based on quantitation of the ATP present. ATP is an indicator of metabolically active cells. The assay procedure involves adding a reagent directly to bacterial cells cultured in medium and measuring luminescence [149].

Virulence test was done on surface-sterilized lettuce leaves with *P. aeruginosa* which is a also plant pathogen that produces tissue damage. The plasma treated bacterial solution was injected into mid-vein of a leaf and tissue damage was observed after three days of incubation [133].

Summary

The direct CFU count and fluorescent LIVE/DEAD BacLight Bacterial Viability Kit are the two methods widely used in biofilm community, although they have limitations (mentioned in subsection 3.5.1 and 3.5.2). Therefore, complementary techniques, listed above can be used.

Some authors showed that plasma-treated cells that are unable to grow on selective laboratory-based culture media are still able to respire. They refer to this state as a sublethal injury. For plasma-assisted biofilm inactivation, it has been reported that some cells remain metabolically active, intact and even virulent, yet non-culturable after a short exposure to plasma [78, 122, 150].

Part II

Experimental part

Objectives of the dissertation

This work is being carried out in two laboratories: in Slovakia at Faculty of Mathematics, Physics and Informatics, Comenius University, and in France at Group of Electrical Engineering – Paris (GeePs) CentraleSupélec, Université Paris-Saclay.

In this dissertation, three different plasma sources are used, two for bio-decontamination of bacterial biofilms: 1) pulsed corona discharge propagated over dielectric surfaces in argon at atmospheric pressure, for the decontamination of long tubes inner surfaces. 2) argon plasma jet enclosed in an argon atmosphere. 3) corona discharge in point to plane geometry in ambient air at atmospheric pressure; we use positive streamer corona and negative Trichel pulse regimes. The electrostatic spraying of water is used with this discharge for decontamination of flat surfaces.

Characterization of the investigated discharges

Argon plasma discharges which spread or propagate on dielectric surfaces will be examined. Different methods allow us to measure electrical characteristics of the discharge such as discharge propagation velocity, mean electric field in the plasma channel, optical characteristic - emission spectroscopy of discharge in infrared, visible and ultraviolet region, discharge temperature measurements. In the case of corona discharges in air, we will measure emission spectra of both corona polarities with or without electrostatic spraying of water. From both plasma sources, all measured characteristics will help us to better understand chemical processes induced by plasma in biological samples.

Bio-decontamination of a biofilm by low temperature plasma discharges

Thermosensible surfaces cannot be decontaminated by standard dry heat or autoclave, because they use high temperature. Our goal is to decontaminate biofilm produced by bacteria *Escherichia coli* using low-temperature plasma and to quantify the bactericidal effect of the plasma by various methods.

Identifying the bactericidal factors of air and argon plasmas

We will try to confirm that plasmas of both air and argon discharges decontaminate biofilm, however, our final objective is fundamental understanding of the process, so we attempt to separate single factors (agents) of the plasma (electric field, UV radiation, radicals, charged particles, heat, water content...) which cause bactericidal effects and asses their contributions. We will try to eliminate negative effects of the plasma on decontaminated surfaces, by keeping temperature close to ambient and monitoring possible surface modifications.

4 DC corona discharges in air

4.1 Introduction

Corona discharges - DC, pulsed or in plasma jets - are popular, easy to implement, and low cost low-temperature plasma sources for easily applicable bio-decontamination. They are usually used in ambient air, therefore they are rich sources of ROS and RNS [151].

The typically used polarity of DC corona discharge is positive, but examples of negative coronas used for decontamination purpose can be found: *Candida albicans* in *Fantova et al.* [152]. It is possible to use corona to initiate interesting discharges e.g. the jetlike or comet discharge using two points, positive and negative, in special arrangement in air [153]. Both anode and cathode initiated streamer was applied to decontaminate bacteria on a petri dish. As was mentioned before, corona discharge is also popular for producing plasma jets. In the paper *Choi at al.* [118], corona discharge jet with dry air as a feed gas was used to decontaminate *E. coli* O157:H7 and *Listeria monocytogenes* on fresh and frozen pork meat. Within 2 min 1.5 $\log_{10}$ reduction was achieved without significant impact on sensory characteristics of the pork. The afterglow of this discharge was used to treat food borne pathogens [154] for 24-hours and 3.5 $\log_{10}$ reduction in viable cell counts of tested food pathogens, especially *E. coli* O157:H7, was observed. Another corona jet, with argon used as a feed gas, was used for root canal disinfection [155]. Corona discharge jet in air [128] without any additional feed gas was used to decontaminate biofilm of *Weissella confusa* and was decontaminated for 20 min and 2.6 $\log_{10}$ reduction was achieved.

Pulsed corona discharge can also be used in liquids. In *Joubert et al.* [156] *Bacillus subtilis* vegetative cells and spores were decontaminated by corona discharges in water. The reduction of vegetative cells by 2 $\log_{10}$ was achieved by 1000 corona pulses and the main bactericidal factor was identified to be H_2O_2. For decontamination of spores by 4 $\log_{10}$ 10 000 pulses was used, and this effect was connected to shock waves produced by the discharge. Other way to decontaminate bacteria is not directly by plasma treatment but indirectly by plasma activated medium (PAM). In water [157] molecules of NO_X and their corresponding acids, H_2O_2 and O_3 are typically formed upon plasma activation. In many reported cases microbicidal effect of such PAM remained active even after 4 weeks of storage, although O_3 completely disappeared and concentration of H_2O_2 was diminished. The artificially prepared PAM was bactericidal but into a lesser extent.

DC corona discharges have been extensively used by our group in Bratislava, Slovakia

for decontamination of polypropylene surfaces from spores of *B. cereus* and *Streptococci* biofilms [24] and *Streptococci* biofilms on extracted teeth [18]. The interaction of the water electrospray with the positive steramer corona and the negative corona was studied [49, 50, 158]. This part of the thesis about DC corona discharges of both polarities with or without electrospray is the continuation of our previous work. A more controlled environment was used to grow biofilms and the effect of plasma on the biofilm structure was analyzed in depth using additional methods. With the help of Barbora Tarabová chemical analysis of electrosprayed water was performed.

4.2 Materials and methods

The non-thermal (cold) plasma generated by both positive corona (PC) and negative corona (NC) discharges in air were applied for eradication of planktonic or biofilm *Escherichia coli* on glass surfaces (cover slides). The effect of water electrospray combined with the discharge was tested on the bactericidal efficiency, the biofilm thinning, and the ability to detach biofilm biomass from the surface.

Stable reactive species produced by discharges in air were analyzed by Fourier transform infrared spectroscopy (FTIR), commercial gas analyzer (KANE) and homemade ozone analyzer. The concentrations of reactive species formed inside the electrosprayed water or transferred to it from the gas phase were measured by UV/Vis absorption spectroscopy by using colorimetric methods.

4.2.1 Experimental set-up and discharges

Corona discharges in atmospheric pressure air were generated in an experimental set-up consisting of a needle-to-plane electrode system placed in a discharge chamber in open air. The needle electrode was a sharp or a clipped hypodermic syringe needle connected to a DC high-voltage (HV) power supply. Opposite to the needle HV electrode, a copper plate was grounded through a 50 Ω resistor. The treated biofilm samples on glass cover slides were placed onto the grounded electrode, 5 mm from the HV electrode. Some experiments were performed with sterile distilled water electrosprayed onto the sample, through a hollow clipped HV needle electrode; this was in turn supplied to the needle by pumping with NE-300 SyringePump (Figure 4.1). Electrical characteristics of the discharges were measured as follows: the applied voltage with a Tektronix P6015A HV probe connected to the needle electrode, and the discharge current by measuring the voltage across the 50 Ω grounded resistor. Both probes were connected through coaxial cables to a Tektronix TDS 2024 digital oscilloscope for signal recording and storage.

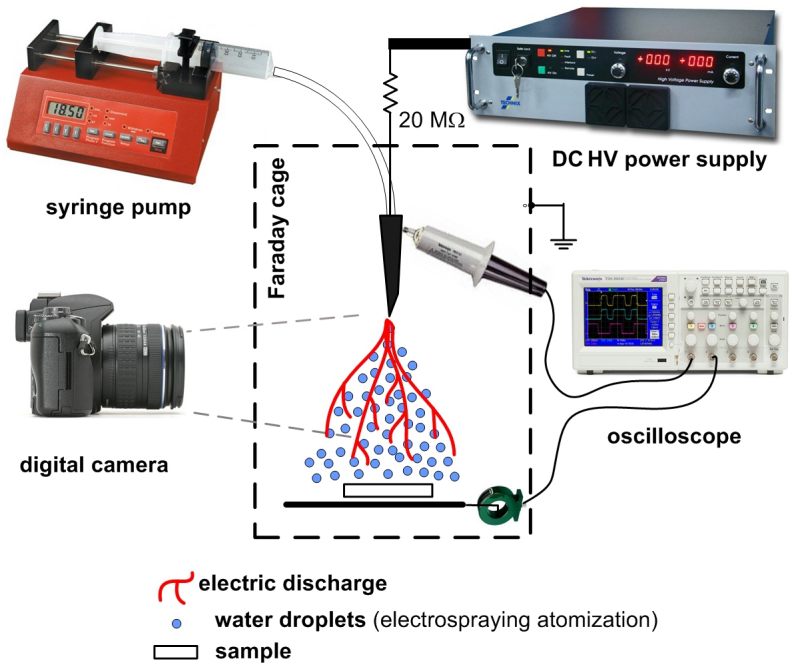

Figure 4.1: Schematic for the set-up of DC corona discharges without/with electro-spraying of water.

4.2.2 Chemical analysis of the electrosprayed water

The water electrosprayed through the PC and NC discharges was analyzed by the methods described above. All these methods are colorimetric, and absorbances were measured on UV/Vis absorption spectrometer UV-1700 SHIMADZU. The electrical discharge parameters were identical to those used for bio-decontamination experiments, but the deionized water flow rate was higher 0.05 mL/min. Water was collected in a glass petri dish with grounded electrode at the bottom, the exposure time was either 15 or 20 min in order to collect enough liquid for the chemical analysis.

Hydrogen peroxide assay

In $TiOSO_4$ colorimetric assay hydrogen peroxide reacts with titanyl ions (Ti^{4+}) in the presence of sodium azide NaN_3 and forms a yellow complex - pertitanic acid H_2TiO_4 with absorption maximum at 407 nm. The method is specific to H_2O_2 and there are no interferences from other compounds present in water. The method is independent on the pH since the measurement of H_2O_2 is carried out in strong acidic solution of sulfuric acid (dilute 1:1) following the modified procedure of Satterfield and Bonnel [20, 159]. In the presence of nitrites, solution of sodium azide was added to the samples with H_2O_2 prior to mixing with titanium reagent to eliminate decomposition of H_2O_2 by nitrites under acidic conditions. With sodium azide, nitrites are reduced into molecular nitrogen under acidic conditions [20, 160].

According to the the Lambert-Beer's law, the yellow color intensity measured as absorp-

tion at 407 nm is proportional to the H_2O_2 concentration giving a linear relationship. The molar extinction coefficient determined in our laboratory from the slope of the calibration plot at the wavelength 407 nm was $\varepsilon = 6.89 \times 10^2$ $\mathrm{Lmol^{-1}cm^{-1}}$.

Ozone measurement

For ozone concentration measurement in the liquid a spectro-photo-metrical method - indigo blue assay is well established. In acidic solution ozone rapidly decolorizes indigo, therefore we can calculate ozone concentration from the difference between the absorption of indigo blue with untreated water and with plasma treated water. This method is not applicable in the presence of the chlorine (www.standardmethods.org [161]). The following equation was used to calculate concentration of ozone in electrosprayed water:

$$O_3[\mathrm{mmol/L}] = \frac{V_{r+s} \times \Delta A_{600nm}}{f \times l \times V_s \times M_{O_3}} \tag{4.1}$$

where V_{r+s} is the volume of the indigo blue reagent and the analyzed sample in mL; ΔA is the difference in absorbance between the sample and the blank at 600 nm; f is the factor 0.42 based on the sensitivity factor for the change of absorbance per mole of added ozone per liter; l is the length of the optical path in cm; V_s is the volume of the sample; and M_{O_3} is the molar mass of ozone equal to 47.992 g/mol.

One should be careful with indigo method for analysis of plasma treated water, this method often gives a false signal due to other ROS interacting with indigo, most likely OH radicals [162].

Nitrates and nitrites

Nitrates (NO_3^-) and nitrites (NO_2^-) in electrosprayed water were both determined by a colorimetric method with Griess reagent 1 and 2 from (Nitrate/Nitrite Colorimetric Assay Kit, Cayman chemical). The Griess reagents react with NO_2^- to form deep purple-coloured azo-product with absorbance peak at 540 nm. To measure NO_3^- concentration, NO_3^- must first react with enzyme and coenzyme to transform to NO_2^-, and then can react with Griess reagents. By this procedure the total concentration of NO_2^- plus NO_3^- can be measured, that by subtracting the NO_2^- concentration previously measured it give the NO_3^- concentration (www.caymanchem.com/pdfs/780001.pdf).

4.2.3 Analysis of the discharge gas composition

The stable species produced by corona discharges in air were analyzed by Fourier transform infrared spectroscopy (FTIR, IRAffinity-1S, Shimadzu), commercial gas analyzer (KM9106 flue gas analyzer, KANE International, ltd.), and a homemade ozone analyzer based on absorption of UV radiation - 254 nm.

The analyzed discharges were enclosed in air-tight box (84×91×95 mm) and the ambient or artificial air (21% N_2 and 79% O_2) has flown (1 slm) through this enclosed box to the analyzers.

Fourier transform infrared spectroscopy

Fourier transform infrared spectroscopy (FTIR, IRAffinity-1S, Shimadzu) of the gas flowing outside the discharge zone inside the 10 cm long cuvette with KRS_5 windows. The spectra were acquired in 4000–600 cm^{-1} with spectral resolution 1 cm^{-1}.

Ozone analyzer

The gas from the discharge chamber is flushed through a $l = 12$ cm long cuvette and the absorption of 254 nm emission from Hg lamp was measured by the optical emission spectrometer (Ocean Optics SD2000).

$$c_{O_3}[m^{-3}] = \frac{A}{\sigma \times l} \tag{4.2}$$

The concentration of ozone per cubic meter was calculated based on linear relationship Equation 4.2 with the measured absorbance (A) based on the Lambert-Beer law with the established photo-absorption cross section $\sigma = 1.15 \times 10^{-21}\,m^2$ for 254 nm [163].

$$c_{O_3}[ppm] = \frac{c_{O_3}[m^{-3}]}{n_0 \times T_r/T_0} 10^6 \tag{4.3}$$

The concentration of ozone in graphs is presented in ppm (parts per million) and it was calculated from Equation 4.3, where n_0 is Loschmidt's number equal to $2.687 \times 10^{25}\,m^{-3}$ at 1 atm and 0°C, and T_r/T_0 is the correction for ambient temperature.

4.2.4 Planktonic bacteria samples

The bacterial suspensions of UV-sensitive *Escherichia coli* DH1 [endA1, recA1, gyrA96, thi-1, glnV44, relA1, hsdR17, (rK- mK+), λ-] [164] and a wild type BW 25113 [BD792 derivative, rrnB, DElacZ4787, HsdR514, DE(araBAD)567, DE(rhaBAD)568, rph-1] [165,166] were used. *E. coli* DH1 was cultured in Miller's modified Lysogeny Broth (LB) (Biolab) at 37°C with agitation until stationary phase, then frozen with 20% (v/v) glycerol in 20 μl aliquots titered at $\sim 10^9$ colony forming units (CFU)/ml. Aliquots of bacterial cultures were thawed and resuspended in 110 μl 1/3X LB. The glass slides (2 cm×2 cm×15 μm) were contaminated by one 10 μL droplet of the bacterial suspension (wet samples). *E. coli* BW 25113 was cultured overnight at 37°C with agitation (400 rpm). The glass slides (2 cm×2 cm×15 μm) were contaminated by one 10 μL droplet of the bacterial suspension. Samples were dried at 35°C for 20 min (dried samples).

Plasma treatment and planktonic sample post-treatment

Cover glasses with dried or wet bacterial samples were placed on the grounded copper electrode 0.5 cm away from the HV electrode. After plasma treatments, bacterial cells were recovered with 10 repetitive rinsings of the cover glass surface with a total of 100 μl sterile distilled water and immediately resuspended in 1/3X LB. Recovered samples were serially diluted and plated on LB agar, incubated at 37°C overnight, and quantified by colony counting.

Control samples were prepared and processed the same way, except they did not go through the plasma treatment.

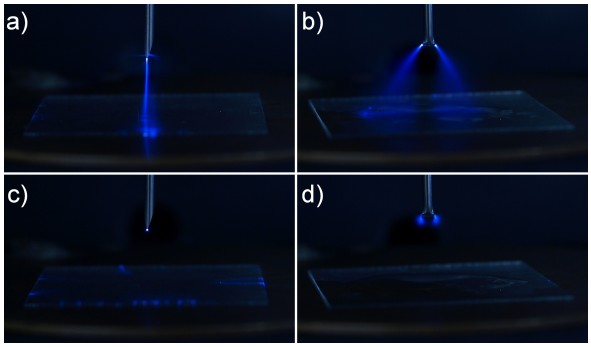

Figure 4.2: Photos of DC corona discharges in air with a hypodermic injection needle as a HV electrode (clipped for electrospray b, d) and a glass cover slide on a copper grounded electrode: a) positive corona, b) positive corona with water electrospray, c) negative corona, d) negative corona with water electrospray (4 s exposure time).

4.2.5 Biofilm samples

Escherichia coli strain BW25113 F+ [BD792 derivative, *rrn*B, DE*lac*Z4787, H*sd*R514, DE-(*ara*BAD)567, DE(*rha*BAD)568, *rph*-1, F+] was used to form biofilm on glass cover slides (2 cm×2 cm×15 μm) on the bottom of a homemade 6-well plate for 48 hours at 30°C. A stationary phase culture grown in Miller's modified Luria broth (LB) (37°C) was diluted 1/100 in buffered (pH 7.4 Phosphate buffered solution) M63 medium (AMRESCO) supplemented with 0.1% casamino acids and 1 g/L glucose. One mL of this suspension was placed into each well of the 6-well plate. The samples were incubated without agitation at 30°C for 48 hours with media refreshment after 24 hours.

Plasma treatment and biofilm sample post-treatment

The biofilms on glass cover slides were taken out from the 6-well plates after 48 hours. The excessive liquid was carefully removed, the samples were dried for 20 min at 35°C, and then placed onto the grounded electrode inside the discharge chamber and treated with plasma. The control samples were dried using the same procedure but not treated with plasma.

Cultivability was determined by repetitive rinsing of the biofilm with 5 mL of 0.85% NaCl saline solution and scraping with another sterile cover glass. The suspension with recovered bacterial cells was vortexed, serially diluted and spread over LB agar in petri dishes and incubated at 37°C overnight; then the bacterial colony forming units (CFUs) were counted.

For imaging using confocal laser scanning microscopy (CLSM), the treated biofilms were stained with solutions of three fluorescent dyes: 1 μL Syto9 (5 mmol.L^{-1}, Life Technologies), 1.5 μL Propidium iodide (PI, 20 mmol.L^{-1}, Cayman chemicals) and 5 μL DAPI (4',6-diamidino-2-phenylindole, 2 mg/mL, Cayman chemicals) in phosphate buffered saline (PBS, pH 7.4), and incubated for 25 min in the dark.

CLSM images were acquired with the OLYMPUS IX81 inverted confocal laser microscope. *Z*-stack acquisitions were performed at 16 bits, with dimensions of 640×640×1 pixels (pixel size 0.33×0.33×0.4 μm), the dimension of the final z-stack was 211.2×211.2×(0.4×N) μm, where N is the number of *z* optical slices taken. Observed excitation and emission wavelength (filters) were as follows:

Dye	Color	Excitation λ	Detected λ
PI	Red	559 nm	575–675 nm
Syto9	Green	473 nm	490–540 nm
DAPI	Blue	405 nm	430–455 nm

Table 4.1: The wavelengths used for excitation and detection of three fluorescent dyes with OLYMPUS IX81 CLSM.

Image stacks (.oif or .oib format) were analyzed using Icy 1.6.1.1v [167] from which the sum of intensity in each channel (red - PI, green - Syto9, blue - DAPI) of each optical slice in the stack and three dimensional projection of stacks were obtained.

E. coli BW 25113 F+ in planktonic form was used to obtain the calibration curve for live/dead ratios (according to supplier manual). Briefly, bacteria in late-log phase were centrifuged to remove nutrient broth and split into two parts: one part with live bacteria diluted in 0.85% NaCl saline solution, and the other part in 70% 2-propanol to kill bacteria. After incubation and washing the live and dead bacteria were mixed together in various ratios, then stained and the fluorescence was measured with CLMS. From the ratios of green (Syto9) and red (PI) fluorescence for the known bacteria live/dead ratio, the calibration curve was constructed (Figure 4.3). From this curve a real live/dead ratio can be estimated.

Biofilm biomass evaluation

Biofilm biomass was evaluated using crystal violet (CV) staining following the established microbiology protocol [168]. The control and plasma-treated biofilms were resealed in the

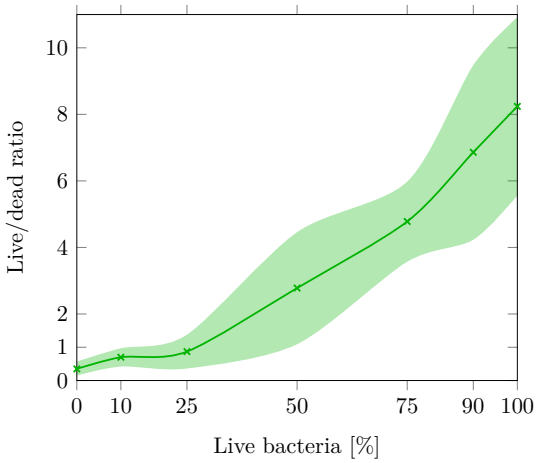

Figure 4.3: Calibration curve for bacteria live/dead ratio (ratio of fluorescence of Syto9 and PI) inside the biofilm measured for the known ratio live/dead for planktonic bacteria (6-10 repeats for each point, mean ± 95% c.i.)

6-well plate after treatment and 200 μL of 0.1% crystal violet was introduced into each well. After 10 min long incubation the CV solution was carefully removed by pipetting and biofilms were rinsed with deionized water until the waste liquid was clear. The 6-well plate was dried upside-down overnight at room temperature. When fully dried, 200 μL of 33% acetic acid was added to each well to solubilize the CV for 15 min, then recovered and diluted in 1/10 deionized water and the absorbance measured at 550 nm.

4.3 Results

In this sections all results obtained by the methods described above are presented.

4.3.1 Discharge characterization

Corona discharges of both polarities were operated in the configuration detailed above (subsection 4.2.1). Positive corona (PC) was supplied with a voltage up to +9 kV and formed streamers with frequencies ranging from 10 to 20 kHz and maximum current pulse amplitudes up to 10 mA (corresponding to a mean input power P ≈100 mW). With water electrospray the pulse frequency was lowered to 10 kHz, although the amplitude was slightly increased but remained under 50 mA (P ≈200 mW). Negative corona (NC) was supplied with a maximum voltage of -9 kV and current pulses with frequencies ranging from 0.5 to 2 MHz and amplitudes up to -1 mA were observed (≈300 mW). With water electrospray, the pulse frequency was lowered to 200–500 kHz and amplitude increased up to -10 mA (P ≈400 mW). The waveforms of the two discharges are presented in Figure 4.4.

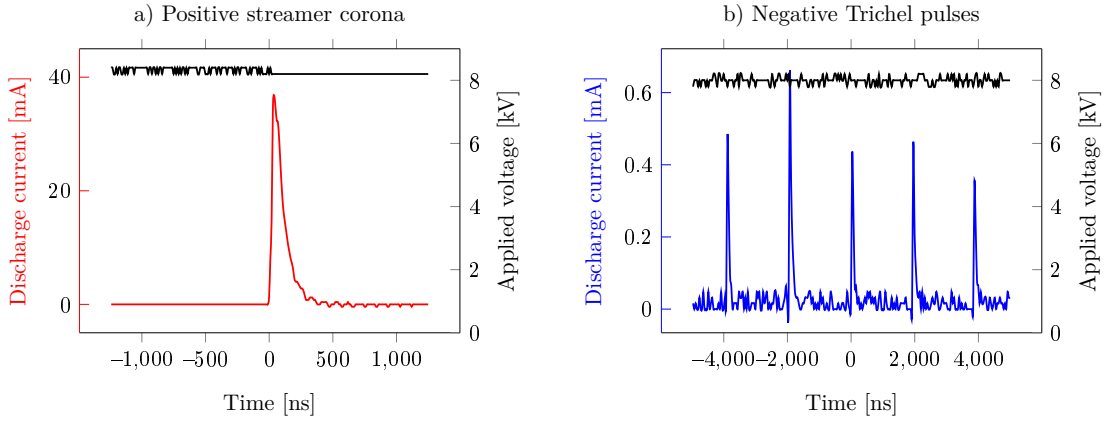

Figure 4.4: Voltage and current waveforms for a) Positive streamer corona, frequency of pulses 13 kHz, b) Negative Trichel pulses, frequency of pulses 473 kHz (current and voltage values were inverted, the supplied voltage and formed pulses were negative).

4.3.2 Analysis of the discharge gases

Gases (dry or humidified air) passing through the positive streamer corona and negative Trichel pulses were investigated using FTIR spectroscopy, commercial gas analyzer, and UV absorption in a home-made ozone analyzer to identify the stable reactive species in the gas surrounding the treated samples.

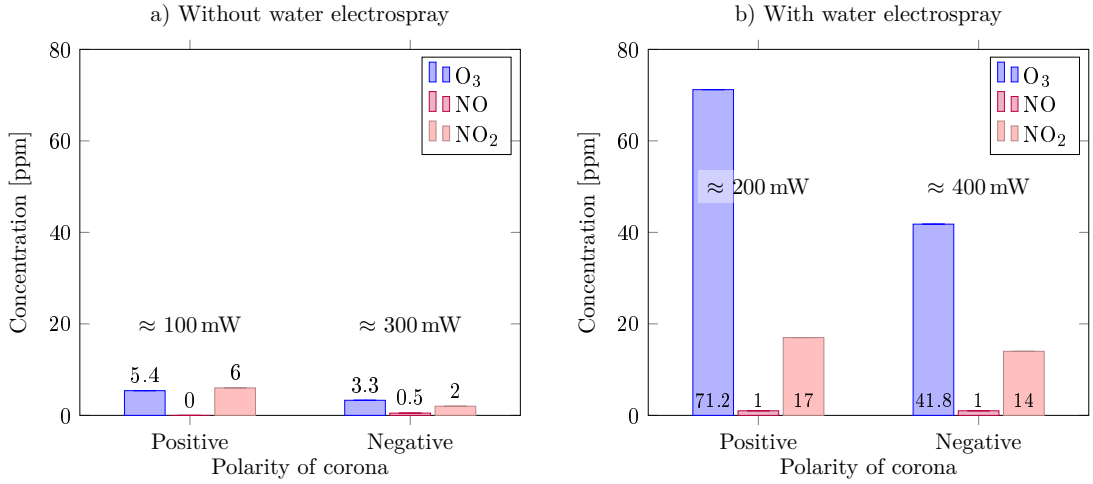

Figure 4.5: Concentration of O_3 measured by the homemade ozone analyzer, and NO and NO_2 measured by the commercial gas analyzer in artificial air (20% O_2, 80% N_2), 15 min accumulation in the zone with the DC corona discharges with or without water electrospray. The mean power of every experimental setup is indicated above the bars.

Figure 4.5 shows the O_3 concentrations obtained by home-made ozone analyzer and NO_X concentrations by the commercial gas analyzer, after 15 min of discharges operation. In the discharge without water electrospray (a), the concentration values of the measured gaseous

RONS are low for both polarities of corona. There is almost no difference between two polarities, the ozone concentrations were 5 and 3 ppm for PC and NC, respectively. NO and NO_2 concentrations were measured by the commercial gas analyzer; NO was undetectable in PC and 0.5 ppm was measured in NC, NO_2 was higher in PC (6 ppm) then in NC (2 ppm). The error of detection for this device bellow 10 ppm is more than 30%. The gaseous RONS concentration values were higher in discharges with water electrospray Figure 4.5 b, the concentration of ozone 71.2 and 41.8 ppm in PC and NC, respectively. NO concentration was in both coronas 1 ppm and NO_2 17 (PC) and 14 ppm (NC).

Typical FTIR spectra obtained form DC corona discharges in air shown in Figure 4.6 measured after 15 min of the discharge operation in dry air (a) or with water electrospray (b). The only identifiable reactive stable species was ozone, NO_X are indistinguishably hidden in the strong water absorption part of the spectra.

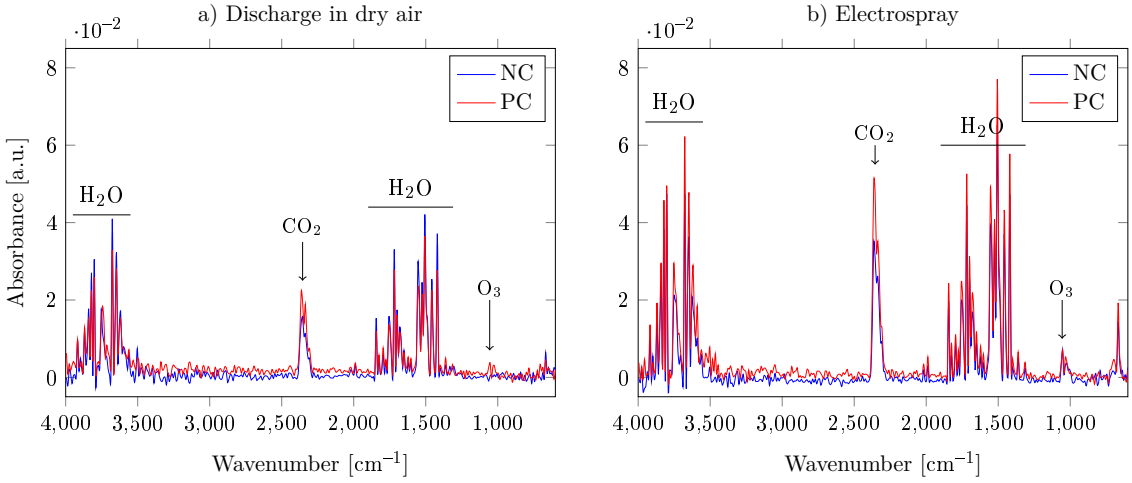

Figure 4.6: Examples of FTIR spectra from positive and negative corona discharge measured in a) dry air, and b) in ambient air with water electrospray. 15 min accumulation inside 1 L chamber the with the discharge running, the gas was then transferred to a vacumated cuvette.

Figure 4.7 shows the time development of ozone absorption spectra in the FTIR in PC and NC discharge with electrospray it the wavenumber range 1000–1080 cm^{-1}. We measured a similar spectrum for PC and NC discharges in dry air, but the O_3 absorption band was almost hidden in the background. The O_3 absorbance was the weakest in the continuous regime, where 1 slm of dry air was flowing through the discharge chamber and then to FTIR. With rising duration of accumulation, the absorbance was increasing and was stronger for PC than for NC. From the absorbance values at 1056 cm^{-1} the concentration of ozone was calculated according to Equation 4.4, where $\varepsilon = 12505$ [1], and A_{1056} absorption at given

[1]This absorption coefficient was previously used in *Hensel et al.* [169] and was experimentally measured by Karol Hensel, Comenius University

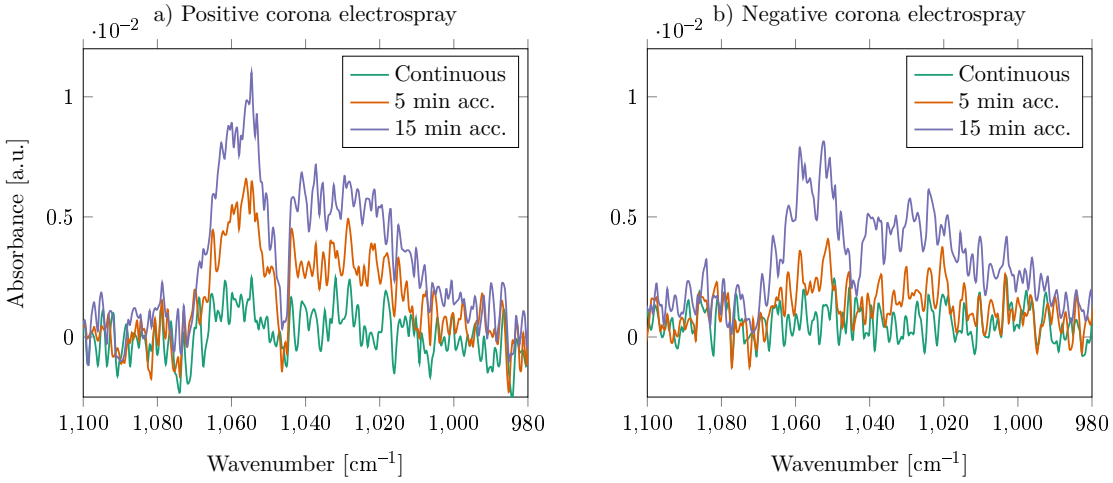

Figure 4.7: Examples of O_3 FTIR spectra formation in time in a) positive corona with electrospray, and b) negative corona with electrospray. Continuous measurement in air flowing through the discharge chamber, 5 and 15 min gas accumulation inside the chamber and then spectra measured.

wavelength.

$$O_3[\text{ppm}] = \varepsilon \times A_{1056} \tag{4.4}$$

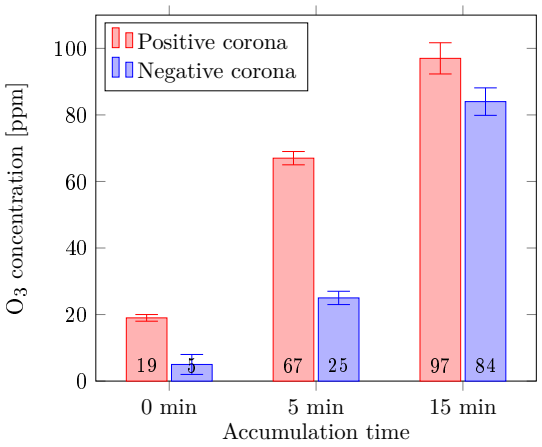

Figure 4.8: Ozone concentration measured by FTIR for PC and NC discharge with water electrospray. The gas from the discharge chamber was flowing to FTIR spectrometer continuously (0 min) or was accumulated for 5 or 15 min and then the concentration was measured. The concentrations were calculated according to Equation 4.4.

The values of ozone concentration measured by FTIR (Figure 4.8) are higher than those measured by UV absorption in a homemade ozone meter (Figure 4.5), especially for NC corona with water electrospray: 84 ppm in (FTIR) vs. 42 ppm (UV). The values were also higher for discharges in dry air, ozone concentration measured by FTIR were 40 and 12 ppm after 15 min PC and NC discharge running, respectively.

4.3.3 Chemical analysis of the electrosprayed water

The measurements of plasma induced chemical changes in the electrosprayed water by PC and NC showed that multiple bactericidal agents were produced (Figure 4.9). The concentration of O_3 in water from PC was two times higher (22.2±1.1 μmol/L) than from NC (10.4±1.7 μmol/L), the same result was obtained for NO_2^- 108.3±23 and 52.9±18.7 μmol/L for water exposed to PC and NC, respectively. NO_3^- was measured in only one independent experiment and the values were 26.8±14.6 (PC) and 37.8±12.5 μmol/L (NC). Lastly, the concentration of H_2O_2 was measured in the water electrosprayed by PC (1039±541 μmol/L) and by NC (32.5±10 μmol/L). The pH of the electrosprayed water decreased from 5.5 to 4 (NC) and to 3.6 (PC), thus generating acidic conditions that influenced the chemistry.

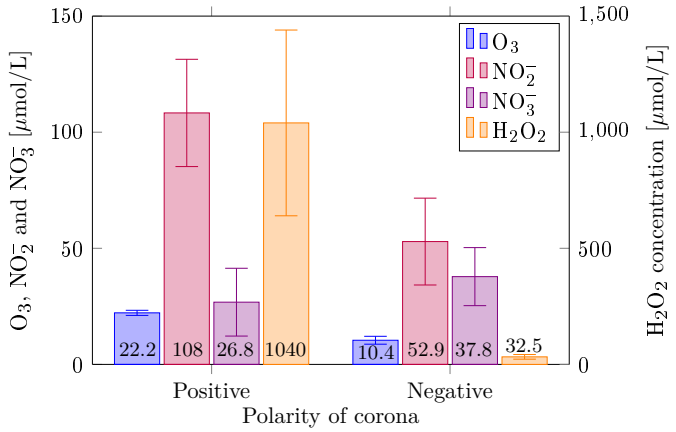

Figure 4.9: Concentration of O_3, NO_2^-, NO_3^- and H_2O_2 measured in the electrosprayed water in positive or negative corona polarity, plotted mean ± SEM, n = 4.

4.3.4 Planktonic bacteria results

Decontamination of planktonic *E. coli* DH1

In Figure 4.10 we present results form decontamination of planktonic *E. coli* DH 1. This bacterial samples were formed from frozen thawed aliquots and were not dried prior to the experiment. Ten μL from prepared bacterial solution was placed onto a glass cover slide and treated with plasma, the initial concentration of control sample was $1.9 \pm 0.5 \times 10^8$ CFU/mL. The electrical characteristics of the NC were differ from those mentioned in subsection 4.3.1, the mean value of the voltage used was -5 kV, the frequency of current pulses did not change but their amplitude was -0.6 mA and -5 mA, without and with water electrospray, respectively. The same bacterial strain and method was used for testing decontamination efficiency of pulsed corona discharge propagated inside the long quartz tube in subsection 5.3.4.

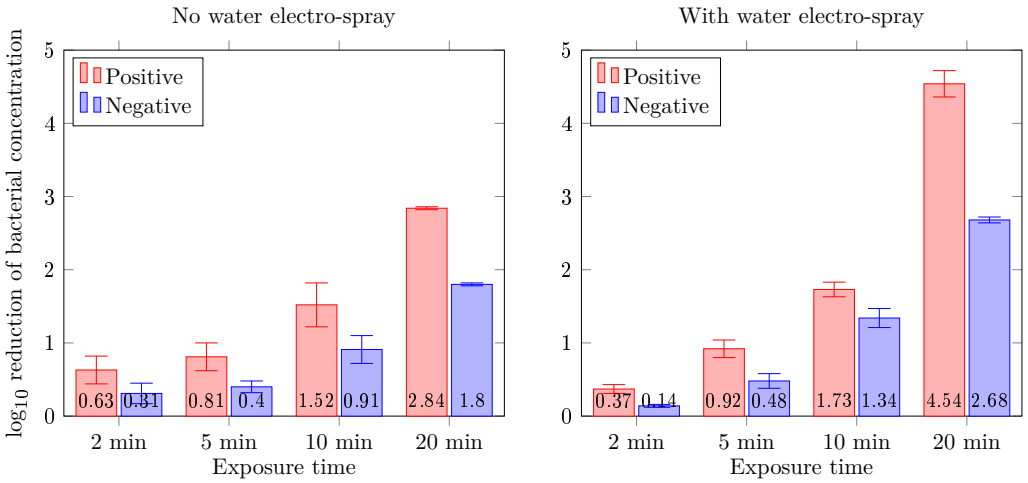

Figure 4.10: Log_{10} reduction of *E. coli* DH1 bacterial population after plasma treatment by positive and negative corona discharge with or without water electrospray (mean±SEM), samples were not dried prior to experiments.

PC reduced bacterial population within 20 min by almost 3 $\log_{10}$, with the addition of water electrospray by 4.6 $\log_{10}$. NC was less efficient: 20 min exposure caused 1.8 $\log_{10}$ and with water electrospray 2.7 $\log_{10}$ reduction. Even from the beginning of decontamination PC efficiency was always higher, this is because the measured input power in experiments with DH 1 for PC was 10 times higher than for NC (∼40 mW as opposed to ∼300 mW). Due to the fact that in the experiments with water electrospray we used a clipped hollow needle, we created two sharp points from which coronas were originated (Figure 4.2). By creating two sharp points, the corona discharges were able to treat larger areas on a sample. This could also contribute to the overall better efficiency of discharges with electrospray.

Decontamination of planktonic *E. coli* BW 25113

In these experiments we also compared decontamination efficiency of electrospraying for PC and NC. The differences from the previous experiments are the the use of *E. coli* BW 25113 strain, which was chosen after failed attempts to form thick-enough biofilms from DH1 10 μL bacterial samples on glass cover slides were dried prior to the experiments and electrical parameters changed to match those used for biofilm treatment (subsection 4.2.1). The results are presented in Figure 4.11.

The initial concentration of bacteria in the 10 μL sample was $3.7 \pm 0.8 \times 10^8$ CFU/mL. The exposure time went only up to 15 min. For the samples exposed to the the discharge only without electrospray, the decontamination efficiency raised slowly with time and reached 2.6 $\log_{10}$ reduction for PC and 3.02 $\log_{10}$ for NC. The water electrospray enhanced the action of the discharge and even in 2.5 min exposure, the higher decontamination efficiency was reached. The water electrospray caused the increase in input power for both PC (100%

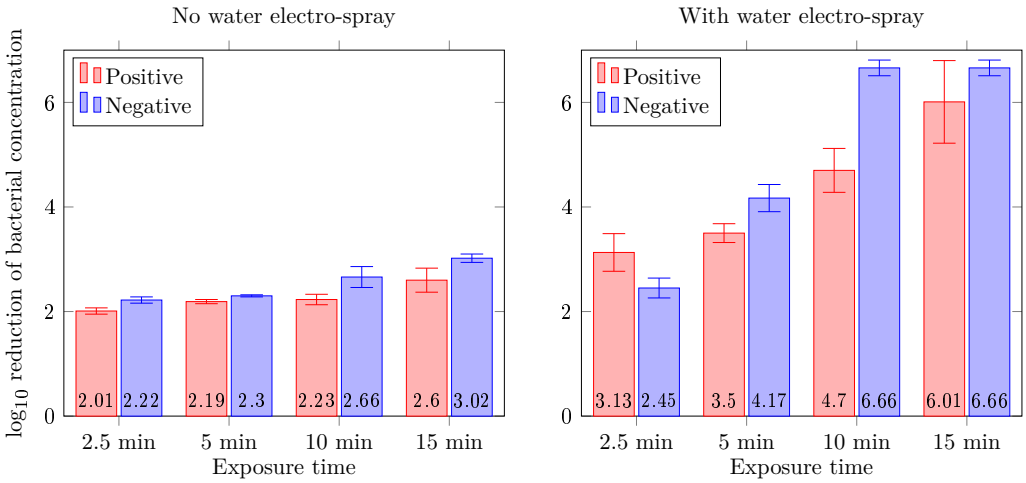

Figure 4.11: Log_{10} reduction of *E. coli* BW 25113 bacterial population after plasma treatment by positive and negative corona discharge with or without water electrospray (mean±SEM), experiments were done in triplicates, samples were dried prior to experiments.

increase) and NC (33% increase). Within 15 min plasma treatment with water electrospray 6.01 and 6.66 $\log_{10}$ reduction of initial concentration was achieved for PC and NC, respectively. For the NC this reduction was achieved for 10 min exposure time.

Effect of separated charged particles from corona discharges on *E. coli*

In this experiment, the reaction chamber was continuously blown by the external ambient air flowing through a tube with the nozzle close to the HV electrode and perpendicular to the inter-electrode gap, the flow rate of air was 4 slm, in the concept similar to [21]. By this configuration neutral reactive species were supposed to be blown away and therefore the bacterial samples with dried *E. coli* BW 25113 were exposed to only charged particles (ions) from the discharge and to the UV emission. From our previous measurements with the streamer corona [77], we had found that UV emission from this discharge had no significant effect on bacterial survival. Comparison of the effect of the full plasma exposure with only charged particles formed in plasma is presented in Figure 4.12.

Within 5 min of decontamination without air blowing the bacterial population was reduced by 3.1 and 2.85 $\log_{10}$ by PC and NC, respectively. With blowing air (4 slm) through the discharge region we obtained slightly lower bio-decontamination efficiency, which might indicate the role of ions in the process. This difference was significant only for NC. This unexpectedly small reduction in efficiency can be caused by insufficient elimination of neutral species and can be improved by increasing the air flow rate. However, increase in the air flow rate (10 and 36 slm) affected the discharge electrical properties (the frequency of current pulses and mean power either increased or decreased compared to the discharge without air blowing on it) and caused the same and even higher efficiency of the discharge decontami-

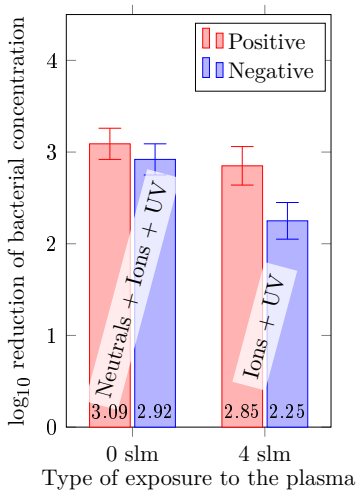

Figure 4.12: Logarithmic reduction of bacterial population by the corona discharges with or without blowing of air through the discharge, the exposure time 5 min (5-8 repeats, mean±SEM).

nation, so these results (not shown) cannot be directly compared to separate the effects of neutral and charged particles. Further experiments are planned with pulsed corona discharge to eliminate the effect of the flowing air on the electrical discharge parameters.

4.3.5 Biofilm treatment results

Results of cold plasma application to the biofilm evaluated by thermostatic cultivation and the analysis of biofilm structural changes by CLSM and CV assay are presented here.

Thermostatic cultivation

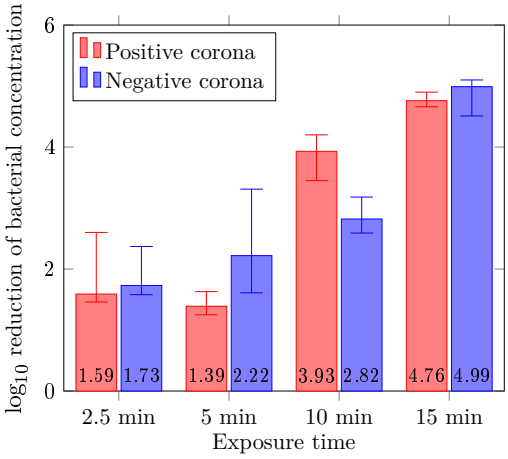

Figure 4.13: Reduction of bacterial concentration in the biofilm on the cover glass by cold plasma treatment of the corona discharges (medians with IQR - interquartile range).

The reduction in bacterial colony forming units after plasma treatment with variable exposure times (2.5, 5, 10, and 15 min) is presented in Figure 4.13. The initial bacterial

concentration in the biofilm was $3.11 \pm 6.59 \times 10^7$ CFU/mL (the biofilms were disrupted and resuspended in 5 mL of NaCl solution). In both corona polarities, the decontamination efficiency increased with exposure time and reached up to 4.76 and 4.99 $\log_{10}$ reduction for positive and negative corona within 15 min, respectively. No significant differences between positive and negative corona were found, except for 5 min exposure time ($p = 0.043$, Mann-Whitney test).

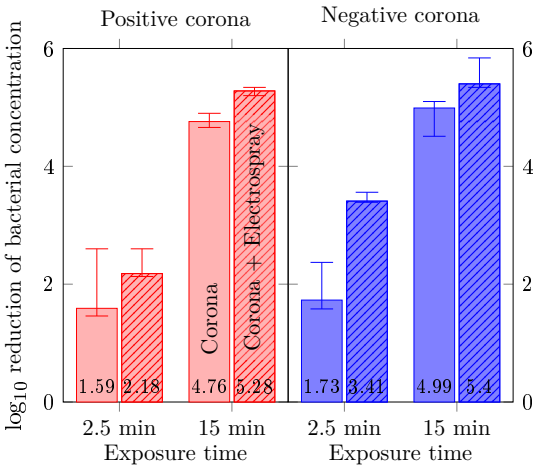

Figure 4.14: Logarithmic reduction of bacterial concentration in the biofilm on the cover glass by corona discharges, effect of water electrospray 0.01 mL/min on the sample - hatched bars (medians with IQR, 5–6 repetitions).

To evaluate the efficiency of water electrospray through the corona discharge we present two exposure times: 2.5 and 15 min (Figure 4.14). For 2.5 min exposure time, the electrospray increased the efficiency from 1.59 to 2.18 $\log_{10}$ for PC, and 1.73 to 3.41 $\log_{10}$ for NC. For negative corona this change was found significant ($p<0.01$, Mann-Whitney test). For the 15 min exposure time, the difference in efficiency between the plasma only treatment and the plasma with electrospray treatment was found to be smaller, but significant (PC, $p=0.048$, Mann-Whitney test) or marginally significant (NC, $p = 0.074$, Mann-Whitney test). Decontamination efficiency increased from 4.76 to 5.28 $\log_{10}$ and from 4.99 to 5.4 $\log_{10}$ for PC and NC, respectively, when the water electrospray was used.

Confocal laser scanning microscopy (CLSM)

The images from CLSM contain information about spatial distribution of the fluorescence in the biofilm from three different fluorescent dyes. DAPI binds preferably to dsDNA and its blue fluorescence is proportional to the amount of the present DNA. In our case DAPI was used to stain all cells in the biofilm. Red PI also stains DNA but does not penetrate through intact cell membranes and is therefore used for dead cells staining, or cells with damaged membranes. Syto9 is a green DNA dye which can penetrate inside all cells. Since PI has a stronger affinity to DNA than Syto9, when both are present in a cell, Syto9 is displaced

from DNA by PI and cells are stained red (according to the protocol - L7012 LIVE/DEAD® BacLight^{TM} Bacterial Viability Kit, Molecular Probes).

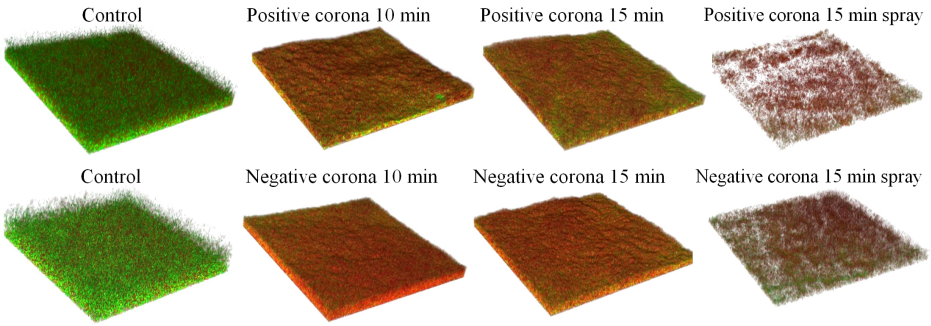

Figure 4.15: Three-dimensional reconstruction of the biofilm z-stacks from CLSM. First column: sections from control biofilm. Biofilms treated by PC (first row) and NC (second row) for 10, 15 min, and 15 min with water electrospray. Green fluorescence Syto9 - live bacteria, red fluorescence (PI) - dead bacteria. Magnification 60×, section size 211.2×211.2 μm.

The fluorescence was acquired from four examined spots on the biofilm: the center and three random places around the center. Examples of reconstructed three-dimensional examined spots (211.2×211.2 μm) of the biofilm (the entire biofilm is a ⌀ 12 mm disc) are presented in Figure 4.15. From this representation we can see that the plasma treated biofilms contain more dead cells (red) at the top than the controls. The structure of the biofilm also changed with plasma treatment: the biofilm seems denser with more compact cellular structure. After plasma treatment with the water electrospray, the biofilm became thinner and patchy.

To quantify the effect of the plasma treatment on the biofilm, the live/dead ratio (Syto9/PI) was calculated. The sums of the red and green fluorescent intensities were measured in each optical slice of the biofilm. The relative values of fluorescence intensity ratios, corresponding to the real live/dead bacteria ratio obtained from the calibration curve (Figure 4.3), were calculated and plotted along the depth position z in the biofilm (from the bottom z=0 to the top of the biofilm - Figure 4.16 - red). In the control samples (Figure 4.16 (a)), the live/dead ratio remained constant at 0.9±0.3 in the bulk of the biofilm (from z=0 to 17 μm), and increased up to 2±1.5 toward the biofilm surface (z=35 μm). After a 15 min plasma treatment (with or without electrospray), the mean live/dead ratio remained constant (around 0.7–0.8) for both polarities in the biofilm bulk, and the topmost layers of cells (with the highest live/dead ratio in the control) were lost. This corresponds to the reduction of biofilm thickness which decreased from 35 μm (control) down to 23 μm by PC with water electrospray, and down to 16 μm without water electrospray. For NC, the biofilm thickness was reduced from 35 μm (control) down to 13 μm with water electrospray, and down to 18 μm without water electrospray.

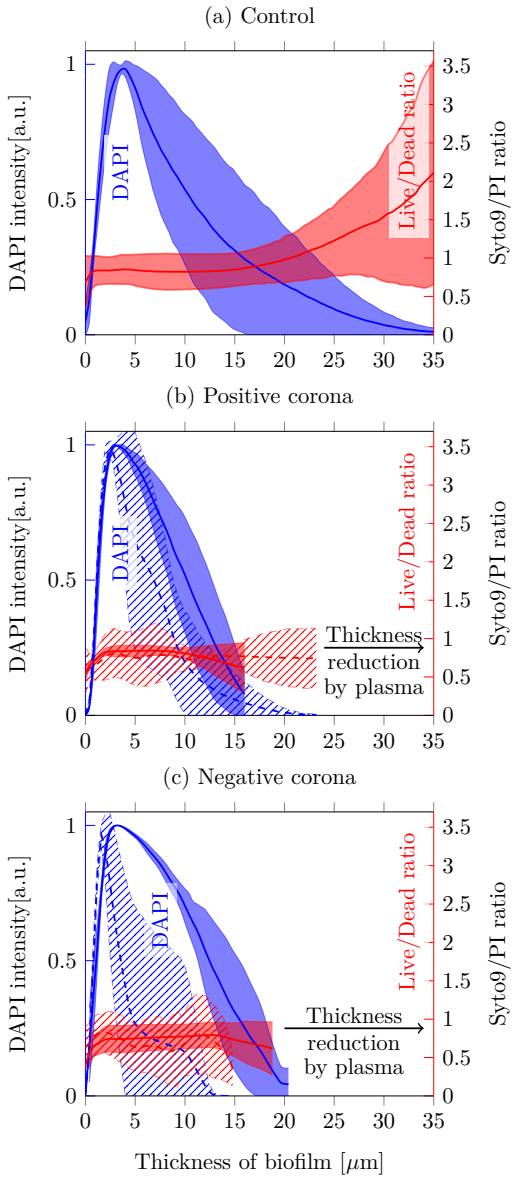

Figure 4.16: Typical development profile of the total fluorescence intensity of DAPI (blue) and Live/Dead ratio (red) in each optical section of the biofilm. (a) Control samples. (b) Samples exposed to positive corona discharge for 15 min. (c) Samples exposed to negative corona discharge for 15 min. Legend: samples with water electrospray (dashed lines, hatched interval), without electrospray (solid line, solid interval). Zero μm represents the bottom of the biofilm - glass cover slide. (Data from one experiment, averaged over 4 random places on one sample per condition, intervals around represent the data range).

The weak influence of the plasma treatment on the live/dead bacteria ratio in the bulk of the biofilm may indicate that the plasma (active species and radiation) does not penetrate sufficiently inside the biofilm. This can be caused by cellular debris and EPS, which protect the deeper layers of bacteria in the biofilm. The values of live/dead ratio calculated from the total fluorescence of Syto9 and PI (not layer by layer but integrated through all

layers) measured on all biofilm samples are presented in Figure 4.17. These results from all experiments summed together (unlike one specific experiment shown in Figure 4.16) showed a slight decrease in the live/dead ratio with plasma treatment that is only significant for PC 15 min exposure time with water electrospray. The live/dead ratio decreased from 0.91±0.02 (control) to 0.61±0.03 in PC, and did not change for NC, at 15 min exposure time and either with or without water electrospray.

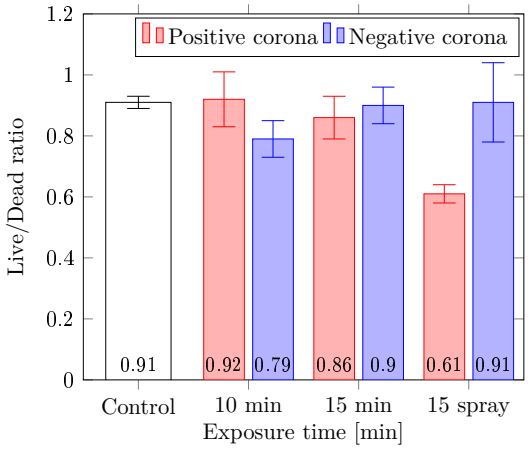

Figure 4.17: Live/Dead ratio calculated from Syto9/PI fluorescence integrated over the entire biofilm thickness for control samples (n = 21), samples exposed for 10 min (PC n = 8, NC n = 12), and 15 min to corona discharge (PC and NC n = 12), and 15 min exposed to corona discharges with water electrospray (PC and NC n = 16) (Mean ± SD).

The same visualization as for Syto9 and PI (Live/dead ratio) was also applied for DAPI, for which the sum of the blue fluorescence in the optical slice depends on the depth position in the biofilm (Figure 4.16 - blue). Using the DAPI staining technique, in the biofilm control samples (Figure 4.16 a) the biofilm reached up to 30 μm in thickness. The obtained results with DAPI staining confirm the trend in the thickness reduction (biofilm shrinking) observed with the live/dead ratio technique. Again, the stronger effect was obtained for NC with electrospray.

To better quantify this loss of the biofilm thickness we chose to set the biofilm beginning and end as slice z-positions with 10% of the maximal fluorescence of the slice in the z-stack. The difference between z position of the end and the beginning was established as the biofilm thickness. The values of the biofilm thickness were calculated for all z-stacks in all biofilm samples and the result mean values are presented in Figure 4.18. There is a trend of reduction of the biofilm thickness with the exposure time and it is enhanced by adding the water electrospray to the discharge. The only significant difference was found for NC 15 min with electrospray in comparison with the control sample ($p<0.05$, ANOVA test - multiple comparisons).

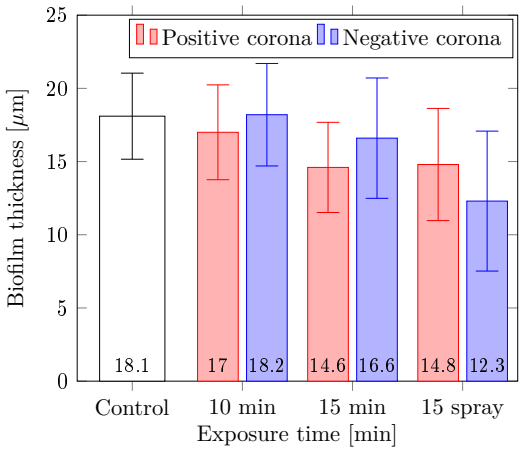

Figure 4.18: Biofilm thickness calculated from DAPI fluorescence integrated over the entire biofilm thickness for control samples (n = 21), samples exposed for 10 min (PC n = 8, NC n = 12), and 15 min to corona discharges (PC and NC n = 12), and 15 min exposed to corona discharge with water electrospray (PC and NC n = 16) (Mean ± 95% c.i.).

Biomass evaluation

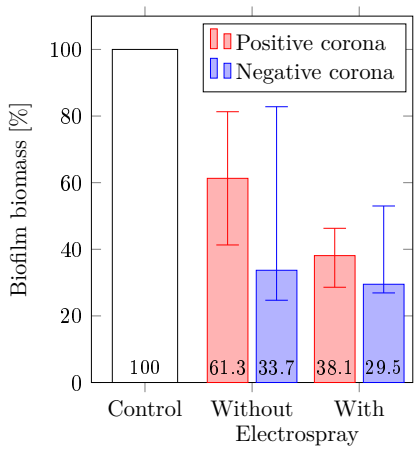

Figure 4.19: Biofilm biomass calculated as percentage of controls from crystal violet absorbance after 15 min PC and NC treatment with or without water electrospray. (Median with IQR, n = 10 in each group).

From the previous results we observed the reduction of the biofilm thickness upon corona discharge treatment. However, the observed biofilm thickness reduction was not very strong: we suppose that disrupted biofilm layers with dead cells still remained on the top of the intact biofilm. By alleviation (wash-out) of the detached bacteria we can observe the true loss of the biofilm biomass, which could have been underestimated by the presence of these detached but still present cells. The biofilm was stained with crystal violet (CV), incubated and the excess dye was rinsed together with the detached bacteria. The absorbance of solubilized CV was then measured. Considering the dispersion in biofilm (controls) thickness over all experiments, the biomass in plasma treated samples was calculated as the percentage of

the control sample absorbance (control sample biomass is equal to 100%). All experiments were done for 15 min exposure time, because of the most significant decrease in the attached biomass (Figure 4.19). For PC 61.3% and NC 32.7% of the biomass was preserved, i.e. remained attached to the surface after exposure to those discharges. When the water electrospray was added to the discharge, stronger bacteria detachment occurred and only 38.1% and 29.5% of the biomass remained attached to the cover glass in PC and NC treatment, respectively. All these correspond to a significant reduction in comparison with the control samples (ANOVA multiple comparisons $p<0.05$, for NC with electrospray $p<0.01$).

4.4 Discussion

In the previous sections, application of low-temperature plasma of corona discharges was used to inactivate planktonic bacteria and bacteria in biofilms. The production of reactive species in the gas phase and in electrosprayed water was measured. The effect of charged ions was tested on planktonic bacteria. Two methods for biofilm viability evaluation were presented: a mechanical disruption of the biofilm followed by a thermostatic cultivation (CFU counts) of bacteria in the resulting solution, and a fluorescent staining and analyzing of the biofilm, layer by layer using the CLMS technique. The reduction of the biofilm thickness and the amount of the attached biomass were investigated by fluorescent DAPI staining, and by colorimetric crystal violet biomass assay. These measurements provided different results but all of them account for different effects of the plasma treatment of biofilms that are discussed in the following sections.

4.4.1 Chemical analysis of the discharge gas and electrosprayed water

The measurement of reactive oxygen and nitrogen species in electrosprayed water (Figure 4.9) showed their presence in considerable amounts. Ozone dissolved in water is known to be an antibacterial agent and could be used as an alternative to chlorination [170]. The toxic effects of ozone for *E. coli* start approximately at concentration 0.19 mg/L ($\approx 4\,\mu$mol/L) according to [171], which is below concentrations produced in our case by both PC (22.2 μmol/L) and NC (10.4 μmol/L). In the gas phase of our discharges the ozone production was higher in discharge with water electrospray than in the discharge alone, although part of it was dissolving into the water, what was shown by chemical analysis of the water. A reason for this higher ozone production might be the cooling effect of the water on the discharge, ozone might have been decomposed at higher temperatures of the discharges without water electrospray.

According to *Hyslop et al.* [172], various concentrations of H_2O_2 have different effects on *E. coli* behavior. Concentrations between 25–50 μmol/L affect the growth, a complete bacteriostasis was observed at 100 μmol/L and a significant cell killing was not observed until

the concentration of H_2O_2 was greater than 500 μmol/L. In our case concentration of H_2O_2 formed in NC (32.5 μmol/L) falls into growth altering window and PC (1040 μmol/L) into bacterial killing region.

The concentration of ozone and hydrogen peroxide was higher in water sprayed through PC, these results were obtained also in previous works, despite negligible difference in the power of PC vs. NC [157]. This difference is especially notable for H_2O_2 production (Figure 4.9). One possible interpretation is that there is much more dissociation of H_2O molecules by electron impact that consequently recombine with each other to make relatively stable H_2O_2 in the streamer corona in the entire interelectrode gap during the propagation of the streamers and their high electric field fronts with a strong space charge and significant generation of electrons.

$$H_2O + e^- \rightarrow H +^{\cdot} OH + e^- \tag{4.5}$$

$$^{\cdot}OH +^{\cdot} OH \rightarrow H_2O_2 \tag{4.6}$$

On the other hand, in the negative corona in electro-negative air, electrons are more efficiently attached to make negative ions and these negative ions drift through the gap, so ionizations and dissociations most effectively occur only in a very limited volume in the close proximity to the cathode tip.

In the gas phase our DC corona discharges produce O_3, NO, NO_2 (Figure 4.5), and H_2O_2 dominantly through the H_2O dissociation to OH and recombination to H_2O_2 mentioned above. These species dissolve directly into the electrosprayed water or a thin water layer on bacterial samples. The decrease of pH in plasma activated water is caused by the dissolution of NO_X [20]:

$$NO_2 + NO_2 + H_2O \rightarrow NO_2^- + NO_3^- + 2H^+ \tag{4.7}$$

$$NO + NO_2 + H_2O \rightarrow 2NO_2^- + 2H^+ \tag{4.8}$$

At lowered pH (in our case NC pH≈4 and PC pH≈3.6), nitrites are quickly oxidized to nitrates [20], and by the reaction with H_2O_2 to peroxynitrites, which are associated with a strong bactericidal effect in plasma activated water [20, 173, 174], besides so-called acidified nitrite (i.e. nitrous acid), which is also associated with a strong bactericidal effect [173, 175, 176]. Despite the fact that these chemicals can act as bactericidal agents by themselves, the final bio-decontamination effect is reached by their combined effects [20]. Previous measurements from our group with the positive streamer corona and the transient spark [77], showed that UV emission from these two air discharges has no significant effect on bacterial survival. By blowing away the neutral species we were able to partially separate the effect of charged particles on bacteria. The slight decrease in bactericidal efficiency suggests that there is a significant contribution (in NC, Figure 4.12) of the charged particles on decontamination. We can speculate that these ions are dominated by superoxide anions O_2^-, since negative ions are abundantly formed in the drift region of the negative corona in air. In the synergy with neutral reactive species, their effect is however greater which agrees

with the results of [21, 177].

However, we must note that the reduction in biocidal efficiency with blown-out neutral species was unexpectedly small compared to the full combined effect of ions and neutral reactive species. This can be caused by insufficient elimination of neutral species by not strong enough blow-out effect and can be improved by increasing air flow rate. On the other hand, the increase in air flow rate affected the discharge electrical properties (including the deposited power) and caused the same and even higher efficiency of the discharge decontamination effect, so these results cannot be directly compared to separate the effects of neutral and charged particles. Further experiments are planned with pulsed corona discharge to eliminate the effect of the flowing air on the electrical discharge parameters.

4.4.2 Biocidal efficiency of DC coronas on the planktonic bacteria

The bactericidal effect of DC corona discharges on *E. coli* DH1 (recA, UV sensitive strain) was presented in Figure 4.10 and on *E. coli* BW 25113 (wild type) in Figure 4.11. Although it would be interesting to compare these two strains, differences in discharge electrical settings (mean power for NC for DH decontamination was 10× lower compare to BW 25113) and sample preparation (DH1 not dried and BW 25113 dried) make the comparison almost impossible. The UV spectra of the positive corona discharge with or without electrospray (Figure 4.20) show that N_2 spectra (Second positive system) were dominant. The OH radical emission was very low probably by fast quenching with other molecules or was overlapped by the higher populated N_2 states. The differences between the emission spectra with or without water electrospray are negligible [178]. Although the UV B emission is present in our discharges and *E. coli* DH1 is more UV sensitive than BW 25113, the main reason is 10× lower deposited mean power. In the next chapter 5, in Figure 5.16 we showed that UV B light had a significant effect on bacterial reduction on *E. coli* DH 1. There might be the possibility that little DNA damage was taking place, and there was an insignificant UV effect [179].

The previous subsection 4.4.1 showed reactive species produced in the DC corona discharges. For both polarities the gaseous ozone concentration was much greater with water electrospray (Figure 4.14) and O_3 concentration dissolved in the electrosprayed water was in the bactericidal range, hydrogen peroxide only for PC and in NC had possible bacteriostatic effect. Both molecules are bactericidal by themselves but especially hydrogen peroxide in the presence of nitrite and nitrate produces secondary reactive species in water e.g. $NO^{\cdot}$, $NO_2^{\cdot}$, $OH^{\cdot}$, and ONOOH [20]. In the NC there is significant effect of negative ions on biodecontamination efficiency, in comparison with PC.

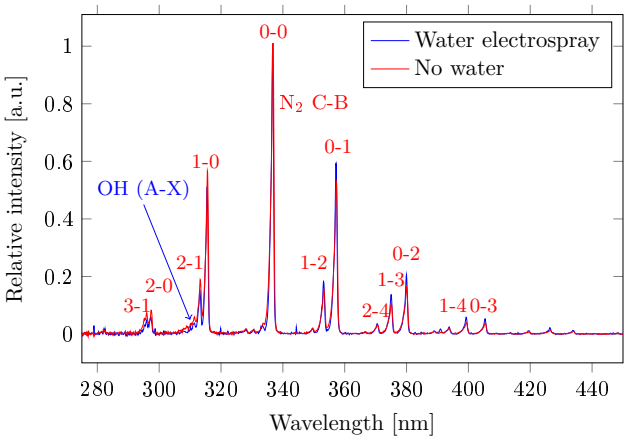

Figure 4.20: Emission spectra of DC corona discharges in the UV region for the positive streamer corona with water (blue curve) and without water (red curve). U_{blue} +12 kV, U_{red} +16 kV, gap 1.5 cm, nozzle 0.6/0.8 mm inner/outer diameter, conductivity 500 μS/cm, water flow rate 0.4 ml/min. (Modified from the PhD Thesis of B. Pongrác [178]).

4.4.3 Biocidal efficiency of DC coronas on the biofilm

Thermostatic cultivation (CFU count method) showed a high biocidal efficiency for both polarities of the corona discharge treatment: almost 5 $\log_{10}$ reduction of the bacterial population was achieved for a 15 min treatment time. Figure 4.13 shows a slightly higher (not statistically significant) decontamination efficiency of NC. This was probably caused by higher discharge input power of NC (P ≈300 mW) in comparison with PC (P ≈100 mW). The only exposure time where PC was more efficient than NC was 10 min; in this case the mean power output of NC was lower than usual at 230 mW, but remained unchanged for PC. Thus, it can be concluded that PC was more energetically efficient than NC, since lower energy deposit of PC provided the same or even higher biocidal efficiency than NC. In PC, positive streamers propagate onto the biofilm surface, so producing in-situ active species (O atoms, OH radicals, and ions) and UV emission (UV-B). Similar neutral active species are also produced by NC, but only in the vicinity of the needle tip (not directly on the biofilm surface), which probably resulted in lower concentrations of RONS both in the gas and in the electrosprayed water, as discussed above in subsection 4.4.1. So the transport of these short-lived species to the cover glass with biofilm placed on the plane electrode is supported by the ionic wind, but lower densities can be assumed to be present at the biofilm/gas interface. In addition, stable species such as ozone and nitrogen oxides are produced in both polarities. These species can also contribute to the biofilm treatment.

By adding the water electrospray to the discharge, the decontamination efficiency increased up to 5.5 $\log_{10}$ reduction. In this case, NC was slightly more efficient than PC (but not statistically significant). Energy deposited by the discharge on the sample increased for both polarities in this case, but was two times higher for NC (P ≈400 mW) than for PC

(P ≈200 mW). In the discharge with water electrospray the tip of a hypodermic injection needle was clipped to enable the spray through the discharge. This resulted in the formation of two sharp points from which corona discharge was developed (Figure 4.2 b, d). Such a configuration can enlarge the plasma treated surface of the sample, which was visible even from the photographs, and therefore may have caused higher decontamination efficiency in the experiments with water electrospray. There was also an increase of the power when the water was electrosprayed onto the sample, because a water layer progressively built up on the cover glass and shortened the distance between the HV and the grounded electrode. Our present results do not clearly show whether the decontamination efficiency increase comes from the higher energy deposit or from other mechanisms such as: increase of the OH radical formation, re-hydration of the biofilm enhancing penetration of active species in its bulk, or others.

CLSM results showed that live/dead ratio distribution through the biofilms (Figure 4.16) remained almost constant in the bulk of the biofilm after plasma treatment. The bacteria in the top layers were killed and their cell debris along with the EPS protected the bottom layers of cells by shielding them from the direct contact with the plasma (PC). The overall live/dead ratio in biofilms (Figure 4.17) confirmed that the plasma effect on the biofilm remained spatially superficial. These results contradict those obtained by the thermostatic cultivation. One hypothesis for explaining this contradiction are possible changes in bacterial metabolism after plasma treatment which might induce the viable but nonculturable state (VBNC), as previously hypothesized by Joaquin *et al.*, 2009 [122]. This change can be induced by oxidative stress, or desiccation from the plasma source [125], visible light, starvation, osmotic stress [180] and other adverse conditions. The cytoplasmic membrane of bacteria in VBNC state may remain intact, therefore the PI fluorescent dye would not penetrate inside the cells and they may have appeared live in CLSM. On the other hand, VBNC bacteria in dormancy state would not proliferate and divide and thus would not form colonies on agar plates, which might have caused the apparent high decontamination efficiency evaluated from CFU plate counts. This problem has been previously reported: plasma treated bacterial cells in a biofilm [122, 125] or a planktonic form [181, 182] seem to be dead based on the culturability test, although the fluorescence and metabolic experiments showed that cells were intact and had a functional respiratory system. Therefore these bacteria could be still viable and may preserve their virulence [133].

4.4.4 Biofilm thickness and biomass reduction

The measurement of the biofilm thickness by DAPI fluorescent staining (Figure 4.18) showed a significant reduction for a biofilm treated 15 min by the plasma with electrospray. However, this decrease in the thickness was smaller than expected and did not agree well with the CV assay that showed almost 50% biomass loss (Figure 4.19). One possible explanation might

be that when bacteria are subjected to the stress they can become smaller [141] and more resistant to adverse environmental conditions [183]. The plasma treatment can also affect the EPS of the biofilm, the polymers surrounding the bacterial cells. As was previously reported in Vandervoot and Brelles-Mariño 2014 [133], after longer exposure to the plasma the extracellular polymeric substance is removed or at least reduced. Since crystal violet only detects the attached biomass, the possibility that the observed biomass loss results from the detached biomass cannot be neglected. The plasma treatment impacted the stability of the biofilm by reducing the EPS and the cell adhesion [125, 133]. Since the biofilm was rinsed during the CV assay, loosely attached and detached bacteria were probably washed away. Rinsing was normally not applied for DAPI visualization, therefore the DAPI biofilm thickness measurements include the detached bacteria and debris in the plasma disrupted biofilm.

For this reason, we performed an additional experiment with rinsing of the biofilm after the corona treatment. Both control and plasma treated samples (15 min, electrospray) were rinsed and compared with unrinsed samples (Figure 4.21) by CLSM live/dead staining. Control samples remained almost intact (visible in Figure 4.21 d, side and bottom frames

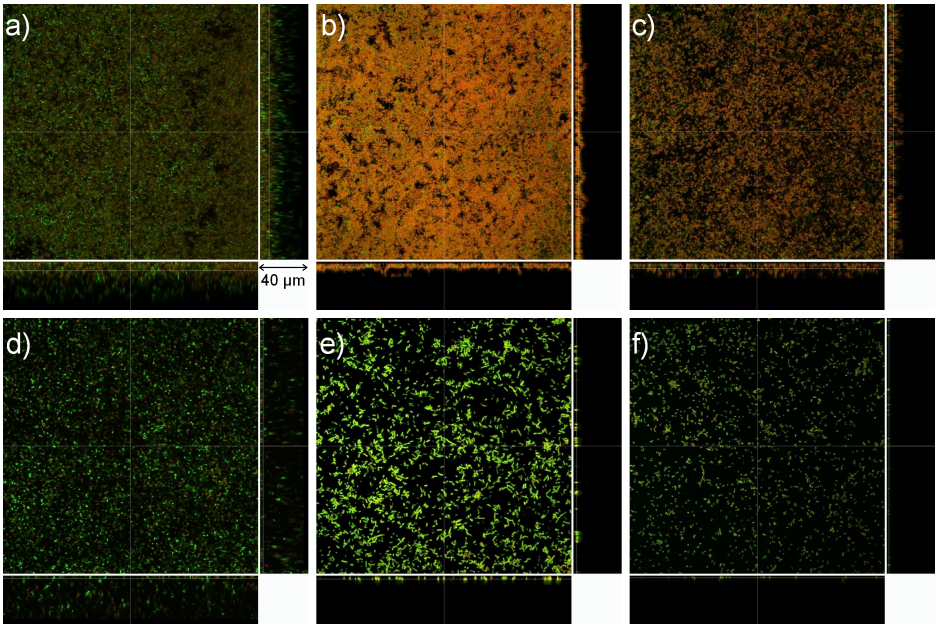

Figure 4.21: The biofilm z-stacks from CLSM Syto9/PI staining, 15 min plasma treatment with water electrospray: a) control, b) positive corona, c) negative corona. Second row: d) rinsed control, e) sample rinsed after positive corona treatment, f) sample rinsed after negative corona treatment. Green fluorescence Syto9 - live bacteria, red fluorescence (PI) - dead bacteria. Magnification 60×, section size (xyz) 211.2×211.2×40 μm. Depth z-cross sections of the fluorescence signal through the biofilm are shown in the frames on a side and bottom of each square x-y image, corresponding to the z-profiles on x and y axes)

showing the depth profile of the fluorescent signal through the biofilm in corresponding x

and y axes), while plasma treated samples were reduced almost to a monolayer of bacteria attached to the glass cover slide. This result confirms that corona discharges were able to disrupt the biofilm structure, which can be then easily detached by washing, while leaving only a monolayer of live single or clustered bacteria attached to the surface of the cover glass. We can assume that by repeating the procedure "plasma treatment + rinsing" we could completely decontaminate and clean the surfaces from biofilms. Testing if this hypothesis remains for future plans.

4.5 Summary

The decontamination effects of the low-temperature plasmas of positive and negative corona discharges in air were tested on *Escherichia coli* in planktonic form and biofilm grown for 48 hours on glass slides. The biofilms were treated by the corona discharge plasma for various exposure times from 2.5 to 20 min. Additionally, water electrospray from the HV electrode onto the bacterial samples was used in some experiments. To quantify the biocidal efficiency of the discharges, different methods were used: thermostatic cultivation of planktonic bacteria and bacteria from the biofilm scraped and disrupted in the solution and CFU counting, or confocal laser scanning microscopy (CLSM) of the biofilm stained with fluorescent dyes (Syto9, propidium iodide and DAPI). Bacteria live/dead fluorescence ratio vertical profiles were visualized through the biofilm thickness. The fluorescence intensity of DAPI was used to evaluate the biofilm thickness loss, and the biofilm biomass loss was measured by the Crystal Violet assay.

The cultivation of planktonic bacteria after 15 min plasma treatment resulted in 2.6 and 3 $\log_{10}$ reduction for positive and negative corona, respectively. The water electrospray enhanced decontamination efficiency and 6 $\log_{10}$ reduction was achieved within 15 min positive corona treatment and 6.6 $\log_{10}$ within 10 min of negative corona treatment. The main bactericidal factors were identified, for positive corona it is a high production of hydrogen peroxide, ozone and nitrates and nitrites. For negative corona the same reactive molecules were detected, hydrogen peroxide production was low, and a significant effect of charged particles, presumably O_2^-, was measured in contrast with positive corona.

From thermostatic cultivation of the bacteria from the biofilm, 4.8 and 5 $\log_{10}$ reductions were observed after 15 min exposure to positive and negative corona discharge, respectively. This decontamination efficiency was significantly enhanced by water electrospray onto the samples to 5.3 $\log_{10}$ for positive and to 5.4 $\log_{10}$ reduction for negative corona. CLSM showed that the live/dead ratio remained constant in the bulk of the biofilm after treatment, only cells on the top layers were affected by the discharge. Although the live/dead ratio did not decrease, the top cells were destroyed and missing. The DAPI staining showed that the biofilm was thinner after plasma treatment; its thickness decreased from 18.1 μm in

the control samples to 12.3 μm after treatment (negative corona with electrospray for 15 min). A substantial biofilm biomass loss (50%) was confirmed by the Crystal Violet assay. Additionally, the live/dead staining of the plasma treated biofilm combined with rinsing after the plasma exposure confirmed the substantial reduction of biofilm thickness, which indicates an interesting possibility for potential applications in future.

5 Atmospheric pressure argon surface discharges propagated in long tubes

5.1 Introduction

Between 4 to 18% all central venous catheters (CVC) are associated with sepsis. Successful therapy of CVC-related infections is difficult to attain. Several approaches to the prevention of CVC infection have been attempted; they include improved catheter care, modification of the intrinsic properties of polymers and the bonding of antimicrobial agents to catheter material [75]. We report a novel method for decontamination of inner surfaces of long narrow tubes by low-temperature plasmas of electrical discharges. In the previous section 2.5 the principles of discharge propagation over dielectric surfaces (e.g. long narrow tubes) is discussed. So-called plasma bullets produced by pulsed dielectric barrier discharges propagating with very high velocities in dielectric capillaries were previously obtained and studied with neon, helium or argon as feed gas [13, 62, 184–186]. Here we name a few plasma devices based on these principles which were used for decontamination of long narrow tubes.

An outer surface of long tubes can be easily decontaminated by special arrangement of plasma jets, or by one jet with adjusted head [187]. Only a few studies have dealt with bio-decontamination of the inside of dielectric tubes by plasma, although lots of devices in medicine have this shape (endoscopes, catheters). Medical endoscopes are the most complex and expensive devices for incorporeal diagnostic and surgery. Medical treatments with such devices always include the risk of endoscopic associated nosocomial infections. Therefore plasmas, which can by ignited inside a long dielectric tube could be a good means of sterilization. Only a handful of laboratories have dealt with the challenge of decontamination of long narrow tubes.

In the first article from *Pollak et al.* [188] a long tube with small diameter (4 mm) contaminated by 10^6 *Bacillus atrophaeus* spores was decontaminated using an argon discharge at reduced pressure. The discharge was sustained using a microwave field-applicator called a stripline, fully enclosing the tube to be treated. The plasma was able to sterilize inner surface of the tube, in less than 10 min. The main biocidal agents were VUV and UV photons. In *Pointu et al.* [189], an afterglow of the discharge in nitrogen was flowing through the small diameter tube (6 mm) 1 m long. *Bacillus stearothermophilus* spores and *Escherichia coli* bacteria were treated by pure nitrogen plasma and within 5 min 3 $\log_{10}$ reduction was achieved for *E. coli*. To obtain the same decontamination efficiency for *B. stearothermophilus*

30–50 min exposure time was required. The same discharge was used in *Limam et al.* [35], but the tube measured 57 cm. The discharge bio-decontamination efficiency was tested on *E. coli* at the beginning of the tube and at its end. Within 40 min of exposure, 5 and 4 $\log_{10}$ reduction from initial bacterial concentration was achieved for both positions. In *Polak et al.* [33], special electrode arrangement on the long lube surface was used to propagate the discharge inside it. The gas flowing inside the tube was argon with oxygen and nitrogen admixtures. 30 cm long tube was contaminated by *B. atrophaeus* spores and treated for 10 min by argon plasma or argon plasma with nitrogen and nitrogen and oxygen admixtures. For pure nitrogen, the observed decontamination efficiency was 3.7 $\log_{10}$, by adding nitrogen it increased to 4.2 $\log_{10}$ and increasing N_2 and O_2 lead to a decrease 1.7 $\log_{10}$. The VUV and UV were important biocidal agents especially in pure argon.

The discharge described and used in this chapter operates at atmospheric pressure is propagated directly on the inner surface of the tube, without necessity of any special electrode arrangement, and with relatively low argon gas flow.

5.2 Materials and methods

5.2.1 Plasma device, high voltage power supply, and electrical measurements

Pulsed corona discharges were propagated on the inner surfaces of a quartz tube (8 mm inner diameter, variable length: 49 cm in the case of Figure 5.1, in which argon (3.9 slm in dry argon conditions and 4.7 slm in a 760 ppm water vapor/argon mixture) was flowing at atmospheric pressure, from a tungsten needle placed at the tube inlet to a grounded counter electrode located at its outlet (a counter electrode in Figure 5.1). The tungsten needle was connected to a low jitter, pulsed high voltage power supply made from a MOSFET solid switch bridge (Behlke HTS 301) with a 2 nF charging capacitor fed by a DC 30 kV-10 mA high voltage power source. Positive voltage pulses of up to 35 kV peak value (due to the inductance of the circuit) and 200 ns – 5 μs width were obtained with a repetition rate of 500 pulses/s. The voltage pulse front rise was ≈1 kV/ns. A voltage probe (Tektronix P6015A, 1 V:1000 V – 75 MHz) connected to the needle electrode and a fast rise current transformer (Tektronix CT-2, 1 mV:1 mA – 200 MHz) connected to the (grounded) counter electrode were used for voltage and current measurements, respectively. Signals were recorded using a LeCroy WaveRunner 62 Xi digital oscilloscope (600 MHz - 10 GS/s).

5.2.2 Optical emission spectroscopy

Optical emission relative intensities and plasma rotational temperatures were measured by optical emission spectroscopy (OES) along the quartz tube. OES was performed in the 250–

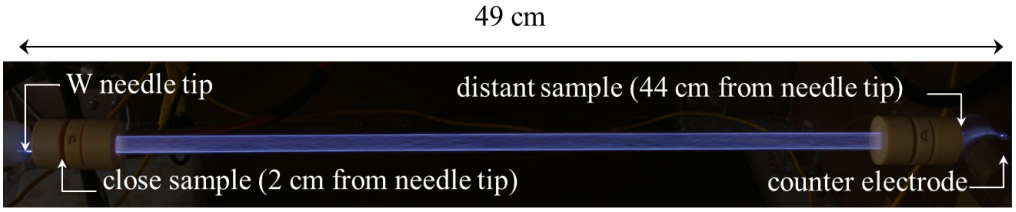

Figure 5.1: Photograph of the pulsed corona discharge propagating in argon gas inside an 8 mm inner diameter quartz tube over 49 cm between a charged tungsten needle and a grounded counter electrode. The bacterial sample locations at 2 and 44 cm are indicated.

850 nm range using an Acton Standard Series SP-2758 imaging spectrograph of the focal length 750 mm. Two gratings were used in the measurements; a 2400 gr/mm ruled grating blazed at 240 nm and a 300 gr/mm ruled grating blazed at 300 nm. This spectrograph was coupled to a Princeton Instruments PI-MAX4:1024f-RB intensified CCD camera with 1024 $\times$ 1024 pixels. The pixel size was 13 $\times$ 13 μm. For the 2400 gr/mm grating, the spectral resolution of the system was found to be 0.025 nm (full-width-at-half-maximum).

For all spectroscopic measurements, light was collected by fiber optic cable pointed perpendicularly at the tube from a distance of 38 cm. This fiber was moved along the tube's length in order to collect light from different positions. A collimator was added to the fiber optic cable and adjusted to collect light from a 1 cm diameter disk centered on the tube axis. For spectroscopic measurements used for the evaluation of the transient plasma temperature, the light was collected at each position along the tube by taking the average of 1000 exposures, each consisting of 100 on-CCD accumulations of 600 ns duration. For time-resolved measurements, the light was collected for durations of 10 ns; 300 of these 10 ns spectra were taken during and after the 2 μs duration voltage pulse. Each of these 300 spectra was obtained using the average of 3 exposures consisting of 100 on-CCD accumulations.

5.2.3 Gas temperature measurements

Local rotational temperature measurements were performed during the discharge propagation. At atmospheric pressure, it is assumed that the rotational temperature is equal to the kinetic (gas) temperature [190]. Thus, 1000 ppm of nitrogen was added to the gas mixture in order to evaluate the neutral gas temperature in the plasma. The spectral emission of the N_2 second positive system between 377 and 381 nm (0-2 band) was measured at various locations (2.5, 5, 15, 25, and 40 cm from the needle electrode) along the tube. Comparisons between the measured spectra and spectra calculated using the line-by-line radiation code SPECAIR [191] were used to estimate the rotational temperature of the plasma.

Under steady-state operating conditions, the bulk gas temperature at the tube outlet and the quartz tube outer surface temperature were measured using an alcohol thermometer. The bulk gas temperature was measured in the flow and behind the counter electrode at 51 cm

from the source electrode (i.e. 3 cm downstream of the discharge region). The external surface temperature of the quartz tube was measured at two locations: 2 and 44 cm from the needle electrode. In this case, the thermometer was sealed in a 2 cm thick Plexiglas casing and its tip coated with a heat transfer silicon paste (HTSP - Electrolube) that was directly applied to the outer quartz surface.

5.2.4 Bacterial sample and test conditions

Bacterial strains and culture conditions *Escherichia coli* strain DH-1 (F-, λ–, *endA1*, *recA1*, *gyrA96*, *thi-1*, *glnV44*, *relA1*, *hsdR17*) was used for all experiments. We have chosen a UV sensitive (*recA*-) E. coli strain [192] in order to obtain a large mortality response to UV light exposure. Bacteria were cultured in Miller's modified Luria broth LB medium (CONDA) at 37°C with agitation until stationary phase, then frozen with 20 % (v/v) glycerol in 20 μl aliquots titered at $\sim 10^9$ colony forming units (CFU)/ml.

Plasma treatment bactericidal assay. Aliquots of bacterial cultures were thawed and resuspended in 110 μl 1/3 × LB. Droplets of 10 μl volume were placed inside or outside the quartz tube (in order to evaluate the UV-B effect on bacteria viability), and either immediately treated as droplets (liquid) or dried at room temperature (2—4 h) or under argon flow (10 min) before treatment. Samples were positioned at 2 and 44 cm from the high voltage (HV) needle electrode (Figure 5.1) and simultaneously exposed to the plasma treatment at room temperature for up to 20 min. Samples exposed for the same duration to the argon flow alone were also included as controls. Bacterial cells were recovered with 10 repetitive rinsings of the inner or outer quartz tube surface with a total of 100 μl sterile distilled water and immediately resuspended in 1/3× LB. Recovered samples were serially diluted or concentrated by filtration through a 0.45 μm mixed cellulose ester membrane (Millipore) when high mortality was expected, plated on LB agar, incubated at 37°C overnight, and quantified by colony counting. Samples and controls were exposed to either 3.9 slm (1.3 m/s average velocity) dry argon, or 4.7 slm (1.55 m/s) humid argon (760 ppm H_2O) with an initial 2 min gas purge. Assays were carried out in triplicates (unless otherwise specified).

5.2.5 H_2O_2 assay

Hydrogen peroxide accumulation in water droplets inside the quartz tube was measured by optical absorption spectroscopy, as H_2O_2 reacts with ammonium vanadate in an acidic environment (dipicolinic acid, distilled water, sulfuric acid) to form a yellow complex with a maximum absorption at 430 nm [193]. A linear relation,

$$[H_2O_2]_{mg/l} = \mathrm{Abs}_{432\ nm} \times 704, \tag{5.1}$$

was obtained between the absorbance of the complex and the hydrogen peroxide concentration for H_2O_2 solution concentrations ranging from 0 to 300 mg/l. Five droplets of 10 μl distilled water (50 μl total) were deposited in the tube at 2 and 44 cm from the HV electrode. After exposure to the discharge in humid argon (760 ppm H_2O, 4.7 slm) for 1 to 5 min, the droplets were collected all together in one volume (max. 50 μl) from the quartz tube and diluted 1/10 in the reagent solution. The bactericidal effect of the measured H_2O_2 concentrations was evaluated by control experiment: incubating 10 μl of bacterial culture aliquots, prepared the same way as for the plasma treatment, for 5 min in final concentrations of 53 to 222 mg/l H_2O_2. Samples were handled with the same protocol following the plasma treatment. Briefly, samples were immediately diluted in 100 μl sterile distilled water and mixed in 900 μl 1/3 LB before being serially diluted and plated for viable titer determination.

5.3 Results

5.3.1 The choice of the discharge operating conditions

Typical voltage and current waveforms are presented in Figure 5.2 for two different distances between the HV needle electrode (tube inlet) and the grounded counter electrode (tube outlet). The current pulse, corresponding to the arrival of the propagating discharge at the counter electrode, is delayed from the voltage front rise (from which the discharge is initiated). For a given constant peak voltage value, this delay τ is associated with discharge propagation velocity, and therefore τ depends on the gap (tube) length d. For given values of the peak voltage and the gap length, the pulse width was adjusted in order to avoid a spark discharge, while ensuring that the discharge propagated along the full length of the tube. This situation corresponds to an optimum pulse width, for which the current pulse is obtained during or immediately after the voltage drop (Figure 5.2). In physical terms, the filamentary discharge tip just reached the counter electrode when the applied voltage approached zero value.

The discharge propagation length, *i.e.* full propagation of the discharge from the needle electrode to the counter electrode, was investigated as a function of both the voltage pulse peak value and width. For a fixed pulse width (700 ns for Figure 5.3 a) and a constant 550 mA current pulse amplitude (occurring after the voltage drop), the propagation length increased linearly with the peak voltage. The inverse slope of this curve can be identified as the mean electric field in the discharge channel, also referred to as the stability field. Values of 520 V/cm and 590 V/cm were obtained in dry and humid argon (760 ppm H_2O), respectively. In dry air at atmospheric pressure, this value is 5 kV/cm, whereas 400 V/cm was found for an atmospheric pressure argon volume discharge [194]. The higher value of the stability field calculated in humid conditions is attributed to electron energy losses in dissociative, vibrational, and rotational mechanisms with water, leading to a higher applied

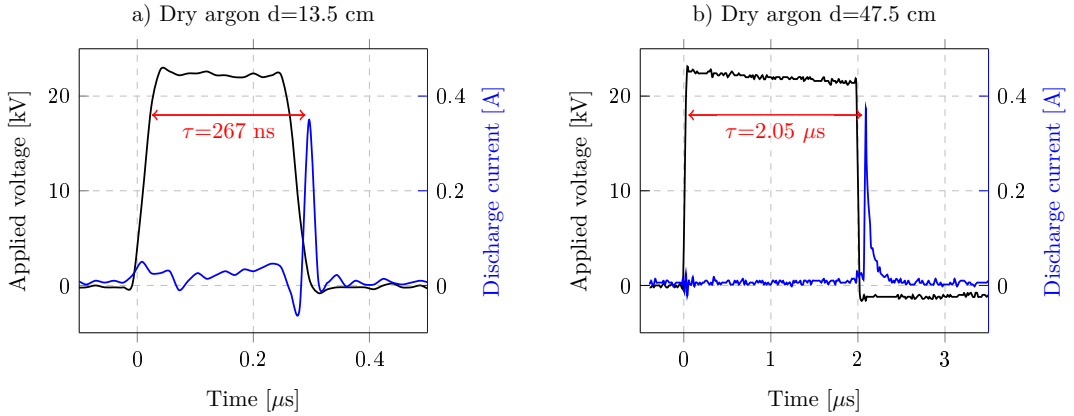

Figure 5.2: Voltage and current waveforms for two needle-to-counter-electrode gap distances for a discharge in dry argon gas (3.9 slm). a) Gap distance of 13.5 cm, and b) gap distance of 47.5 cm, with τ being the delay from the voltage pulse rise to the arrival of the propagating discharge to the counter electrode.

voltage for a given propagation length. For a fixed peak voltage value (23.3 kV for Figure 5.3 b) and a constant 450 mA current pulse amplitude (occurring after the voltage drop), the propagation length increased with pulse width, until it reached a saturation point 2.5 μs beyond which increasing the pulse duration no longer increased the propagation length. Such results were previously observed for the length of plasma jet (helium plasma jet propagated in open air [62]).

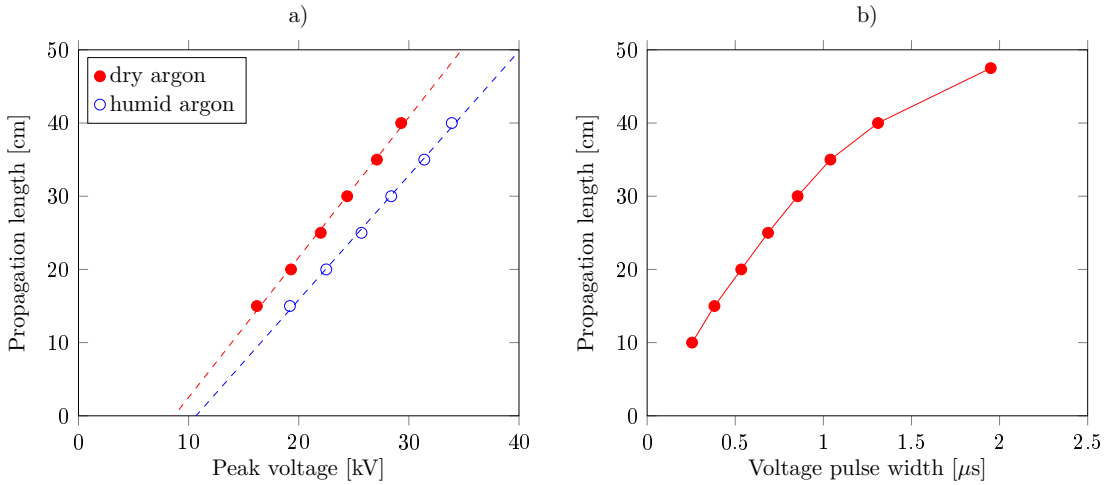

Figure 5.3: Pulsed corona discharge electrical characterization. (a) Discharge propagation length at constant pulse width (700 ns) for increasing peak voltage in humid argon (4.7 slm, blue symbols), and dry argon (3.9 slm, red symbols) with linear fits (dashed lines). (a) Discharge propagation length at constant peak voltage (23.3 kV) for an increasing pulse width in dry argon.

By measuring voltage and current waveforms as presented in Figure 5.2, it was possi-

ble to estimate the average discharge velocity using the ratio d/τ. Average velocities of 5×10^5 m/s and 2.3×10^5 m/s were calculated for short (13.5 cm) and long (47.5 cm) gaps, respectively. These values are consistent with those measured optically in a comparable situation - streamers propagating in argon over a dielectric surface [61].

Streamer velocity, electrical measurements: To measure the velocity of streamer propagation inside the quartz tube, we introduced the second (movable) current probe - a coil with Teflon cylinder inside it to easily slide the probe outside of the 49 cm long quartz tube without touching its surface. A time delay between the current pulse in the movable probe and the leading edge of the voltage signal was measured. The width of HV pulse had fixed width. The streamer velocities were calculated as ratios of the distance (between the tungsten tip and the movable probe) and the delay (Figure 5.4).

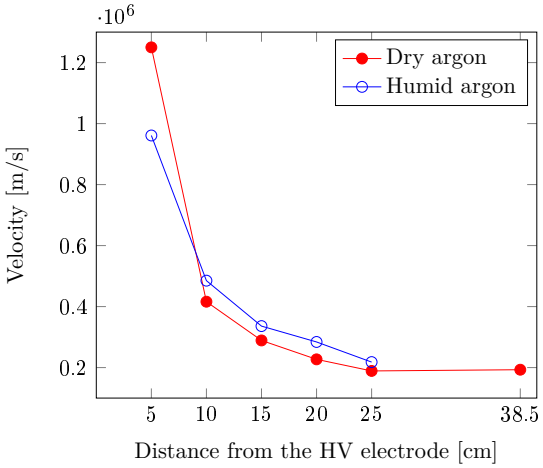

Figure 5.4: Dependence of the streamer velocity in dry and humid argon on the distance from the HV electrode measured by the movable probe. The discharge settings (flow rate and applied HV) were the same as for biological experiments

Final settings: The water vapor concentration for which the discharge could be fully propagated along the tube with a peak voltage value lower than 30 kV was found to be 760 ppm. The above mentioned measurements led to the final settings for electrical parameters according to the propagation length. For all bactericidal tests, the plasma was generated with a 2–2.2 μs voltage pulse at 500 pulses/s with a 20.6–27.9 kV peak voltage depending on the sample and the gas humidity.

It is worth mentioning that by using the same electrode arrangement and high voltage power supply, a propagation length of more than one meter was obtained in a thin (2 mm inner diameter) silicone tube with pure argon flowing at atmospheric pressure (Figure 5.5). This result has important medical implications since the plasma source device under investigation could possibly be applied to catheter and endoscope duct decontamination. However, for the research reported here, aimed at the decontamination mechanism investigation, the

Figure 5.5: Photograph of the pulsed corona discharge propagating in argon gas inside an 2 mm inner diameter silicone tube over 105 cm between a source (a tungsten needle) and a counter electrode.

shorter quartz tube device described above was preferred.

5.3.2 Plasma optical emission

Optical emission spectra of the pulsed corona discharge plasma in dry and humid argon (Figure 5.6) showed the presence of emissive OH radicals. In the presence of water (even traces, as it is for "dry" Ar condition), the argon plasma generates ultraviolet (UV-B) emission through the de-excitation of $OH^*[A^2\Sigma^+ - X^2\Pi]$ radicals (305–311 nm). OH radicals are themselves produced by a water dissociation mechanism involving excited argon Ar^*:

$$Ar^*(4p) + H_2O \rightarrow Ar(3p) + OH^*(A^*\Sigma^2) + H \tag{5.2}$$

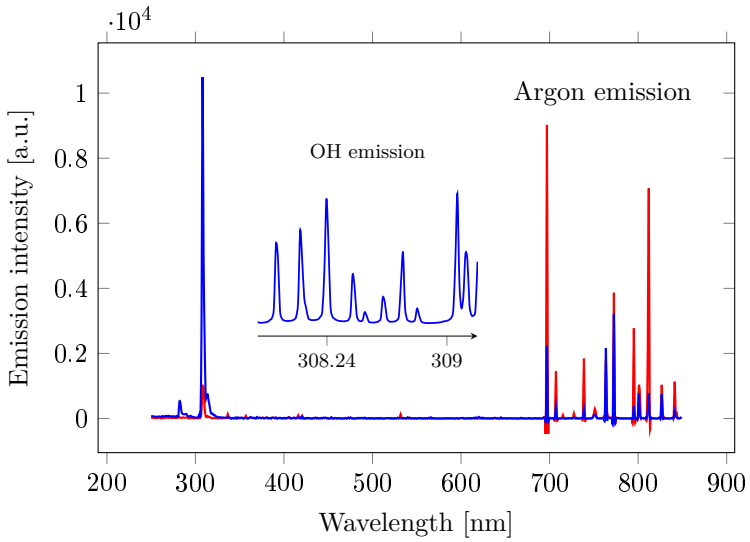

Figure 5.6: Optical emission spectra of the pulsed corona discharge in dry (red line) and humid argon (blue line) acquired at 5 cm from the HV electrode. Detector integration time 600 ns, grating 300 lines/mm. The insert represents a spectrum of the rotational bands of $OH^*[A^2\Sigma^+ - X^2\Pi]$ measured in humid argon (760 ppm water vapor), grating 2400 lines/mm.

As expected (Figure 5.7), the relative intensity of the OH band depends on the humidity present in the feed gas and it is greater in argon with 760 ppm of water vapor than in dry argon. In our conditions, 760 ppm was the water vapor concentration for which the discharge could be fully propagated along the tube with a peak voltage value lower than

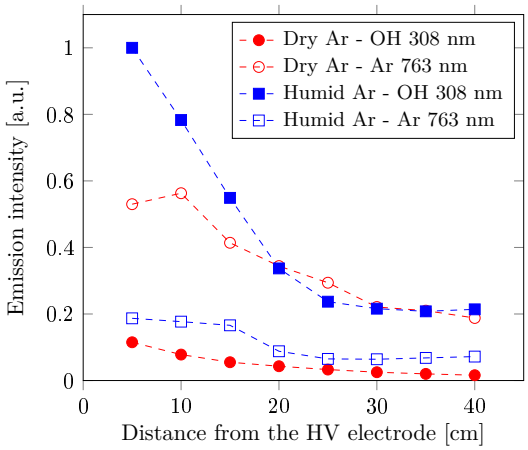

Figure 5.7: Optical emission measurements of the OH radical band (maximum emission intensity at 308.2 nm, full symbols, grating 2400 lines/mm), maximum of argon emission (763.6 nm, hollow symbols, grating 1800 lines/mm), in dry (red) and humid argon (blue) plasma with increasing distance from the source electrode. The peak voltage was adjusted to maintain the average current intensity value at the counter electrode constant in the presence of the fiber optic near the propagating discharge. Data are normalized to the maximum emission intensity of OH in humid argon at 5 cm.

30 kV. This water vapor concentration is slightly below the optimum value, above which increasing the water vapor content does not lead to an increase in the OH line intensity, but on the contrary leads to its decrease. This result was previously observed and was found to be caused by quenching mechanisms that become the dominant phenomena in high water vapor concentration conditions [195, 196] as per:

$$OH^*(A^2\Sigma^+) + H_2O \rightarrow OH(X^2\Pi) + H_2O \tag{5.3}$$

The presence of humidity in the feed gas has thus a dual benefit of producing both reactive OH radicals and UV-B emission.

The time-resolved and spatial distribution of the OH radical emission intensity along the length of the quartz tube was measured by recording the optical emission centered at 308 nm (305–311 nm range). Figure 5.8 shows the evolution of OH emission intensity profile with time (the time delay from a command pulse rise) for 9 different light collecting positions along the tube. The time delay of the OH emission maxima with respect to the voltage front rise increases with the enlarging distance between the high voltage electrode and the light collecting position, so confirming a streamer type propagation mechanism, and allows for calculation of the instantaneous propagation velocity (Figure 5.9). The obtained values are again in good agreement with the average velocity values previously calculated using the electrical measurements (Figure 5.4) and with velocity values from literature with argon gas [61], and helium gas [197, 198]. The values of propagation velocity obtained here in humid argon are lower than those obtained in dry argon conditions. As an example, at the fixed applied voltage (26.5 kV), the average propagation velocity was reduced by 8% for a

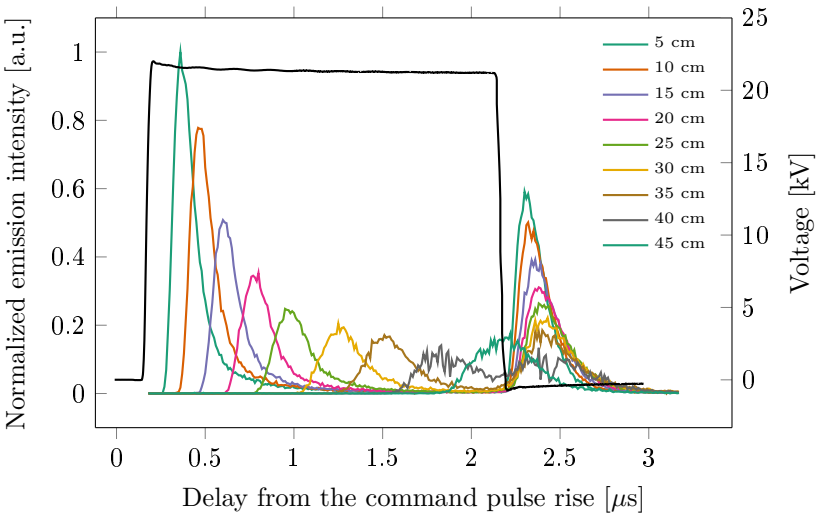

Figure 5.8: Excited $OH^*[A^2\Sigma^+ - X^2\Pi]$ radicals emission (305-311 nm) relative intensity profile evolution with time for different light collecting positions along the tube (distance from the needle electrode: 5, 10, 15, 20, 25, 30, 35, 40, 45 cm) and synchronized applied voltage signal. Humid argon (760 ppm H_2O, 4.7 slm)

10 cm propagation length and up to 30% for a 35 cm propagation length when discharge feed gas was changed from dry to humid argon. This is attributed to electron energy losses in dissociative, vibrational, rotational and attachment mechanisms with water.

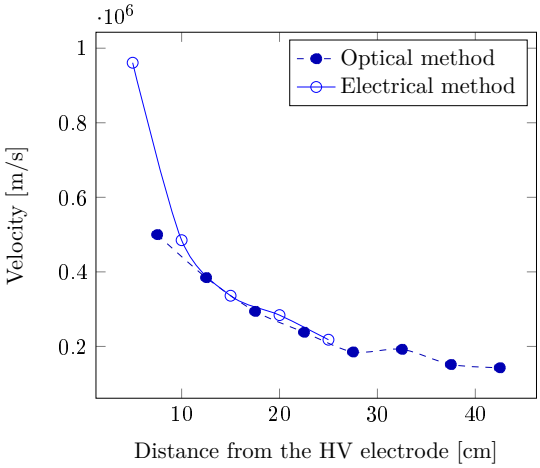

Figure 5.9: Discharge instantaneous velocity of propagation in argon with water vapor (calculated from a fit of the data of Figure 5.8) and compared to the velocity in argon with water vapor obtained from electrical measurement (data from Figure 5.4).

Another interesting feature is that for each measurement location, the second emission maximum occurs just after the applied voltage drop (Figure 5.8 at 2.4 μs), suggesting a back discharge mechanism. This second emission peak also exhibits propagation mechanisms, but with higher velocity (4 to 6 times higher), and it accounts for a significant part of the overall emission intensity per propagation event: from 40 to 50% of the integrated relative intensity

according to the location. This integrated relative intensity per discharge event corresponds to a relative dose per discharge event which exponentially decreases with increasing distance from the HV needle electrode (Figure 5.10). According to this exponential decrease of the emission with the distance, the bacteria sample located at 2 cm is exposed to a dose 4.2-times higher than the bacteria sample located at 44 cm from the HV electrode.

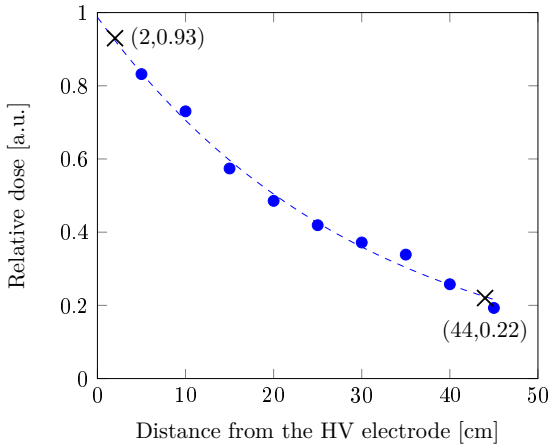

Figure 5.10: Relative UV-B dose (305-311 nm) per discharge event calculated for each position from the data of Figure 5.8, including the second emission maximum at 2.4 μs. Relative dose one corresponds to the relative dose at the tip of the HV electrode.

5.3.3 Temperature

Measurements of the gas temperature are required because any considerable increase of the temperature can play an important biocidal role.

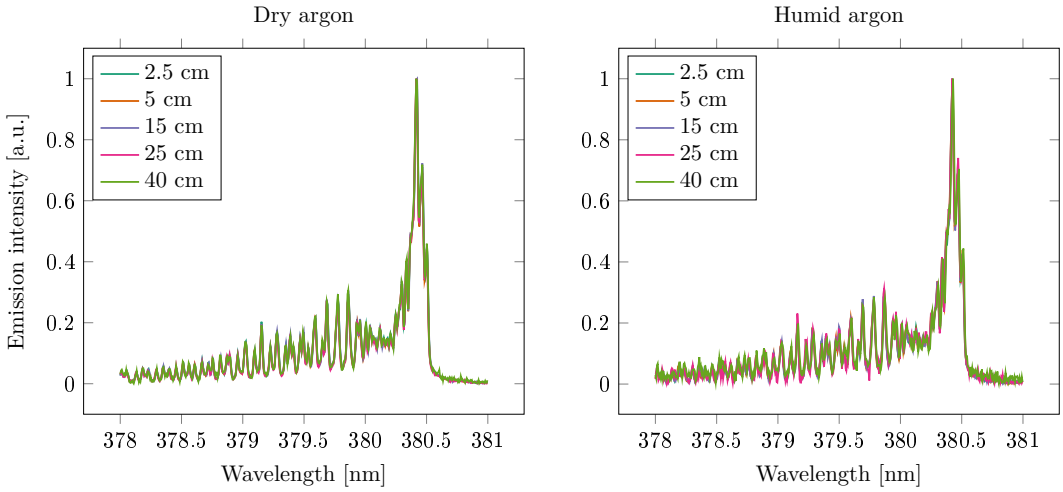

Figure 5.11: Optical emission spectra of the N_2 second positive system between 378 and 381 nm (0-2 band) measured at various locations (2.5, 5, 15, 25, and 40 cm from the needle electrode, overlaid) along the quartz tube in dry argon and humid argon (760 ppm H_2O).

Therefore, the rotational temperature in the discharge channel was measured by emission spectroscopy of the 2nd positive N_2 system, and found to be 450 ± 50 K for both dry and humid argon gas conditions at all measurement locations between 2.5 and 40 cm from the needle electrode (Figure 5.11). This rotational (i.e. gas) temperature was a maximum value measured over a 600-ns time interval for a discharge phenomenon with overall duration of 2–2.2 μs and a 500 pulses/s repetition rate.

We also measured the mean gas temperature increase in the bulk gas phase (at the tube outlet) and on the outer surface of the quartz tube at 2 and 44 cm from the HV electrode in both dry and humid argon. A maximum temperature elevation of 2.2°C (Figure 5.12 a) was recorded for the post-discharge argon flow (at the counter electrode), while a maximum increase of 4.0°C (Figure 5.12 b) was measured on the external tube surface at 2 cm after 20 min of discharge operation in humid argon. The presence of water traces in the argon gas required a higher applied voltage to propagate the discharge over the same distance and resulted in a higher measured temperature at the quartz surface. The increase of the surface temperature during the plasma treatment was smaller at higher distances from the source electrode. As the plasma process was carried out at room temperature (25°C), the measured temperature always remained below 30°C.

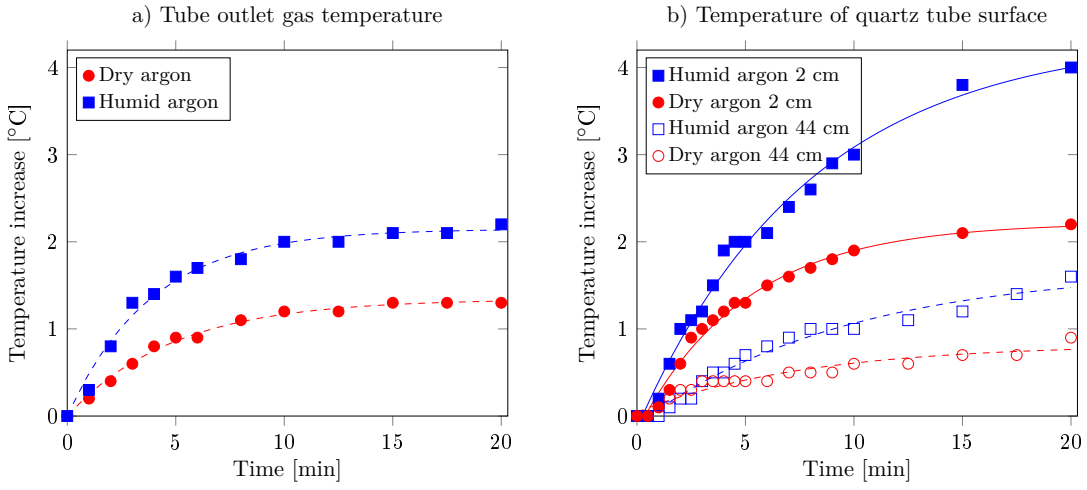

Figure 5.12: Absolute temperature increase over treatment times of: a) the feed gas measured at the counter electrode in dry (red) and humid argon (blue), and b) quartz tube surface at 2 (full symbols) and 44 cm (hollow symbols) from the HV electrode, with one phase exponential fits (lines).

5.3.4 Bactericidal effect

We investigated the decontamination efficiency of the pulsed corona atmospheric pressure argon plasma at the inner surfaces of the quartz tube. Starting from a population of $\sim 10^6$ cultivable *E. coli* DH-1 cells, we evaluated the bactericidal effect of the plasma for samples placed inside the tube at two locations, 2 cm and 44 cm from the HV needle electrode. The

survival curves of bacteria in argon (a) or argon with 760 ppm water vapor (b) plasma are presented in Figure 5.13. Although dry or humid (760 ppm water vapor) argon may cause desiccation, our control measurements showed they had no significant effect on bacterial survival in our experiments (two-tailed Wilcoxon matched-pairs signed rank test; p value = 0.25). The same bacterial strain and method was used for testing decontamination efficiency of DC corona discharge in air (Figure 4.10).

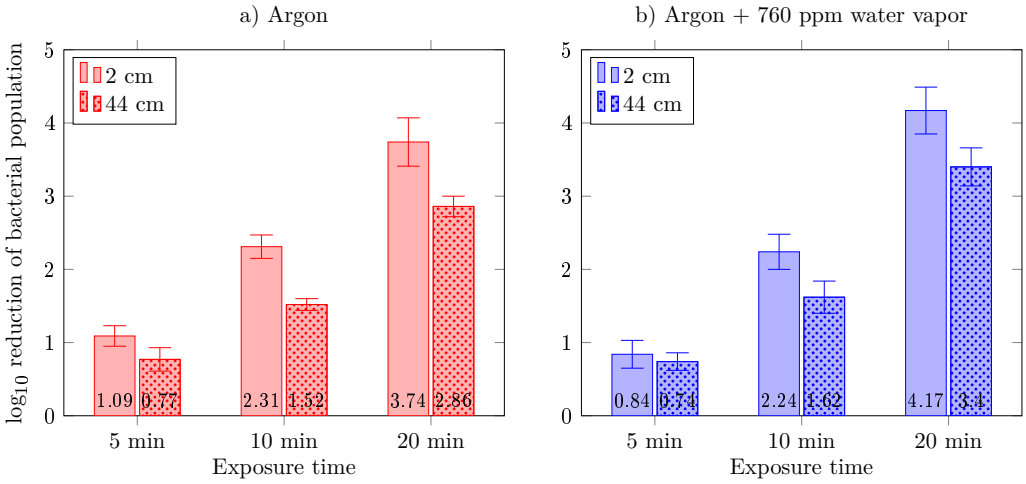

Figure 5.13: Log_{10} reduction of *E. coli* bacterial population after plasma treatment in dry argon and argon with 720 ppm of water, HV frequency 500 Hz (mean±SEM).

The plasma in dry argon reduced the bacterial population by up to 3.8 $\log_{10}$ after a 20 min exposure for the sample located 2 cm from the needle electrode. For the sample at 44 cm distance, the reduction in viability was 2.9 $\log_{10}$ after 20 min. Two intermediate time points were also measured, with smaller differences between the 2 and 44 cm samples: a 5 min exposure reduced the bacterial population by 0.8 and 1.1 $\log_{10}$ and a 10 min exposure by 1.5 and 2.3 $\log_{10}$, for the 44 and 2 cm bacterial samples, respectively.

In the humid argon plasmas, a 0.8 $\log_{10}$ reduction in bacteria viability was observed after a 5 min exposure for both sample locations. After a 10 min exposure, we obtained reductions of 1.5 and 2.2 $\log_{10}$ for 44 and 2 cm bacterial samples, respectively. Up to 4.2 $\log_{10}$ reduction was reached after a 20 min exposure for the sample at 2 cm, and 3.4 $\log_{10}$ for the 44 cm distance. The decrease in the bactericidal activity over the tube length (Figure 5.13 b) is likely related to a decrease in the concentration of OH radicals and associated UV-B radiation.

Higher HV pulse frequency 1000 Hz

To improve bio-decontamination efficiency, the frequency of voltage pulses was increased from 500 to 1000 Hz. Figure 5.14 shows logarithmic reduction for planktonic *E. coli*; as the

average of three experiments with initial concentration 10^6 cfu/ml, one with 10^5 cfu/ml and one with 10^4 cfu/ml.

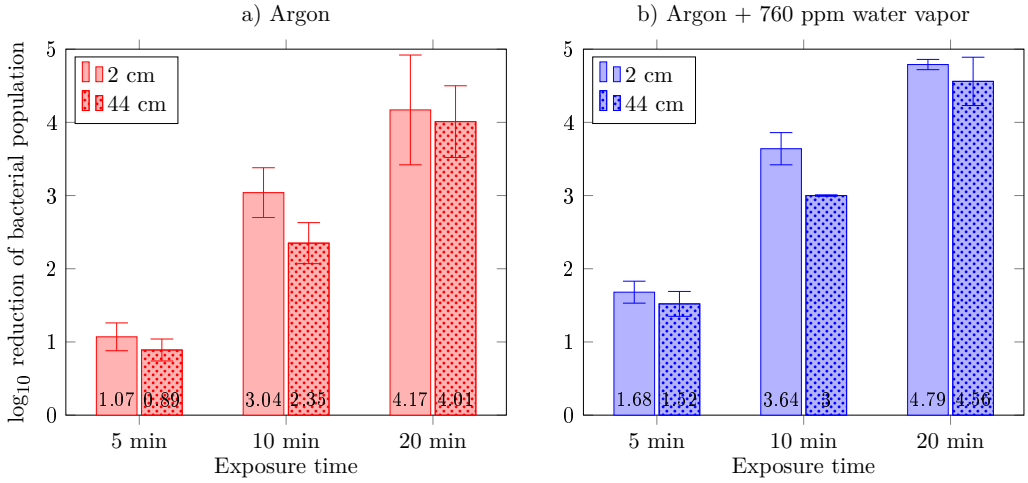

Figure 5.14: Log_{10} reduction of *E. coli* bacterial population after plasma treatment in a) dry argon and b) argon with 720 ppm of water vapor, HV pulse frequency 1 kHz (mean±SEM).

The reduction of bacterial concentration was enhanced in all exposure times in comparison with lower pulse frequency (500 Hz, Figure 5.13), we reached 4 $\log_{10}$ reduction within 20 min at 44 cm location in dry argon and 4.6 $\log_{10}$ with humid argon. This is significant enhancement because in 10 min with 1000 Hz, the decontamination efficiency is only a half $\log_{10}$ below the efficiency reached within 20 min treatment with 500 Hz frequency. In addition, the difference in reduction between 2 and 44 cm positions is less significant with 1 kHz than with 500 Hz.

Dried samples with oxygen admixture to the gas flow

To improve the bio decontamination efficiency of the discharge we added 1000 ppm admixture of oxygen gas into our gas. The bacterial samples were dried prior to the experiment to limit contamination of the gas flow with additional water vapor. The initial concentration of bacteria was $1.05 \pm 0.07 \times 10^8$ cfu/ml. The comparison of bio-decontamination efficiencies between argon and argon with O_2, and humid argon and humid argon with O_2 admixture is presented in Figure 5.15.

There was not a significant difference between the bactericidal efficiency of the discharge in the argon flow (with or without water vapor) with or without O_2 admixture (Mann-Whitney test, p=0.05). As was previously observed, the discharge in humid argon was much more effective.

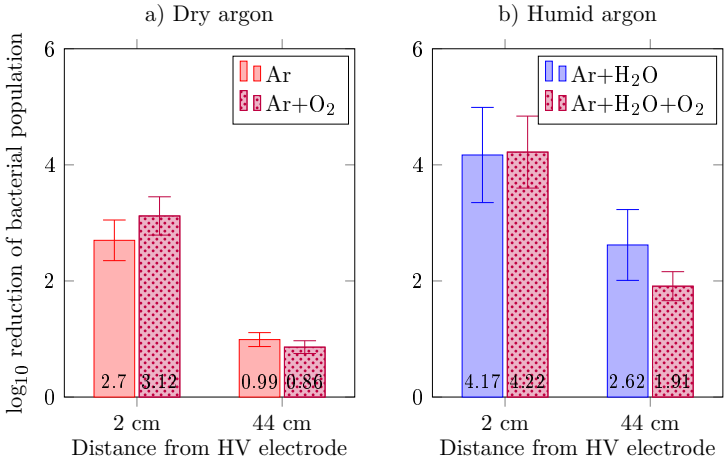

Figure 5.15: Log_{10} reduction of *E. coli* bacterial population after 30 min of the plasma treatment in a) dry argon and b) argon with 720 ppm of water vapor, without or with admixture of oxygen, HV pulse frequency was 500 Hz (mean±SEM), 3 repetitions for each experiment, samples were dried.

Sample and gas admixture water content

The water content (in argon gas or in the bacterial sample, dried or not) was an important parameter in our experiments since it was shown to be a key parameter that strongly influenced the generation of reactive species by atmospheric-pressure argon plasma jet and its effect on cells [16]. In order to get better understanding of the factors affecting plasma bactericidal effect, several combinations of humid/dry argon gas and liquid/dried bacterial samples were investigated over time (Figure 5.16). The bactericidal effect of the treatment is presented in terms of "reduction factor", defined as: $\log_{10}(\mathrm{N}_0/\mathrm{N})$ where N_0 is the control sample CFU and N the sample after plasma treatment CFU. First, let us focus on the samples located inside the tube. As expected, increased treatment times resulted in increased bio-decontamination efficiency. In general, when comparing treatments of liquid versus dried samples, we measured greater decontamination efficiency on dry samples for both positions (2 cm and 44 cm). For example, up to a 5.5 reduction factor ($\log_{10}$ bacterial reduction) was achieved in the case of humid argon with dry samples 2 cm from the needle electrode and 20 min exposure. In the same conditions, a 4.9 reduction factor was obtained at 44 cm. At 20 min exposure time, comparison between humid and dry argon plasma demonstrated greater or equal decontamination efficiency for humid argon. The best decontamination efficiency was obtained in humid argon plasma on dried samples.

Similarly, we measured the bactericidal effect of UV-B plasma radiation alone on liquid and dried samples located on the outer surface of the quartz tube (OUT samples in Figure 5.16) for argon plasmas produced with both dry and humid feed gas.

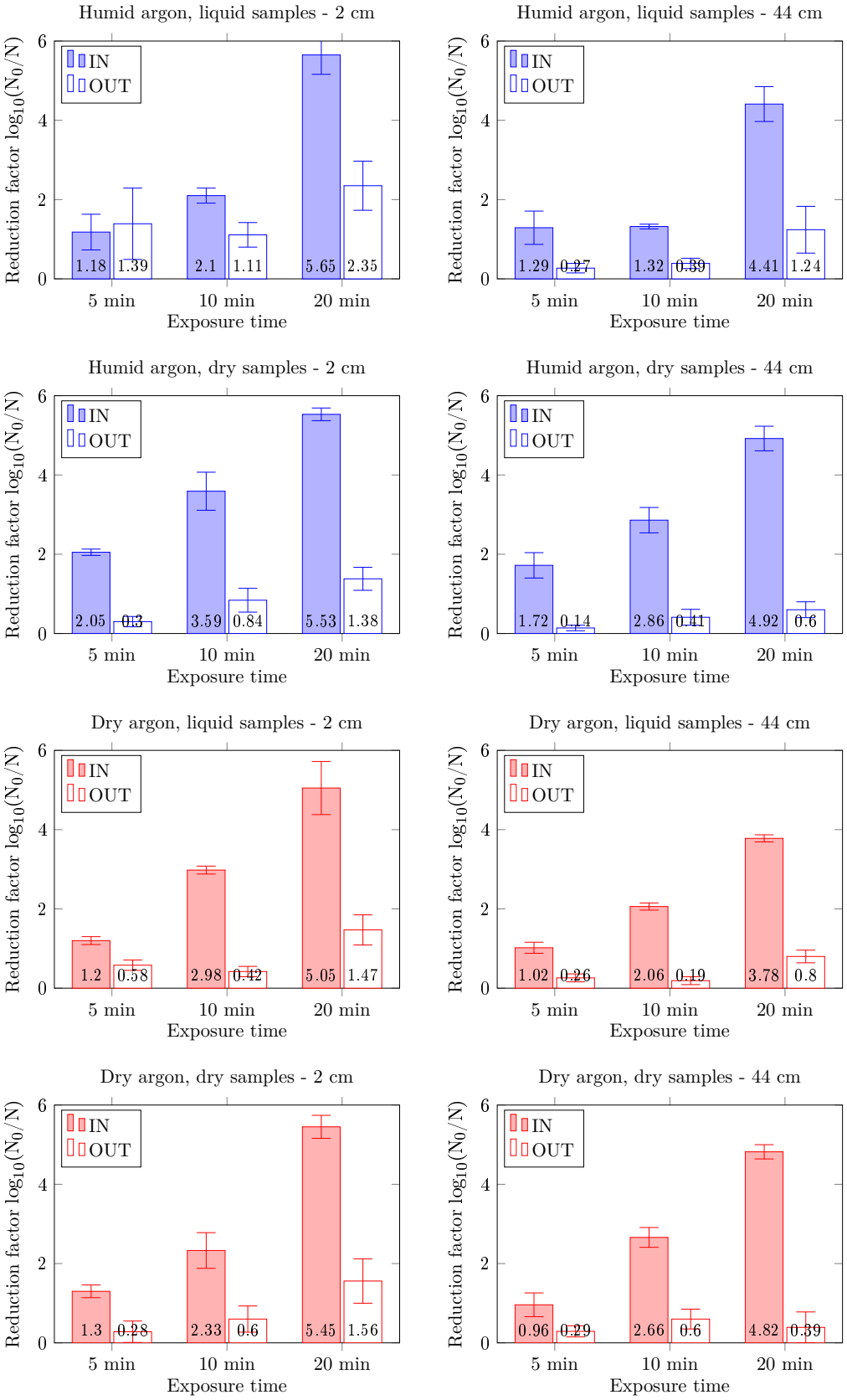

Figure 5.16: Reduction factor measured after the argon plasma treatment (IN, filled bars) and the argon plasma-generated UV-B radiation only (OUT, white bars) for increasing exposure times at 2 (left panels) and 44 cm (right panels) in various humidity conditions (feed gas and bacterial sample). Reduction factor is $\log_{10}(N_0/N)$ where N_0 is the CFU control sample and N the sample after plasma treatment. Assays were carried out in triplicates (except for humid argon/liquid sample in duplicates at 5 and 20 min). Graphed: mean ± SEM.

As expected from the OES results acquired at different locations along the discharge propagation length (Figure 5.8 and 5.10), UV-B emission is more intense closer to the HV electrode and generally has a greater biocidal efficiency at 2 cm than at 44 cm in all conditions tested. The biocidal activity of emission at 308 nm is cumulative, and the decontamination efficiency tends to increase with treatment time in all conditions, reaching a maximum efficiency of 2.35 reduction factor for 20 min treatment of a liquid sample with a humid argon feed gas at 2 cm. The discharge in humid argon with a liquid sample, while not the most efficient when looking at the decontamination efficiency of the overall plasma treatment process (inside tube), generated the best efficiency of decontamination for UV-B radiation alone (outside tube).

5.3.5 The effect of hydrogen peroxide

The impact of H_2O_2 was investigated and its concentration measured in five 10 μl water droplets exposed to a humid argon discharge inside the tube, similar to as described in *Dodet et al.* [193].

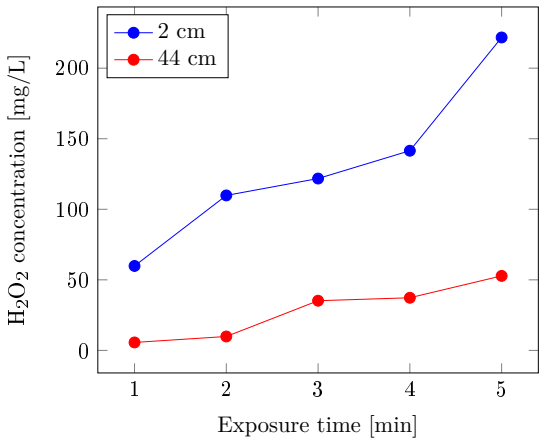

Figure 5.17: H_2O_2 concentration at 2 and 44 cm from HV electrode produced in water droplets ($5 \times 10\mu$L) over increasing exposure times to the plasma discharge in humid argon (760 ppm H_2O). Experiments were carried out in triplicates.

Due to evaporation, exposure times greater than 5 min did not allow for the recovery of sufficient liquid volume (10 μl), and thus prevented measurements of H_2O_2 accumulation in the liquid phase (Figure 5.17). The reduction of volume through desiccation concentrates H_2O_2 in the liquid phase, resulting in a non-linear concentration with time. As shown in Figure 5.17, with 760 ppm water vapor content, H_2O_2 accumulated faster and in higher concentration near the HV electrode (2 cm distance), where the surface temperature was slightly higher (Figure 5.12 b). For a 5 min exposure time, 222 mg/l H_2O_2 was measured at 2 cm and 53 mg/l H_2O_2 at 44 cm.

5.4 Discussion

Even though bactericidal, cytotoxic, fragmentation, and denaturation effects have been shown to be stronger in air plasmas such as transient spark than in noble gas plasma jets [55], the latter allow propagating the discharge in the insulating tube and prevents the formation of species leading to the degradation of polymers (ozone, nitrogen oxides, nitric acid). The overall objective of this work was to identify various factors accounting for the bactericidal effect of the non-thermal atmospheric pressure argon plasma generated by pulsed corona discharge propagated over long distance on the inner walls of an insulating tube (treatment of the inner walls of long tubes, such as those used for colonoscopy). The biocidal factors generally invoked were UV emission and oxidative chemical species. Damage to DNA may occur through chemical modification (alkylation or oxidation), cross-linking, or base removal such as depurination [199, 200]. The efficiency of the plasma is based on a combination of these factors [201]. Therefore, the bacterial cell death likely resulted from the accumulation of irreversible oxidative damage to the membrane layers, proteins, and DNA caused by the synergy of the plasma biocidal factors [202–204]. Additional sources of stress generated by the plasma process should be considered, such as damage from desiccation and thermal stresses which could contribute to the overall decontamination effect.

5.4.1 Temperature and desiccation

The argon pulsed plasma process is carried out at room temperature. The steady state temperatures measured on the quartz surface and in the gas flow at the outlet always remained within the permissive range for the bacterial species. In the case of *E. coli* used here as the model bacteria, the measured temperature of 30°C would not induce a thermal shock response (temperature step with a fast rise). In addition, this temperature is below the optimal temperature of growth for this bacterium. Based on the absence of significant bacterial viability loss in the control treatments, the desiccation effects of the gas flow are not significant bactericidal factors by themselves either. Nevertheless, desiccation is enhanced during plasma operation: a hydration loss from phospholipids of the bilayer membrane induces membrane separation, leading to protein aggregation, and upon rehydration, membrane modifications leads to solute leakage and loss [205]. Moreover, a fast desiccation can induce protein conformational changes, resulting in dysfunctions in enzymes and electron transport chains that cause free radical accumulation. This can influence the cell's capacity to alleviate the damages generated by the plasma and may result in lipid peroxidation, protein denaturation, and DNA mutation [199].

We also measured local and transient (duration $\sim$2 μs) high temperatures (450$\pm$50 K) at different positions along the path of the discharge propagation. This was done using spectroscopic measurements (Figure 5.11) compared with modeling of the nitrogen second

positive system. The effect of this transient thermal stress on bacteria is unknown. However, the same thermal stress (within the ±50 K error range) was applied on the sample whatever its location inside the tube (2 and 44 cm), and yet, this thermal stress cannot account for the difference in decontamination efficiency observed between these two locations, so its contribution to the overall bactericidal effect can be neglected. It can be added that the surface discharges, during their propagation, may induce transient electric field changes on the cell membranes but this effect does not seem important from our results and was not further studied here.

UV emission

Emissive argon species and hydroxyl radicals generate UV-A, and -B emissions that inflict further damage on cells. While DNA is the primary target for UV-induced damage [206,207], other UV-absorbing cell components can be targeted as well, such as proteins. The high energy photons from the short-wavelength UV radiation can lead to singlet oxygen and free radical formation when absorbed by molecules of chromophores, and can generate molecular singlet oxygen O_2 $^1\Delta_g$ ($^1O_2$) through type II photosensitization reactions that will target membranes and other cellular components [208,209]. Furthermore, a single photon impact on the DNA molecule may have a lethal effect at the cellular level. Most damage to the DNA can be attributed to UV-B (280–315 nm) emission that is absorbed by cellular DNA. UV-A (315–400 nm), while less potent, may generate indirect damage to the DNA via photoreactions and photosensitization [210]. UV-induced DNA modifications are presented by pyrimidine dimers of thymine-thymine or thymine-cytosine [211]. These lesions will result in DNA helix distortion and block transcription and replication that can generate punctual mutations and lead to cell death [212, 213].

In Figure 5.10, the relative UV-B dose (305-311 nm) per discharge event calculated for each sample position along the tube is presented. This relative dose can be extrapolated to calculate an accumulated relative UV-B dose for the two different positions at different treatment durations. This accumulated relative dose (now normalized to the 2 cm, 20 minute treatment) is then used as the abscissa for Figure 5.18. In Figure 5.18 a, the reduction factor of bacteria samples deposited onto the external surface of the quartz tube (OUT samples: only submitted to the plasma UV-B emission) increases with the accumulated relative UV-B dose. The most important result extracted from data in Figure 5.18 a is that no major difference in the trend may be discerned between points at the two positions (open and closed symbols), which means that the bactericidal efficiency on the OUT samples only depends on the relative UV-B dose. From a qualitative point of view, the observed tendency is in agreement with *E. coli* (wild type and mutants) UV irradiation studies [214]. Another interesting point is that greater efficiency is observed for liquid samples as compared to dried ones (square symbols compared to circles). The influence of the sample form (dried or liquid)

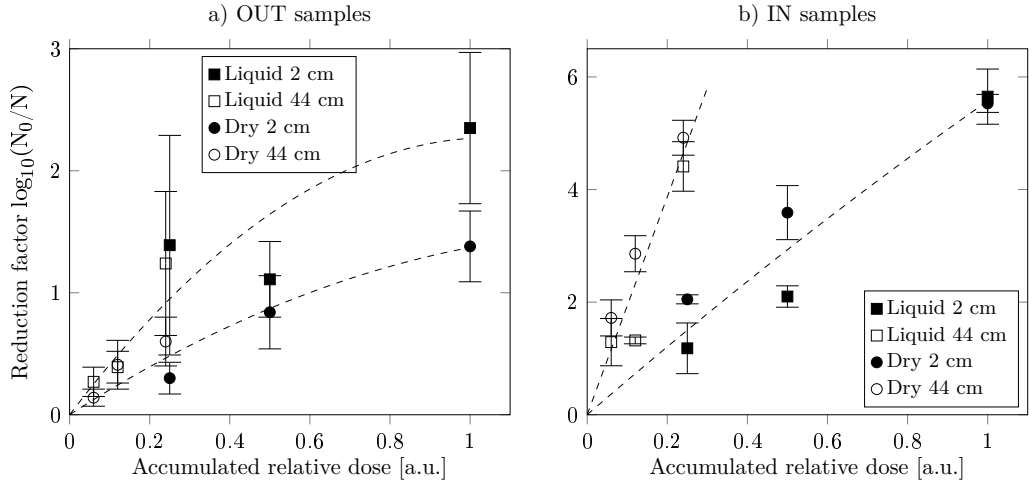

Figure 5.18: Reduction factor (Figure 5.16) as a function of the calculated accumulated relative dose (with regard to the samples position IN and OUT the tube and the exposure time) from humid argon plasma. Dashed lines are only guides for the eye. Graphed: mean ± SEM.

could be interpreted as due to a shadow effect previously invoked for the UV irradiation of multilayer microorganism samples [215], which occurs more in the dried samples.

In the case of a direct exposure of bacteria to the plasma (IN samples deposited inside the tube - Figure 5.18 b), the reduction factor is no longer influenced by the form of the sample, but is strongly dependent on the sample location: for a given value of the accumulated relative UV-B dose (e.g. 0.25), the reduction factor at 2 cm is 3 orders of magnitude lower than at 44 cm, either for dry and liquid samples. When focusing on bacteria exposed to the plasma for the same duration, e.g. 20 min (open symbols at 0.25 accum. relative dose and closed symbols at 1.0 accum. relative dose), a similar reduction factor was obtained for 4-times higher dose received by the 2 cm sample (than the 44 cm sample). The bactericidal decontamination mechanism in the IN samples is therefore not governed by the accumulated UV-B irradiation dose but other stress factors dominate. It was observed that exposure of DNA to radiation from noble gas radiofrequency discharge did not lead to single strand nor double strand break [216]. Although, direct contact of DNA with a helium plasma needle (propagating in open air) induced single strand break [217], and exposure to humid argon post-discharge induced DNA fragmentation [34].

Another potential biocidal factor is VUV radiation (200–10 nm) from the second continuum of the argon excimer Ar_2^* (maximum intensity at 126 nm). Ar_2^* results from a three-body collision mechanism of two ground state Ar atoms with an excited Ar^* atom. This type of radiation has a low penetration depth in air, but in the case of an argon atmosphere the penetration depth is much longer because the excimer radiation is not subject to self-absorption [218]. The rare gas excimer emissions produce photons with energies that can break most chemical bonds and initiate chemical reactions [219]. The maximum intensity of

the argon excimer emission at 126 nm corresponds to energy of 9.84 eV, which is sufficient to cause photodissociation of water (4.77 eV being the dissociation energy for O – H bond). The quenching of Ar^* by H_2O molecules, as seen by the reduction of the argon emission intensity (700–850 nm) in the presence of water (Figure 5.6), should lead to a decrease in the excimer second continuum emission intensity. Therefore, the bactericidal effect of VUV emission should be greater in dry argon and might be relatively limited in our most efficient plasma treatment settings that involve humid argon feed gas. In the specific case of dry argon and dried samples, the VUV emission could be considered as important for the samples placed inside the tube, and may contribute to the rather high decontamination efficiency shown in Figure 5.16 d.

This VUV emission could also decrease or be quenched because of gas impurities, especially oxygen and nitrogen species [33, 219]. VUV/UV emission by itself can cause damage even on spores, but its biocidal effectiveness varies markedly with wavelength and power densities [28].

Samples placed onto the outer surface of the tube cannot be submitted to the VUV emission because of its absorption in the tube material (quartz). Results show that the higher the water vapor content, the higher the decontamination efficiency (Figure 5.16 a). During experiments with liquid samples placed outside of the quartz tube, there were liquid samples placed inside, too. Through evaporation the inner samples contributed to an increase in the water vapor concentration inside the tube; and thus to an increase (at least for a period of time) in the OH emission intensity (UV-B) received by the outer samples.

Results obtained for samples placed inside the tube show that the conditions providing the greatest bactericidal effect are the humid argon discharge on dried samples, considering samples located 44 cm from the HV electrode. The H_2O molecules at a constant concentration in the argon gas generate both UV radiation and reactive species (i.e. OH in ground and excited states) that directly affect the dried bacterial cells. In the case of liquid samples, there is a dilution of the reactive species and so a delay in the bactericidal effect compared to the dried samples.

5.4.2 Reactive oxygen species

Plasma generated in humid gases is known to produce hydrogen peroxide [193], the most stable reactive species generated by this process. The production rate of H_2O_2 is dependent upon the water content of the plasma environment (feed gas and samples) that determines the production of OH radicals, which are precursors of H_2O_2, and the degree of conversion of water into H_2 and O_2 [195]. Traces of hydrogen peroxide were accumulated in water after the plasma process. The impact of hydrogen peroxide on bacterial survival was examined. The incubation of bacterial cells in a solution of 222 mg/l H_2O_2 for a 5 min period, representing the same H_2O_2 concentration as the one measured in the wet sample at 2 cm

and 5 min plasma exposure (Figure 5.17), resulted in only 0.1 $\log_{10}$ reduction of bacterial viability, whereas a 5 min exposure time to the plasma (humid argon/liquid sample) led to a 1.2-1.3 $\log_{10}$ reduction (for both 2 cm and 44 cm positions). We can thus conclude that H_2O_2 alone is not responsible for significant bacterial population reduction, although longer treatment times may affect the dryness of the sample and may interfere or amplify this effect in our current procedures. Nevertheless, higher hydrogen peroxide concentrations than those presented in Figure 5.17 are expected since H_2O_2 accumulates in liquid phase with time until the point when advanced evaporation takes place and when bacteria are only submitted to gas phase H_2O_2 (low concentration). There should be an optimum exposure time corresponding to a maximum liquid phase H_2O_2 concentration. At this point before full desiccation, the bactericidal effect of hydrogen peroxide cannot be excluded, especially in combination with UV light.

Despite the low concentrations of formed H_2O_2 were not shown to have an important decontamination effect, H_2O_2 precursors, gas-phase OH radicals are known to be extremely reactive although very short-lived. They can be one of the major decontamination factors for the IN samples where the effect of UV-B was not found dominant.

As with the other stressors of argon plasma studied here, synergistic effects may occur allowing an efficient decontamination of bacterial cells even with stressors in limited concentrations. One of these may be the *in-situ* production of OH radicals by UV photolysis of hydrogen peroxide [220].

5.5 Summary

This chapter reports on biocidal results obtained with an atmospheric pressure non-thermal pulsed corona discharge plasma source adapted to the treatment of the inner surfaces of thin long tubes such as endoscope ducts or catheters. We report the full propagation of a streamer-like discharge inside a 2 mm diameter silicon tube over a distance of one meter. We investigated the bactericidal factors accounting for the decontamination effects, in particular the UV-B emission, in a quartz tube adapted to bacteria sample treatment and recovery and to optical emission diagnostics. To obtain a large enough mortality response to UV light only exposure, we chose to use a (UV-sensitive) recA- *E. coli* strain.

The discharge feed gas was argon, (dry or with water vapor admixture). Although the treatment duration was longer than other non-thermal atmospheric pressure plasmas using air (which also produce harmful and stable species such as nitrogen oxides and ozone), the investigated plasma process resulted in, using this *E. coli* strain, $\approx 5 \log_{10}$ reduction from a 10^6 initial population for samples placed 44 cm away from the HV electrode and 20 minute exposure time.

Among the factors accounting for the observed bactericidal activity, it was determined

that desiccation did not lead to strong population reduction (less than $1\,\log_{10}$). For the selected operating conditions, the temperature measured on the tube wall did not exceed 29°C (at a 25°C room temperature) and thus should not be an important stress factor either. On the other hand, short-duration ($\approx 2\,\mu$s) temperature increases were measured in the discharge channel during its propagation on the inner surface of the tube (up to 450 ± 50 K). Given that (i) the temperature was found to be constant (within the error range) with distance, and (ii) the decontamination efficiency was, for a given exposure time, strongly dependent on the sample location; it was concluded that this transient heating did not play a major role in the decontamination.

By calculating the accumulated relative UV-B dose and comparing samples placed either inside or outside the quartz tube, it was determined that increased bacteria population reduction observed inside the tube may be either due to a direct attack by reactive species such as OH or by synergistic effects such as UV hydrolysis of the formed hydrogen peroxide. The hydrogen peroxide production and its impact on bacterial survival were examined for short exposure duration. Bacteria incubation in a H_2O_2 solution of the same and higher concentrations as those measured in wet samples led to a negligible population reduction. It is thus concluded that hydrogen peroxide by itself is not responsible for significant bacterial reduction in these conditions. However, higher hydrogen peroxide concentrations are expected with longer treatment times, and therefore a bactericidal effect of hydrogen peroxide cannot be completely excluded.

OH production depends on water vapor content, and the latter can come from both liquid sample evaporation and/or addition of water vapor to the feed gas. This point was investigated, and from a practical point of view it was found that it is more effective to dry the surfaces prior to exposure to the plasma process and to add water vapor to the discharge feed gas.

6 Atmospheric pressure argon jet in argon atmosphere

6.1 Introduction

Plasma jets are convenient and widely used plasma sources for bio-decontamination of surfaces - solid or liquid (this was detailed in the chapter 3 and Table 3.1). Working gas is usually a noble gas, often helium or argon with admixtures of other gases such as are oxygen, nitrogen, and water vapor. In the case of plasma jets propagated into open air, the use of helium as a discharge feed gas is problematic, because it is lighter than air and therefore does not reach distant samples when the discharge is off (lack of electric wind, problem for control samples [221]). The advantage of argon in comparison with helium is that it is heavier than air and much cheaper. The jet in this chapter is the continuation of our work with long discharge tube. Argon jet was more convenient and practical for treatment of the biofilms on cover glasses for subsequent analysis with CLSM.

6.2 Materials and methods

In this section we will describe our argon plasma jet and methods used for its characterization. We will also detail methods used for biofilm growth and its subsequent analysis after plasma treatment.

6.2.1 Argon DBD plasma jet

Plasma source used for experiments was an argon dielectric barrier discharge (DBD) jet sustained in argon atmosphere at atmospheric pressure (Figure 6.1). High-voltage (HV) power supply (waveform shown in Figure 6.2) was connected to a blunt stainless steel rod electrode (2 mm in diameter), inserted in Pyrex glass tube (10 cm long, 3 mm inner diameter). A grounded electrode consisted of two copper strips connected with copper mesh placed on the outside surface of the glass tube (Figure 6.1 a). Discharge was ignited in the gap between HV electrode and the dielectric tube inner surface. Three different gas mixtures were used during the experiments: argon (dry argon), 760 ppm of water vapor admixed to the argon flow (humid argon), and argon fully saturated with water vapor at room temperature; the flow rate of gases flowing inside the tube was two standard liters per minute (slm). The jet was enclosed inside the box so the gas mixture flowing from the jet tube and the atmosphere

inside the box were of the same composition. All measurements were done at atmospheric pressure, two openings in the box back wall allowed the gas to exit (Figure 6.1 b).

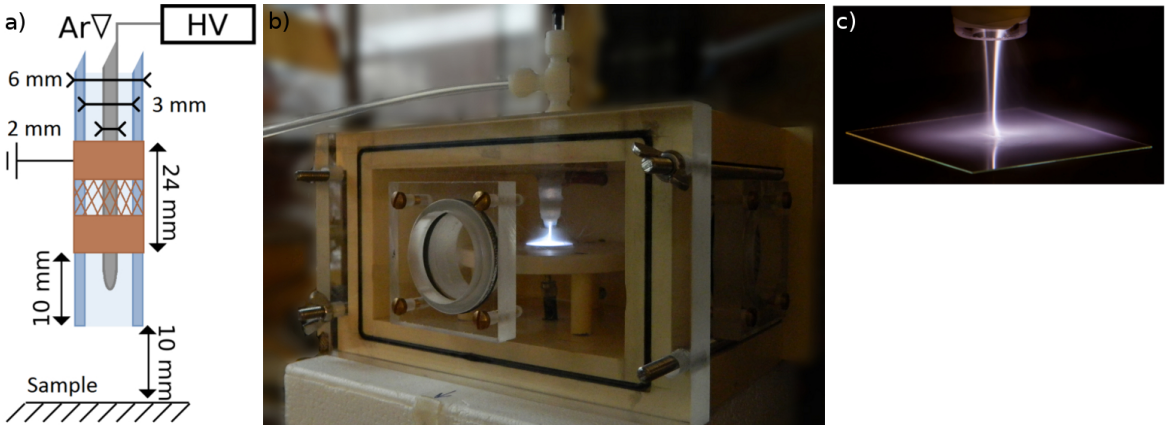

Figure 6.1: DBD argon jet set up for bacteria treatment. a) HV electrode consists of stainless steel rod centered in a 10 cm long Pyrex tube (3 mm inner diameter), two copper strips (orange) connected with copper mesh placed on the outside surface of the Pyrex tube form a grounded electrode. b) The photograph of the box with the jet in controlled atmosphere. c) Close up of the plasma jet during biological sample treatment with the microscopy cover glass with the biofilm sample 1 cm from the jet nozzle.

Three settings were used for biological decontamination assays: dry argon with peak to peak voltage of 8.1 kV and mean power of 1.2–1.4 W, humid argon (760 ppm of water vapor admixture to argon flow) with peak to peak voltage of 11.7 kV and mean power of 4.2–4.4 W, and argon saturated with water vapor with peak to peak voltage of 12.2 kV and mean power of 4.8–5.0 W. The HV probe (Tektronix P6015A 1 V:1 000 V - 75 MHz) connected to the needle electrode and a fast rise current transformer (Tektronix CT-2 1 mV:1 mA - 200 MHz) connected to the grounded counter electrode were used for voltage and current measurements, respectively. The electrical signals were recorded with a LeCroy WaveRunner 62 Xi digital oscilloscope (600 MHz - 10 GS/s).

6.2.2 Spectroscopy

OES: for non-quantitative optical emission spectroscopy of the discharge, light was collected directly by optical fiber in a proximity to the discharge through an opening on the side of the box, or indirectly through a window (Figure 6.1). The 200 – 850 nm range was measured using a Spectrometer UV VIS LT 12 (StellarNet INC.). One spectrum results from the averaging of 10 spectra captured during a 200 – 1000 ms integration time.

OH-PLIF: Planar Laser Induced Fluorescence of OH radicals was measured for saturated argon regime (relative humidity >95%, ambient temperature and atmospheric pressure). To detect OH radical presence in the post-discharge gas, it was excited by laser light at

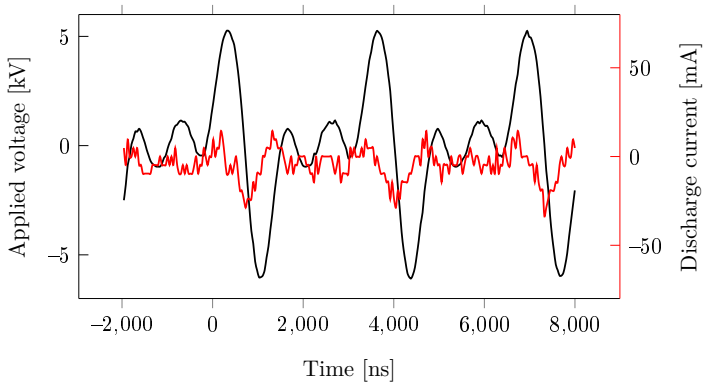

Figure 6.2: Waveform of the dielectric barrier discharge inside the argon jet. The high voltage development over time (——) and time development of the electric current measured on the grounded copper electrode (——), frequency of pulses is 30.2 kHz.

282.935 nm (saturated regime) and fluorescence was collected by an ICCD camera with 10 nm filter centered on 313 nm. This experiment was performed with cooperation with Dr. Florent Sainct (Lab EM2C, CentraleSupélec)

6.2.3 Planktonic bacteria samples

Escherichia coli BW 25113 (the same bacteria and method as used in experiments with DC corona discharges in air, subsection 4.2.4) were cultured overnight at 37°C with agitation (400 rpm). The glass slides (1.8 cm×1.8 cm×18 μm) were contaminated by one 10 μL droplet of the bacterial suspension and dried by argon flow for 5 min.

Plasma treatment and planktonic sample post-treatment

Cover glasses with dried bacterial samples were placed on silicon surface inside the box 1 cm from jet nozzle (Figure 6.1). After plasma treatments, bacterial cells were recovered with 10 repetitive rinsings of the cover glass surface with a total of 100 μl sterile distilled water and immediately resuspended in 1/3 LB. Recovered samples were serially diluted and plated on LB agar or filtered through the membrane (0.45 μm mixed cellulose ester membrane, Millipore), when the high decontamination efficiency was expected. Agar plates were incubated at 37°C overnight, and decontamination efficiency was quantified by colony counting. Control samples were prepared dried in argon flow and then processed the same way as plasma treated samples.

Effect of UV and VUV on planktonic bacteria

To test the effect of UV light from our discharges on bacteria we placed 10 μL of bacteria on quartz or MgF_2 windows. Bacteria were consequently dried by argon flow, and the dried sample windows were flipped upside down so that bacteria were not exposed to the

discharge directly, but only to UV and VUV and some diffusing long lived species. The quartz windows (thickness 3 mm, diameter 25 mm, UQG Optics) were used for evaluation of the effect of UV B. The MgF_2 windows (thickness 3 mm, diameter 25.4 mm, Eksma optics) should transmit the UV B together with VUV.

6.2.4 Biofilm samples

Escherichia coli strain BW 25113 F+ (The protocol for bacterial biofilm cultivation was developed by Dr. Magali Leroy. The same bacteria and method was used in experiments with DC corona discharges in air, subsection 4.2.4) were used for all experiments. Biofilms were grown in homemade 6-well plates with microscopy glass cover slides (1.8 cm × 1.8 cm × 18 μm) at the bottom. Biofilms were seeded with 1/100 dilution of stationary phase culture grown in LB (Miller's) medium at 37°C with agitation, then grown without agitation in M63 growth media, buffered PBS (Phosphate Buffered Saline) pH 7.4, supplemented with 0.1% casamino acids and 1 g/L glucose at 30°C for 48 hours with dilution of planktonic bacteria and replenishment of $7/10^{\text{th}}$ of the growth media at 24 hours.

Plasma treatment and viability assays

Biofilm cultured on microscopy glass cover slides were placed inside the box 1 cm from the jet nozzle (Figure 6.1). Bacterial samples were partially dried for 5 min under argon flow (2 slm) prior to plasma treatment. To ensure humid argon atmosphere inside the box before the treatment by humid argon, the box was purged for 2.5 min with the desired water admixture followed by 10 to 20 min plasma treatment. Control samples were also partially dried for 5 min under argon flow and then exposed solely to the same gas flow and for the same duration as plasma treated samples.

Culturability assay. For CFU counts, bacterial cells in biofilm were recovered by repetitive rinsing with a total of 10 mL of sterile PBS and scratching with a sterile cover glass. Cells were immediately resuspended in 1/3 LB and dispersed by vortexing at maximum speed. Recovered samples were serially diluted or concentrated by filtration through a 0.45 μm mixed cellulose ester membrane (Millipore) when low density was expected, plated on LB agar, incubated at 37°C overnight, and quantified by colony counting.

Confocal laser scanning microscopy (CLSM). For microscopic observations, biofilms were stained with a solution of 5 μmol/L Syto9, 30 μmol/L propidium iodide (PI) from LIVE/DEAD BacLight Bacterial Viability Kit and 10 mg/mL DAPI (4',6-diamidino-2-phenylindole) in PBS pH 7.4, for 25 min in the dark. Samples were immediately mounted, inverted on a hybridization frame (1.5×1.6 cm, Gene Frame 65 μL) with BacLight mounting oil.

Images were acquired on the Leica SP8X inverted confocal laser microscope. Excitation and emission spectra were determined on bacterial samples stained with a single fluorophore (PI or Syto9), with wavelength steps of 10 nm from 470 to 670 nm. The fluorescence excitation and emission matrix were generated using the integrated processing tools of the software. *Z* stack acquisition were performed at 16 bits to allow for signal quantification, 1024×1024×N pixels (pixel size 0.56×0.56×0.34 μm), 400 Hz speed bidirectionally, and sequentially. Observed excitation and emission wavelength (filters) were as follows:

Dye	Color	Excitation λ	Detected λ
PI	Red	525 nm	585–625 nm
Syto9	Green	480 nm	495–535 nm
DAPI	Blue	405 nm	445–485 nm

Table 6.1: The wavelengths used for excitation and detection of three fluorescent dyes with Leica SP8X CLSM.

Image stacks (.lif format) were analyzed using Fiji 1.47v [222] and the LOCI plugin to split channels and *Z* slices, and the integrated signal density of individualized images measured. 3D *Z* stack projections were generated using Icy 1.5v [167].

Crystal violet assay for biofilm biomass evaluation

Biofilm biomass was evaluated using crystal violet staining following established microbiology protocol [168]. The control and plasma-treated biofilms were resealed in 6-well plate after treatment and 200 μL of 0.1% crystal violet (CV) was introduced in each well and incubated for 15 min, after which CV solution was carefully removed by pipetting and biofilms were rinsed 4 times with deionized water. The 6-well plate was dried upside-down for two hours at room temperature. When fully dried, 200 μL of 33% acetic acid was added to each well to solubilize the CV and incubated for 15 min, then recovered and diluted in 1/10 in deionized water and the absorbance was measured at 550 nm.

6.3 Results

We investigated the bactericidal effect of non-thermal atmospheric pressure argon plasma jet on planktonic *E. coli* and its 48 hour-old biofilm on glass surfaces. As described in the subsection 6.2.1, the electrodes set up was encased in a sealed box to control the gas composition at and around the DBD discharge and the sample, with small exhaust holes to maintain atmospheric pressure (Figure 6.1 b). This setting permits the treatment of flat surfaces such as microscopy glass cover slides that allow both for biofilm samples growth

and subsequent microscopy analyses to evaluate the bio-decontamination efficiency of non-thermal atmospheric pressure argon plasma jet on *E. coli* biofilm.

6.3.1 Discharge characterization

Optical emission spectroscopy

We previously established that humid argon plasma was one of the most effective for bio-decontamination of planktonic bacterial samples, the presence of water molecules in the feed gas producing both reactive OH radicals and UV B emission [14]. Here, we investigated the OH and argon emission spectra by optical emission spectroscopy of this plasma set up at different water vapor concentrations in the argon feed gas. In order to test the suitability of our discharge conditions for the production of excited hydroxyl radical (OH^*) and resulting UV B emission (290–320 nm) we increased the water vapor content of our feed gas from 500 up to 3000 ppm while electrical parameters for humid argon were kept identical. Spectra were measured for each condition (Figure 6.3 a) and the dependency of the emission maxima of hydroxyl and argon on water content were plotted (Figure 6.3 b). In our usual conditions of humid argon, 760 ppm water vapor content is above the optimum value for OH emission (Figure 6.3 b). As discussed in chapter 5, increasing water vapor content above 500 ppm leads to an increase of OH overall production but also to a decrease of the OH emission (due to a quenching effect).

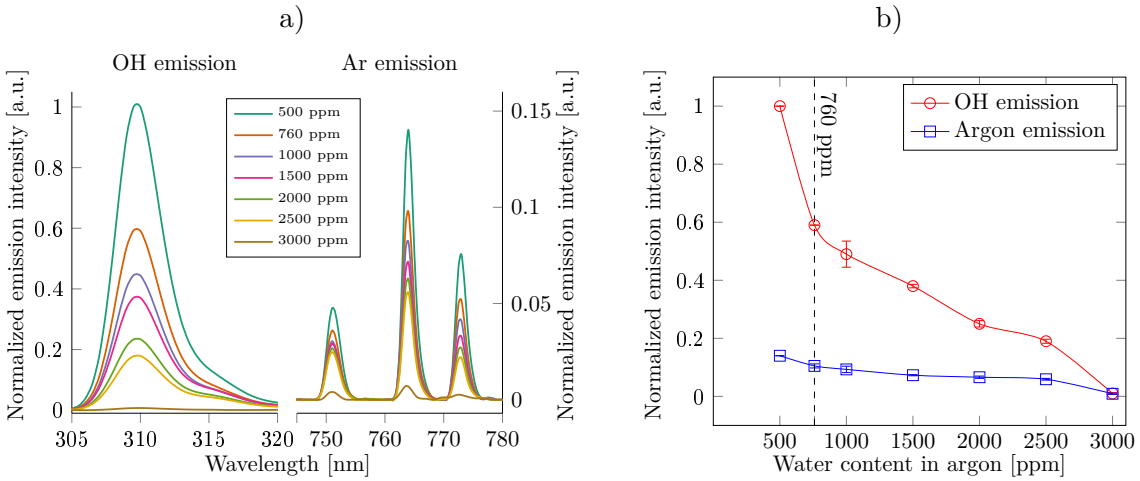

Figure 6.3: Optical emission spectroscopy of argon jet with varying water vapor content. a) Normalized emission spectra of OH (305 – 320 nm) and argon emission (745 – 780 nm) intensity dependence on water content in argon gas. b) Dependence of OH and argon emission maxima on water content in argon (normalized, average of two experiments). Electrical parameters for humid argon were kept constant during the whole experiment.

Laser induced fluorescence

The second condition suitable for bio-decontamination was in the working gas argon saturated with water vapor. In this case plasma did not propagate outside the inter-electrode gap and was enclosed inside the Pyrex glass tube between HV electrode and grounded electrodes; only gas with reactive species was interacting with the samples (indirect exposure). Although the water content was, according to our previous result (Figure 6.3 b), too high for production of UV B radiation, we were producing non-emissive hydroxyl radical whose presence at the tube outlet was revealed by planar laser induced fluorescence (OH-PLIF) (Figure 6.4). This could also be a case for humid argon working gas. While OH radical is short lived, it can still reach the sample 1 cm from jet nozzle (Figure 6.4). Therefore even if UV B can contribute to the overall decontamination efficiency [14], hydroxyl radical by itself is an important antimicrobial agent [63].

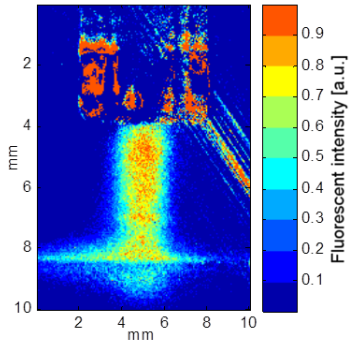

Figure 6.4: Indirect exposure of biological samples to the plasma jet. OH-PLIF of the jet fed by saturated argon, the fluorescence intensity (color scale) linearly corresponds to the concentration of OH radicals (Measured by Florent Sainct, CentraleSupélec).

Temperature measurement

To measure the jet temperature, an alcohol thermometer was used instead of glass cover slide 1 cm from jet nozzle. Increase of temperature above the initial temperature (18–23°C) is plotted in Figure 6.5. The discharge parameters were the same as those used for bacterial decontamination.

In the usual settings (Figure 6.5 a) with the discharge frequency 30.2 kHz, the temperature raised up to 30°C for the discharge with saturated argon, up to 28°C for humid argon (760 ppm water vapor) and up to 16°C for dry argon. This temperature is quite high especially for saturated and humid argon feed gas; if the ambient temperature was around 20°C, the temperature of the sample surface in these conditions could have risen to 50°C. Therefore the frequency of HV pulses was halved while preserving their the amplitude to 14.5 kHz. The temperature increase measured (Figure 6.5 b) in discharges in dry and humid

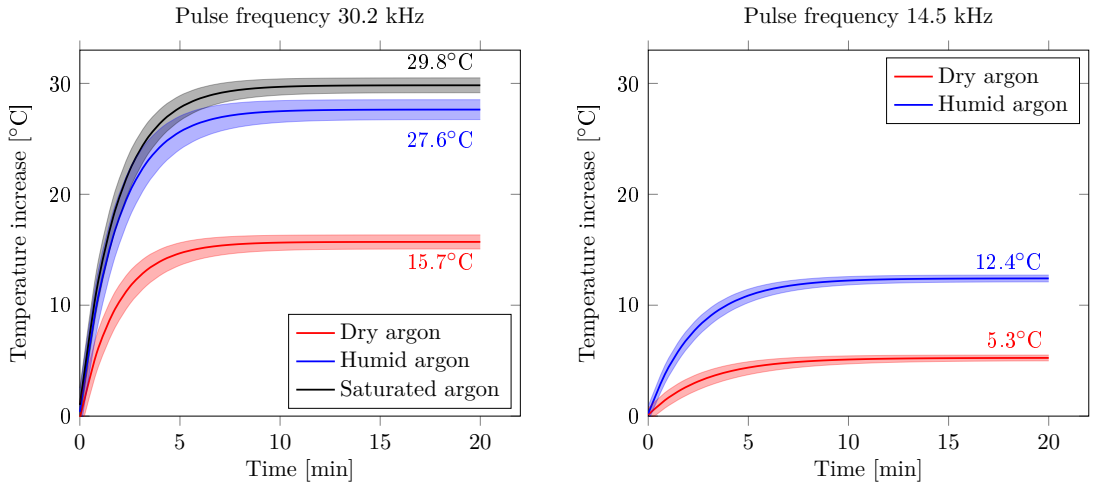

Figure 6.5: Temperature increase over the ambient temperature of the cover glass 1 cm from the jet nozzle in the dry, humid and saturated argon discharge. Values represent the final value of the surface temperature increase over ambient after 20 min of discharge running. The initial (ambient) temperature varies between 18 – 23°C. Frequency of HV pulses: a) 30.2 kHz, b) 14.5 kHz (fits with 95% confidence intervals).

argon was smaller, 5.3 and 12.4°C above the ambient, respectively.

To test the biocidal effect of high temperature the bacterial sample on cover glass was put on hot plate with temperature 50.5°C for 20 min, by this method we lost 2.1 $\log_{10}$ of the bacterial population. The second method we used was to place 10 μL bacterial sample inside the microtube at then in the water bath with temperature 51°C, this resulted in losing 1.1 $\log_{10}$ of the bacterial concentration within 20 min.

6.3.2 Planktonic bacteria treatment

Decontamination of planktonic bacteria by three regimes of argon jets are presented in Figure 6.6 a. Dry and humid argon corresponds to direct exposure to the discharge (plasma in contact with the sample, as it is in Figure 6.1 c), and saturated argon is in indirect exposure - only effluents were reaching the sample. The initial bacterial concentration deposit on glass cover slide was $8.6 \pm 1.8 \times 10^8$ cfu/mL. Dry argon plasma treatment reduced initial concentration of bacteria by 1.6 ± 0.2 $\log_{10}$ in 10 min exposure time and 3.4 ± 0.2 $\log_{10}$ within 20 min. In humid argon plasma bio-decontamination efficiency was significantly (Mann-Whitney test, $p<0.001$) increased to 3.6 ± 0.2 and 5.9 ± 0.4 $\log_{10}$ in 10 and 20 min exposure time, respectively. The saturated argon discharge was tested only for 10 min exposure time and caused 2.3 ± 0.4 $\log_{10}$ reduction of initial bacterial concentration.

The results from temperature measurements (Figure 6.5) showed us that temperature of the surface could reach up to 50°C in the jet with humid argon plasma within 20 min. By decreasing the frequency of HV pulses down to 14.5 kHz the temperature also decreased to

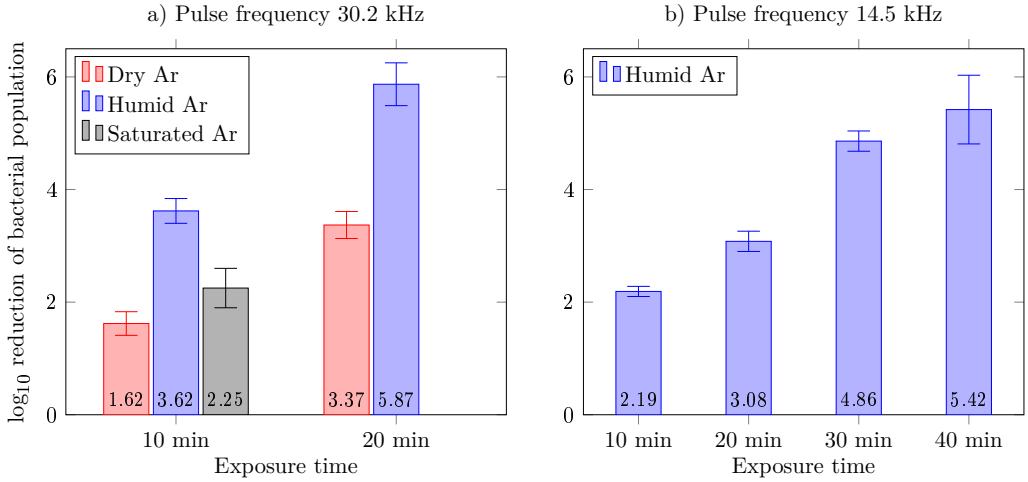

Figure 6.6: Log_{10} reduction of planktonic *E. coli* bacterial population after treatment with the jet: a) HV pulse frequency 30.2 kHz with three working gases - dry (n=6), humid (n=8) and water saturated argon (n=2); b) HV pulses frequency 14.5 kHz in humid argon working gas (n=3-4). Data are represented by mean ± SEM.

32.4°C and 25.3°C for humid and dry argon jet plasma, respectively. Therefore we tested decontamination efficiency of humid argon discharge with lowered frequency of HV pulses (Figure 6.6 b). Within 20 min exposure, our usual time for bio-decontamination, the initial bacterial concentration ($6.3 \pm 2.8 \times 10^8$ cfu/mL) was reduced by 3.1 ± 0.2 $\log_{10}$, what was only half efficiency as it was with original setting (Mann Whitney test, $p<0.05$). Consequently we extended exposure time of the sample to the discharge up to 40 min. By doubling the exposure time the initial bacterial concentration was reduced by 5.4 ± 0.6 $\log_{10}$, approaching the 5.94 ± 0.4 $\log_{10}$ obtained at 30.2 kHz.

Effect of UV and VUV on planktonic bacteria

Optical measurements (Figure 6.3) evidenced UV B emission from the plasma jet especially in humid argon. In dry argon discharge, the emission from excited hydroxyl radical is low, but we can assume a possible VUV emission from argon excimer (Ar_2^*, maximum intensity at 126 nm). Therefore we tested the impact of UV B and VUV on planktonic bacterial samples (Figure 6.7).

Bacteria were exposed to the dry or humid argon discharge for 20 min directly and decontamination efficiency of 3.4±0.2 $\log_{10}$ and 5.9±0.4 $\log_{10}$, respectively, was reached (initial concentration was $6.8 \pm 1.3 \times 10^8$ cfu/mL). The quartz window allowed through only UV B radiation, this decreased decontamination efficiency to 1.7±0.3 $\log_{10}$ for dry argon and 4.8±0.5 $\log_{10}$ for humid argon. In the case of MgF_2, bacteria should be exposed to UV B + VUV radiation. Decontamination efficiency for dry argon remained almost the same as for the experiment with quartz window 1.9±0.2 $\log_{10}$. For humid argon, efficiency

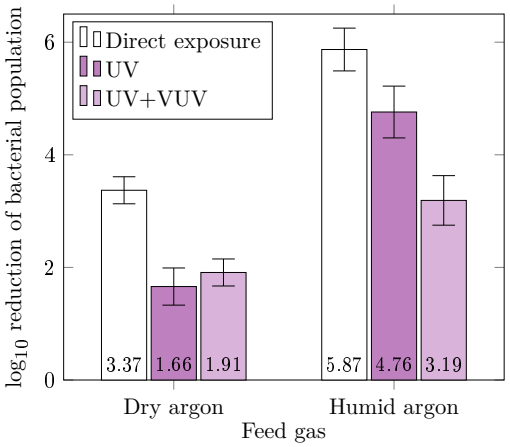

Figure 6.7: Log_{10} reduction of planktonic *Escherichia coli* bacterial population after 20 min treatment with the jet (HV pulse frequency 30.2 kHz), n = 6. Data are represented by mean ± SEM.

decreased in comparison with quartz to 3.2±0.4 $\log_{10}$. For dry argon plasma there was a significant difference of the effect of UV B in comparison with direct exposure (ANOVA, $p<0.05$), but not between UV B and UV B + VUV effect. For humid argon the effect of UV B + VUV was surprisingly lower than UV B alone (ANOVA, $p<0.05$). The external transmission according to suppliers manuals[1] is aroun 90% for both windows at 300 nm, therefore there must be another reason for this result. There is not evidence of the effect of VUV on the decontamination efficiency.

6.3.3 Biofilm treatment

In the previous section we had demonstrated that cold atmospheric pressure argon plasma treatment was efficiently reducing viable bacterial loads and that 760 ppm of water admixture was most efficient for bio-decontamination of *E. coli* cells in the planktonic state.

Here, we evaluate the bio-decontamination efficiency of cold atmospheric pressure humid argon plasma treatment of *E. coli* biofilms grown for 48 hours in static conditions.

Culturability biofilm results

To allow for comparison with our and other previously published work, we evaluated the bio-decontamination efficiency by determining the reduction in viability by plating the samples with and without treatment and counting colonies after incubation in appropriate conditions.

As shown in Figure 6.8, bacterial load decreases with increasing plasma treatment time, with an observed reduction in colony forming unit (CFU) of 4 to 5 $\log_{10}$ in 10 min of humid argon plasma treatment and up to 7 $\log_{10}$, corresponding to a full decontamination, after 20 min of humid argon plasma treatment. At the same time, we observe up to 2 $\log_{10}$

[1] Eksma optics - magnesium fluoride and UQG optics - Vitreosil® 077 Optical Fused Quartz

reduction in CFU of control samples which were exposed only to humid argon flow for 20 min. Such a decrease in non-treated samples was not observed on planktonic cells.

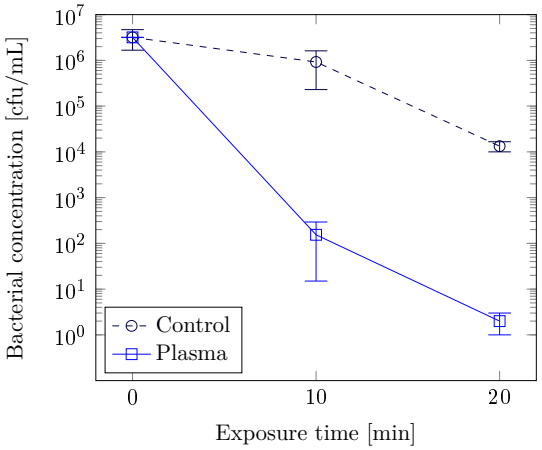

Figure 6.8: Survival curves for bacteria from 48-hour old *E. coli* biofilm after treatment with argon plasma with 760 ppm of water vapor. Cultivable bacterial cells count (colony forming units, CFU) recovered after 0 (initial bacterial load), 10 and 20 minutes of exposure to the plasma (plasma treated, plain line) and to 760 ppm humid argon flow only (control, dashed line). Results are from two experiments with duplicates (n=4, mean±SEM)

CLSM biofilm results

The observed bio-decontamination efficiency of humid argon plasma treatment of biofilms was validated using live/dead BacLight bacterial viability assay (Invitrogen, Thermo Fisher Scientific) two-color fluorescence assay (described in previous subsubsection 4.3.5). Live/Dead BacLight recommendations for fluorescent measurement and data analysis are: excitation at 485 nm and emission acquisition centered about 500 nm for Syto9 (480/530 nm) and 630 nm for PI, and the use of different longpass or bandpass filters for simultaneous or single fluorophore viewing, respectively.

We measured the fluorescence excitation-emission matrix in our experimental conditions on samples stained with a single dye at a time. We determined that the optimum excitation wavelength was at 525 nm for PI and 480 nm for Syto 9, and the fluorescence was acquired over a 40 nm window centered over the maximum of emission at the set excitation wavelength for each dye. The excitation of PI at 525 nm will not excite Syto 9 as PI optimum excitation wavelength falls outside of Syto 9 excitation range ($<$500 nm). On the other hand, excitation of Syto9 resulted in some level of excitation of PI. In addition, excitation of Syto 9 resulted in emission within the acquisition window set for PI and could result in artificially increased measured signal for PI from residual Syto9 emission. On the contrary, PI does not emit within the wavelength window fixed for Syto9 fluorescence acquisition. For these reasons and to insure an exclusive measure of each fluorophore's signal intensity, we resolved from the

excitation spectra that the fluorescence should be acquired sequentially with PI fluorescence measured first (Figure 6.9).

We also verified that bacterial autofluorescence, in the absence of the dye, did not interfere with the exclusive signal acquisition set up as just described (data not shown).

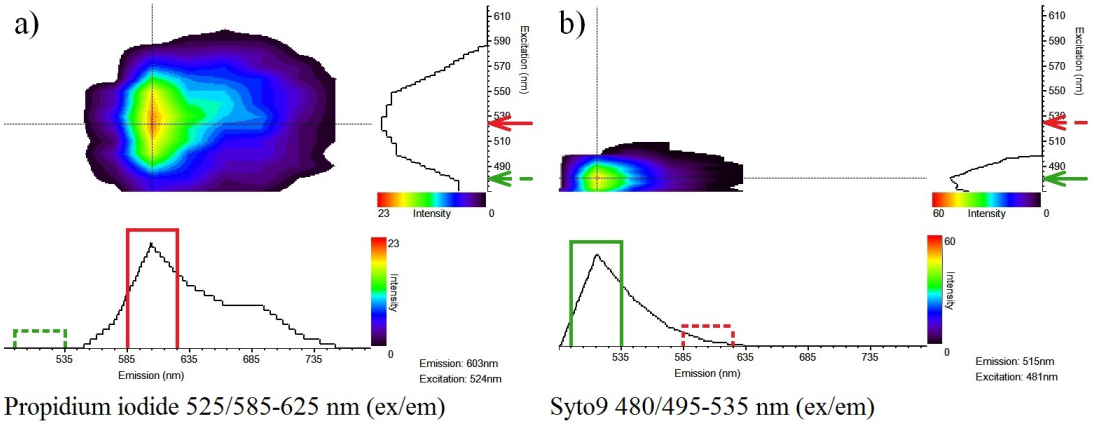

Figure 6.9: Excitation and emission matrices for fluorophores: a) propidium iodide and b) Syto9. Exclusive emission and excitation spectra were determined with wavelength steps of 10 nm over a 470 to 670 nm range on bacterial samples stained with a single dye at a time. To acquire an exclusive signal for each fluorophore, sequential acquisition was carried out at these wavelengths (excitation/emission) and in this order: propidium iodide 525 nm/585–625 nm, Syto9 480 nm/495–535 nm, and DAPI 405 nm/445–485 nm (Table 6.1).

Comparison of plasma-treated and control biofilm samples was achieved using live/dead BacLight bacterial viability two-color fluorescence assay using our exclusive sequential acquisition set up as described above. Samples were stained using the same dye mix and for the same time duration. Images were acquired at 3 to 5 locations across the sample, specifically - for plasma-treated samples - at the point of impact of the plasma plume and on each side of this impact point. Image series including fibers, salt crystals or other foreign elements that could alter the fluorescence signals were discarded. Figure 6.10 shows the 3D plot rendering z-stack and xyz projections for typical non-treated (control) and treated (20 min humid and saturated argon) samples. This allows for visual, qualitative comparison of samples.

When both fluorescence signals are overlaid, it is apparent that the plasma-treated biofilm is now composed of a substantial number of cells emitting red fluorescence, indicating membrane damages, possibly lethal. The overall fluorescence of the treated sample is orange compared to the almost exclusively green aspect of the control biofilm. In addition, 20 min of exposure to humid or saturated argon plasma results in the considerably reduced density of cells, regardless of their viability, with patches almost entirely stripped of cells. This is further evidenced by the considerable reduction in biofilm thickness as can be seen on xz and yz projections on sides of xy pictures (Figure 6.10 - second row). The qualitative comparison of treated vs. non-treated samples corroborates the bio-decontamination efficiency

of humid argon plasma on biofilms initially calculated using CFU counts. However, no calibration curve could have been established for biofilm samples to calculate the proportion of live/damaged cells.

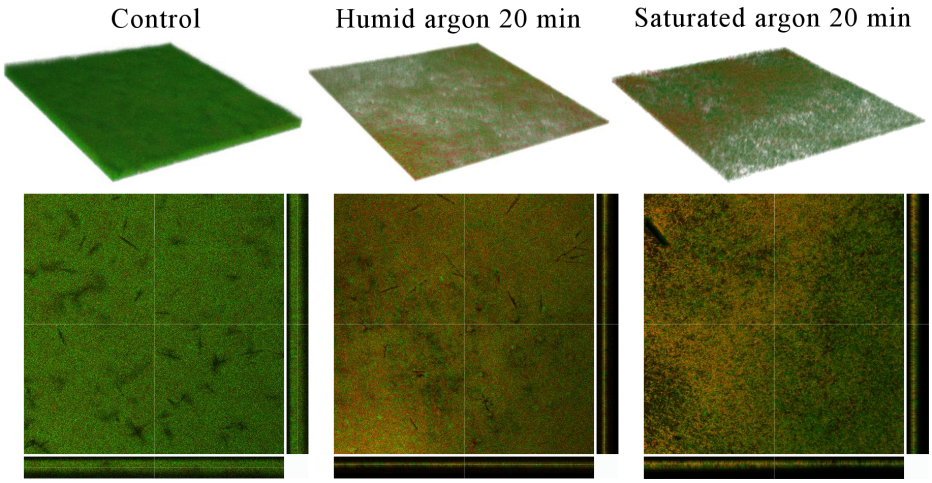

Figure 6.10: Three-dimensional reconstruction of the biofilm z-stacks from CLSM (first row). Qualitative comparison of control (first column) and plasma-treated biofilms: humid (second column) and water saturated argon plasma (third column) treatment biofilms. Second row contains cross sections of the z-stack above (xyz size is 512×512×24.14 μm), a cross hair on x-y image corresponds to the z-profiles on x and y axes (magnification 40×).

Live/dead ratio. To allow for a more quantitative comparison of plasma-treated and non-treated biofilm viability, green/red fluorescence ratios were calculated. The ratios were normalized to the background value of this green/red fluorescence ratio acquired outside (value = 1) of the biofilms samples in the mounting oil (most right hand side values). This normalization enables comparison across samples and experiments. As seen in Figure 6.11 a and c, the green/red ratio is above one for the non-treated biofilm sample, indicating that the biofilm is composed for the most part of viable bacterial cells.

For the humid argon plasma treatment of the biofilm (Figure 6.11 b), the calculated ratio is slightly below one, indicating that the proportion of cells emitting green fluorescence is reduced and that the proportion of red-emitting cells has increased. The plasma-treated biofilms' cells have experienced membrane damage that may interfere with their viability.

When we compare the result from "indirect exposure" - saturated argon plasma (Figure 6.11 d), when only the effluent from discharge active zone reached the sample, to its control sample (Figure 6.11 c) we see no decrease in the live/dead ratio.

Biofilm thickness from DAPI fluorescence

To produce another quantifiable variable to evaluate argon plasma bio-decontamination efficiency of *E. coli* biofilms, we introduced the third fluorophore to the staining mix, DAPI

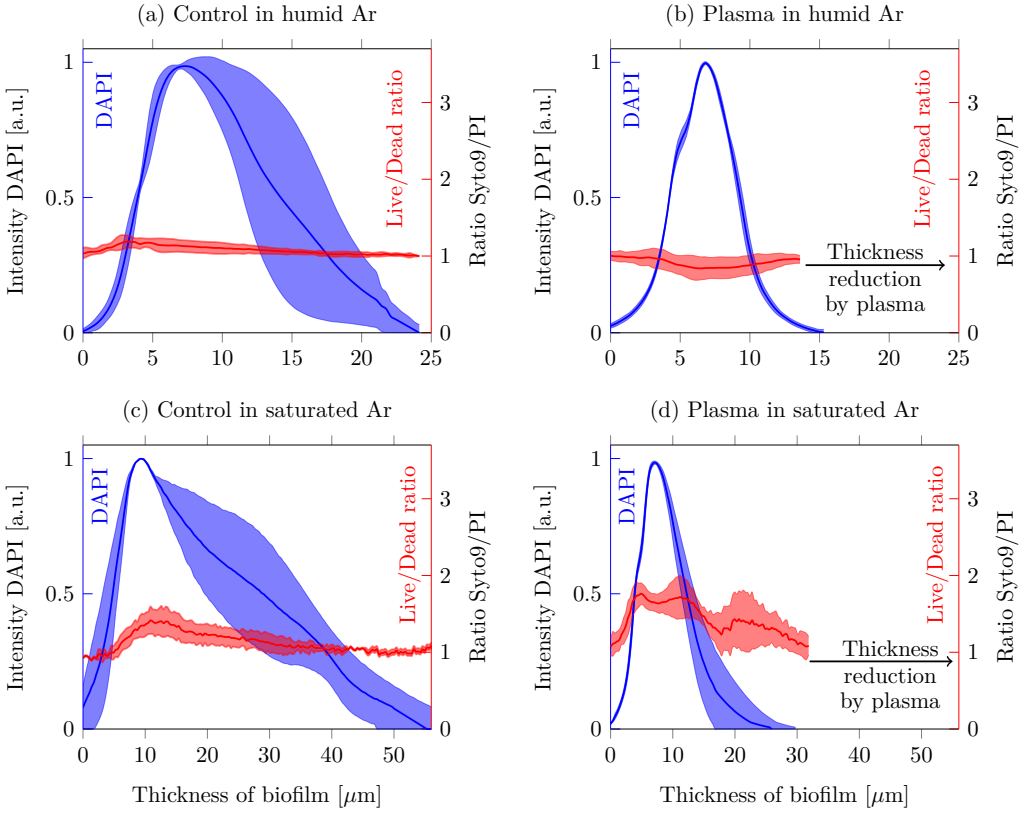

Figure 6.11: Typical development profile of the total fluorescence intensity of normalized DAPI (blue) and normalized Live/Dead ratio (red) in each optical section of the biofilm. (a) Control samples. (b) Samples exposed to humid argon discharge for 20 min. (c) Control samples. (d) Samples exposed to saturated argon discharge for 20 min. Zero μm represents the bottom of the biofilm - glass cover slide. (Data from one experiment, averaged over 4 random places on one sample per condition, intervals around represent the data range).

(4',6-diamidino-2-phenylindole) at a final concentration of 10 ng/mL. This dye allowed for cells containing dsDNA to be visualized and biofilm thickness to be estimated. When comparing two controls from two independent experiments (Figure 6.11 a and c) we can see that DAPI fluorescence was detectable in one case 25 μm and in the other case up to 55 μm from the bottom of the biofilm. However, in both experiments thickness of the plasma treated biofilms was reduced (Figure 6.11 b and d) and DAPI fluorescence was detectable only up to 15 μm and 25 μm.

Biofilm thickness was measured between the 10% and 90% percentile of the raw integrated density signal captured for DAPI through the z-stacks. Biofilm thickness was measured and compared for controls and plasma-treated samples from eight experiments (Figure 6.12). Following 20 min plasma treatment in humid argon biofilm thickness is significantly (ANOVA test, $p<0.0001$) reduced by 63% from an average of 31.1±6.5 μm for controls, to 11.7±2.3 μm for humid argon plasma-treated samples. The indirect treatment by saturated argon plasma for 20 min reduced thickness by 31.3% (ANOVA test, non significant $p=0.05$) to 21.4±5.4 μm.

This confirms the qualitative observations that biofilm thickness is reduced more by humid argon plasma "direct" treatment than saturated argon plasma"indirect" treatment.

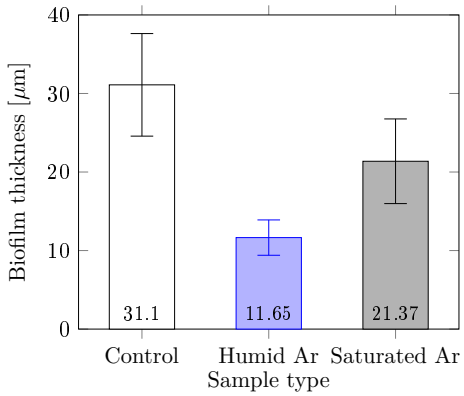

Figure 6.12: Biofilm thickness calculated from DAPI fluorescence for control samples (n = 26), samples exposed to humid argon (direct exposure, n = 19), and samples exposed to saturated argon (indirect exposure, n = 7) (Mean ± 95% c.i.).

Biofilm biomass evaluation

The microscopy observations of DAPI staining of the biofilms show the thinning of the biofilm after plasma treatment in comparison with control sample. In order to test if this is the result of drying and shrinking of the biofilm structure or the actual eradication of cells and reduction of the biofilm biomass, we used crystal violet assay for biofilm biomass assessment. Results shown in Figure 6.13 were obtained after 20 min plasma treatment.

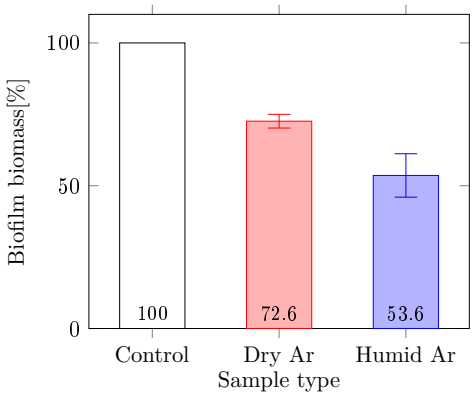

Figure 6.13: Biofilm biomass calculated as percentage of controls from crystal violet absorbance. Control sample exposed to only argon flow as 100% of biomass, samples exposed to dry and humid argon plasma (Mean ± SEM, n = 8 in each group).

The biomass of control biofilms was set as 100%. After treatment with the plasma jet with dry argon the biomass of bioflims was significantly reduced to 72.6±2.4% of the control within 20 min (ANOVA, $p<0.0001$). With the same exposure time, the humid argon plasma jet left 53.6±7.6% of initial biomass preserved only (ANOVA, $p<0.0001$).

6.4 Discussion

Three gas mixtures were used in our plasma jet: dry argon, argon with 760 ppm of water vapor and argon fully saturated by water vapor at room temperature.

6.4.1 Discharge characterization

The optical emission spectroscopy of the jet was used to test the efficiency of production of UV B emission by deexcitation of OH^* (Figure 6.3), and we found out that our usual 760 ppm water vapor in argon flow condition is above an optimal value for OH emission intensity (lower concentration 500 ppm of water vapor was more efficient). Additional increase of water content decreases emission in UV B together with overall emission. This is caused by quenching mechanisms that become the dominant phenomena in conditions with high water vapor concentrations [195, 196]: $OH^*(A^2\Sigma^+) + H_2O \longrightarrow OH(X^2\Pi) + H_2O$. Laser induced fluorescence of saturated argon post-discharge showed that even if plasma of the jet no longer propagates from the tube outlet, non emissive OH radicals which are present in the flow, can spread on the sample surface (Figure 6.4). In this situation the bacteria biofilm treatment only results from a chemical actions of OH radicals.

6.4.2 Planktonic bacteria

The bactericidal effect of the plasma jet in three gas mixtures was tested on planktonic bacteria *E. coli* BW 25113, which were later used for biofilm formation. To compare all three discharges, 10 min exposure was used: the most efficient regime of the jet was humid argon discharge that reached 3.6±0.2 $\log_{10}$ reduction of initial bacterial population. This regime was the most efficient although the water vapor saturated argon discharge used higher input power. This can be because the plasma was enclosed between in the inter-electrode gap and only reactive species, especially OH radicals reached the sample. The dry argon was the least efficient regime of the jet. In this case water vapor comes from the sample itself (and to the lesser extent from the walls of the reactor). This results in a low OH production in comparison with a continuous water vapor supply (humid argon discharge).

Effect of temperature. Surface temperature of glass cover slides, exposed 1 cm from the jet nozzle, was measured in steady state conditions (20 min of discharge running) for three different working gases (Figure 6.5 a). It was found that the surface temperature increase was dependent on the discharge input power: low input power (1.2–1.4 W) for dry argon discharge led to 16 K, whereas higher input power (4.2–5 W) for humid argon (760 ppm) and water vapor saturated argon discharges led to 28–30 K. The impact of such temperature values (36°C and 50°C respectively for experiments performed at 20°C ambient temperature) on bacteria survival could not be neglected. Bactericidal tests for the highest

temperature (50°C) were therefore conducted, by directly placing contaminated glass cover slides onto a hot plate. This may be the highest margin value because during the plasma treatment, temperature steady state is reached after ≈7 min of the jet operation and bacteria are therefore not exposed to the highest temperature value during the whole treatment duration. With such an experiment, bacterial population decreased by 2.1 $\log_{10}$ from the initial population.

The HV pulse frequency was then lowered to 14.5 kHz in order to reduce the overall energy deposit and therefore limit the heating of the glass cover slide (32.5°C in steady state conditions - Figure 6.5 b). Bactericidal test in humid argon discharge at 14.5 kHz showed lower bio-decontamination efficiency as was expected. But by comparing cases with almost the same energy deposit in the discharge (Figure 6.5 a and b), 10 min - 30.2 kHz versus 20 min - 14.5 kHz on the one hand, and 20 min - 30.2 kHz versus 40 min - 14.5 kHz on the other hand, we obtain similar decontamination efficiencies (there is not a significant difference between cases, Mann-Whitney test, p=0.05). Therefore it can be assumed that the bio-decontamination effect is not caused by higher temperature during the treatment with 30.2 kHz frequency.

6.4.3 Bacteria in biofilm

Biofilm cultivability. CFU assays only account for cultivable cells, while bacteria grown in biofilm are known to have a recalcitrant growth phenotype in laboratory conditions. In addition, bacterial cells encased in biofilm cannot be easily separated and dispersed before cultivation due to the extracellular polymeric matrix; this effect might further be enhanced by the desiccation due to exposure to the gas flow. The observed reduction in the number of viable cells recovered from control samples after 20 min of exposure to the gas flow likely reflects the combination of these two effects, since the assays on planktonic bacteria cells revealed less than 1 $\log_{10}$ decrease in viability after 20 min exposure to humid argon gas [14] and no more than 1 $\log_{10}$ decrease in viability was reported for *E. coli* biofilm after up to 12 hours of desiccation [223]. This is further supported by the fact that biofilm encased bacteria cells are more efficiently protected against the adverse effect of desiccation and thus should be less affected in their viability than planktonic cells [223–225]. The reduction observed for control samples exemplifies the difficulty to separate and cultivate bacteria cells collected from a biofilm structure.

If we take into account only the decontamination efficiency from control samples (not the initial bacterial load), after 10 min of the plasma jet treatment, the bactericidal efficiency of the jet remains constant ~ 4 $\log_{10}$. This may be the effect of forming of a protective layer from cells or cell debris after longer exposure (more than 10 min exposure time) [120, 122]. There is also a possibility that after 10 min treatment bacteria enter the viable-but-non-cultureable (VBNC) state, and finally are killed after longer exposure times [133].

Biofilm live/dead ratio Confocal laser scanning microscopy was used to visualize three fluorescent dyes, Syto9, PI, and DAPI. Syto9 and PI allowed for 3D reconstructions of biofilms. Figure 6.10 shows that green live and thick control sample is turned into thin biofilm with patches of red dead cells after 20 min of plasma treatment with humid or saturated argon. The live/dead ratio of control biofilm was above one in the bulk of the biofilm and after "direct" treatment with humid argon plasma, the ratio in the biofilm bulk decreased. After an "indirect" treatment by saturated argon plasma, the live/dead ratio of the treated biofilm samples remained the same and even had grown (Figure 6.11). These two results, visual and semi-quantitative, are in contradiction. In the case of saturated argon plasma we did not find any proof for proliferation of bacterial grow after plasma treatment as was previously reported in studies on eukaryotic cells [226–229].

Biofilm thickness and biomass A biofilm thickness reduction to 37% of control thickness by humid argon discharge was measured after 20 min exposure time (DAPI fluorescence). In comparison, after the same exposure time to the humid argon discharge, the biofilm biomass was reduced to 54% (CV assay). The cause of this difference might be that bacterial cells are destroyed during plasma treatment, and therefore could no longer concentrate DAPI; but the biomass remains lodged inside the EPS and is not washed away during crystal violet assay.

To test this hypothesis, we washed the biofilm control and humid argon plasma treated samples, and stained them with the dyes according to the usual protocol. The comparison between washed and unwashed samples is presented in Figure 6.14.

Thickness of the washed control biofilm in comparison with unwashed was reduced by 65% (in Figure 6.14 a $\rightarrow$ c). Thickness of the plasma treated biofilm sample washed after treatment was also reduced by 60% (Fig. 6.14 b $\rightarrow$ d). In the case of unwashed sample, the biofilm thickness was reduced after plasma treatment by 77% (Fig. 6.14 a $\rightarrow$ b), and the washed sample by 73% (Fig. 6.14 e $\rightarrow$ d) in comparison with the control sample. We can conclude that there was not a significant difference between the loss of thickness in washed and unwashed samples. Therefore rinsing of sample will not detach the dead bacteria and EPS from the sample, perhaps only planktonic or loosely attached cells, which are also removed by rinsing from the control sample.

6.4.4 Comparison of biofilm treatment by DC corona discharges in air and DBD argon plasma jet

The 48 hour old *E. coli* biofilm was also treated by DC corona discharges in air and the results are presented in subsection 4.3.5. Although there were some differences such as the model of the confocal microscope used, magnification used for acquiring the data, and wavelengths used for excitation of the fluorophores and detection of their florescence, the differences are

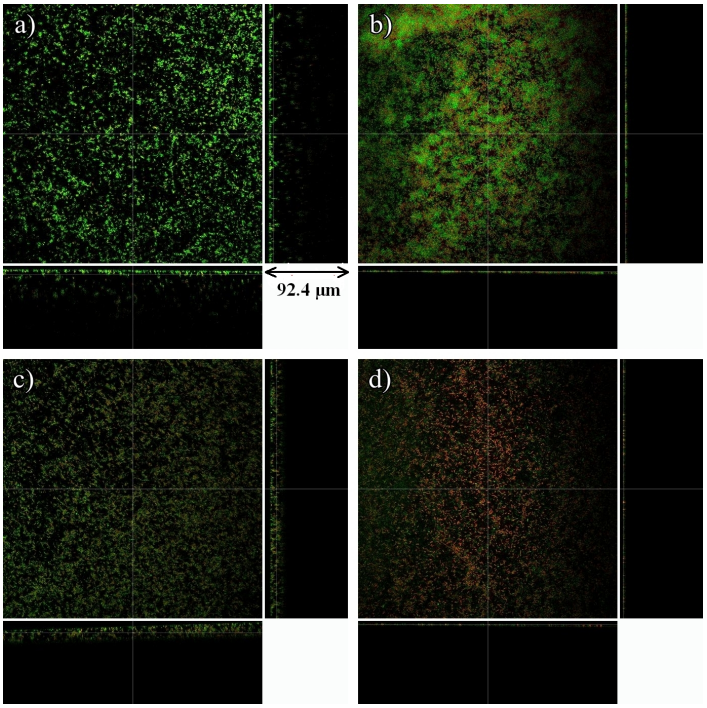

Figure 6.14: The biofilm z-stacks from CLSM: First row, unwashed samples a) control, b) humid argon plasma, Second row, washed samples: c) control, d) humid argon plasma. Magnification 40×, section size 290.63×280.63 μm.

negligible for our comparison. We used the same method for a viability assessment - the culturability of bacterial cells and the live/dead fluorescent staining by Syto 9 and PI. In the case of DC corona discharges, within 15 min plasma treatment 4.76 and 4.99 $\log_{10}$ reduction of initial concentration of bacteria was achieved by PC and NC, respectively (Figure 4.13). This efficiency was enhanced by water electrospray from the HV electrode to 5.28 and 5.4 $\log_{10}$ by PC and NC within 15 min, respectively (Figure 4.14). A higher decontamination efficiency was achieved using humid argon plasma jet, 7 $\log_{10}$ reduction in bacterial culturability was measured, but after 20 min of the plasma treatment (Figure 6.8). The plasma treatment with the argon jet was more efficient from the viewpoint of culturability, the reason might be the higher mean input power, 4.2–4.4 W (and surface temperature), compared to DC corona where only ≈100 mW were used. The CLSM live/dead ratio of the reconstructed 3D parts of biofilms in both cases showed an increase in the red fluorescence indicating dead cells. DC coronas were able to reduce the live/dead ratio in the top layer of the biofilm, but the live/dead ratio remained almost constant after treatment with argon plasma jet. The thickness of the biofilm was reduced by plasma treatment in both cases, humid argon plasma reduced the biofilm thickness to $1/3^{\text{rd}}$ of its original value, DC corona discharges caused only minor changes and reduced thickness by a few μm. The biofilm biomass measurement by CV, which includes washing unattached cell and debris of the sample, showed a massive loss of the biomass for both types of plasma sources. Negative corona with water electrospray

left only 30% of the initial biomass attached on the cover glass (Figure 4.19), compared to 54% left by humid argon jet plasma (Figure 6.13). This result was very repeatable for the jet, compared to relatively scattered results obtained by DC corona discharges; it might have been caused by precisely defined and easy to maintain conditions for the jet in contrast with the DC corona discharge, where the sharpness of the used HV needle can influence the electrical parameters. A final test carried out on biofilms was rinsing them after plasma treatment and staining them with fluorescent dyes for CLSM observations. This showed a significant difference between both low-temperature plasma sources. After DC discharges treatment and washing of samples, only live bacteria remained attached on the glass and all cell debris and dead bacteria left over on unwashed treated samples disappeared. On the other hand, after humid argon treatment, dead bacteria and debris remained attached to the cover glass.

6.5 Summary

In this chapter argon plasma jet in argon atmosphere was studied for bio-decontamination of *Escherichia coli* 48-hour-old bacterial biofilms, because of its convenience for the treatment of flat surfaces, such as glass cover slides. First, the optical characterization of the discharge was performed: the light from the discharge was collected in order to determine the most suitable water vapor content for production of excited hydroxyl radicals. We found out that water content of our mostly used condition (760 ppm) is above optimal value value for maximum OH emission. In the case of water vapor saturated argon, although the water content was too high to propagate the plasma out of the inter-electrode region, the OH-PLIF showed high production of non-emissive (ground state) hydroxyl radical. Temperature measurements of the glass surface showed an increase in temperature by almost 30 K within 7 min of the discharge exposure. This high temperature was decreased by lowering the HV pulses frequency from 30.2 kHz to 14.5 kHz; in this case the temperature increased only by 12.4 K. The treatment of planktonic *E. coli* by humid argon discharge reduced the initial bacterial population by 5.9 $\log_{10}$ within 20 min. The same discharge regime running on half frequency (14.5 kHz) was able to achieve the same bio-decontamination efficiency within 40 min; this might indicate that the high bio-decontamination efficiency in not caused by higher temperature during treatment with 30.2 kHz HV frequency. The biofilm viability after plasma treatment was assessed by cultivability and live/dead fluorescent staining. Special excitation and emission wavelengths for PI ad Syto 9 were used after analysis of their excitation-emission matrices, in order to obtain exclusive signal for each fluorophore. By CFU counting, up to 7 $\log_{10}$ reduction was achieved within 20 min of humid argon plasma treatment. The CLSM of biofilms stained by fluorescent dyes showed increase in red fluorescence after plasma treatment. This increase was not seen on live/dead ratio plotted as

a function of the biofilm thickness. The biofilm thickness and biofilm biomass were also analyzed. The biofilm thickness was measured by the third fluorescent dye - DAPI and biofilm biomass by crystal violet assay. The biofilm thickness after 20 min of humid argon plasma treatment was reduced to 37% of control biofilm thickness. The same discharge and exposure time reduced biofilm biomass to 54%. The biocidal effect of humid and water vapor saturated argon plasma jet is governed by the production of OH radical, which presence was measured near the glass cover slide by the OH-PLIF, and in the case of humid argon by UV B emitted from excited OH. In the humid environment, the production of hydrogen peroxide is also expected. The effect of VUV especially in dry argon was not observed but cannot be excluded. The argon plasma jet was shown to be an inexpensive and efficient plasma source for decontamination of bacterial biofilms.

7 Conclusions

In this PhD thesis entitled "Bio-decontamination of biofilms on surfaces by cold plasma", three different set-ups for generating low-temperature plasma at atmospheric pressure were used. The first one used was a DC corona discharge in ambient air in point to plane geometry. The HV electrode was connected to either positive polarity forming positive streamer corona discharge, or to negative generating negative Trichel pulses.

The second used set-up was a positive pulsed corona discharge propagated in the inner surface of a 49 cm long quartz tube filled with flowing argon or argon with water vapor (760 ppm).

The third set-up was a DBD plasma jet enclosed in the box filled with the same working gas. Three working gases were used: dry argon, argon with water vapor (760 ppm) and argon saturated with water vapor at ambient temperature. The conclusions summarized in three groups follow as the objectives of this thesis were defined. The suggestions for future work are listed below the conclusions.

7.1 Characterization of the investigated discharges

DC corona discharges were characterized by electrical measurements: the typical voltages, currents, mean power consumptions, etc. The processed gas (air) was analyzed by FTIR, UV absorption (homemade ozonemeter), and a commercial gas analyzer. The concentrations of stable reactive species in gas such us ozone, nitric oxide, and nitrogen dioxide were measured for DC corona discharges with or without water electrospray, with considerable concentration of ozone (up to 97 ppm) in PC with water electrospray. The chemical analysis of the electrosprayed water was performed and micromolar to millimolar concentrations of ozone, nitrite, nitrate, and hydrogen peroxide in the water were measured.

Pulsed corona discharge propagated inside long quartz tube filled with argon or argon with water vapor was analyzed. Electrical characteristic such as discharge propagation length as a function of HV amplitude and the stability field inside the discharge channel were measured. Optical emission spectroscopy in dry argon showed that argon emission dominates the spectrum at 680–850 nm. In humid argon, argon emission is accompanied by emission from excited hydroxyl radical in UV B region. The hydroxyl radical emission time evolution alongside the tube showed the first emission maximum corresponding to the discharge propagation in the tube from the HV electrode at the tube inlet to the grounded electrode at the tube outlet and the second emission maximum occurring just after the applied voltage drop. The

discharge propagation velocities inside the tube in dry and humid argon were obtained from electrical and optical measurements, and for humid argon were around 0.2 and 1×10^6 m/s at the outlet and inlet end of the tube, respectively. The discharge temperature was measured from the optical emission of the N_2 second positive system (1000 ppm N_2 added to the gas mixture), and was found out to be 450 ± 50 K, the temperature of the quartz tube surface and argon flowing from the tube outlet measured by alcohol thermometer, remained below 30°C.

Argon jet in argon atmosphere was characterized by optical the emission spectroscopy and by OH-PLIF. OES showed that 760 ppm water vapor content is above the optimum value for UV B emission production from excited OH. Although the jet working with water saturated argon is not ideal for UV B production, since the plasma is no longer propagating from the jet outlet. OH-PLIF showed that it is very efficient in production and transport of OH radicals even 1 cm far from the jet nozzle. Temperature measurements by alcohol thermometer 1 cm from the jet nozzle showed a temperature increase, reaching steady state conditions after 7 min of the discharge operation, by 30 K for water saturated argon, 28 K for humid and 16 K for dry argon (above ambient temperature 20°C).

7.2 Bio-decontamination of biofilms by low-temperature plasma

DC corona discharges and the argon plasma jet were used for bio-decontamination of *Escherichia coli* 48 hour biofilm. The same methods for a viability assessment were used - culturability of bacterial cells and live/dead fluorescent staining by Syto 9 and PI. DC corona discharges up to 5 $\log_{10}$ reduction of initial concentration of bacteria was achieved within 15 min plasma treatment. This decontamination efficiency was enhanced by water electrospray from the HV electrode up to 5.4 $\log_{10}$. The higher decontamination efficiency was achieved using humid argon plasma jet, 7 $\log_{10}$ reduction in bacterial culturability was measured after 20 min of the plasma treatment. The confocal laser scanning microscopy showed an increased appearance of dead cells inside the biofilm after plasma treatment. The live/dead ratio decreased especially in the top layers of the biofilms after exposure to DC coronas and remained constant after the argon jet treatment. The thickness of biofilm was reduced by plasma treatment in both cases, humid argon plasma reduced the biofilm thickness to $1/3^{\text{rd}}$ of the original value, DC corona discharges caused only minor changes and reduced the thickness by few μm. The biofilm attached biomass measurement showed a massive loss of the biomass after exposure to the plasma. Negative corona with water electrospray left only 30% of the initial biomass attached on the cover glass compared to 54% left by humid argon jet plasma. The remaining attached biomass could be removed by washing the surface of samples after plasma treatment and repeat the treatment again.

Both types of low-temperature plasma sources were able to inactivate bacterial growth and kill bacteria in biofilms. They were able to reduce biofilm thickness and erode the biomass which allowed for washing away cellular and extracellular debris.

7.3 Identifying the bactericidal factors of air and argon plasmas

The bactericidal effect of DC corona discharges is reached by the possible combination of the high electric field and the detected species such as ozone and nitrogen oxides in the gas, and ozone, hydrogen peroxide, nitrate, nitrite and their products in the electrosprayed water. Ozone and hydrogen peroxide concentrations by themselves were found to be in bactericidal region, especially for positive streamer corona. At lowered pH, nitrites react with hydrogen peroxide and form short-lived unstable peroxinitrites. Acidified nitrites and peroxinitrites are associated with strong bactericidal effect of the plasma activated water. In the negative corona, charged particles play a significant role in decontamination efficiency of this discharge. We can speculate that these ions are dominated by superoxide anions, since they are abundantly formed in the drift region of negative corona in air. UV emission was shown to have no significant effect on the bacterial survival.

The electrical discharges in argon, both pulsed corona discharge and argon plasma jet produce UV B emission from the excited OH radicals in humid argon. The effect of UV B by itself on *E. coli* DH1 (*recA1-*) and BW 25113 strains was significant. In dry argon, the possible bactericidal factor might be VUV radiation. Although its effect was measured, the results were not conclusive, therefore we cannot confirm or rule out the effect of VUV. OH-PLIF of water saturated argon jet showed the formation of OH radicals even 2 cm far from the active discharge region, which makes OH radical one of the key bactericidal factors of humid argon plasma. There was no effect of higher temperature on bacterial survival in both set-ups for argon plasma production, or temperature played only synergistic effect with other active components of the plasma.

7.4 Suggestions for future work

Based on our extensive research summarized in this thesis, the following suggestions for future work can be proposed:

For experiments with DC corona discharges, better discharge characterization would be in place. As some OES of the positive streamers in air with and without water electrospray has been performed in our laboratory [178, 230]. We propose to perform optical emission spectroscopy of the discharges especially in negative Trichel pulses with or without water electrospray. FTIR measurement of the gas coming out of the discharge region with more

control over water vapor impurities would clean the FTIR spectra and enable us to better distinguish the low concentration components interfering with water bands, such as NO_X. To test the effect of charged particles on bacteria and biofilms by selective blowing of the neutral particles away, with pulsed corona discharge for more controlled discharge characteristics. In order to complete bio-decontamination of biofilms study, we would like to perform resazurin metabolic test, to find out whether the uncultivable bacteria are still metabolically active, i.e. are in the VBNC state. We also propose to visualize the biofilms by atomic force microscopy or scanning electron microscopy to study cell morphology after the plasma treatment and measure the strength of biofilm attachment before and after the plasma treatment.

For the argon plasma jet we propose the same measurements concerning biofilms. We would like to continue measurements on VUV effect on bacteria and confirm or rule out its contribution. For the discharge propagation inside the quartz tube, the analysis of secondary discharge formed after HV pulse drop together with calibrating the UV B measurement would be of interest. The treatment of biofilm cultivated on the inner surface of the tube would also be of high interest to complete the study of its biocidal efficiency.

Bibliography

[1] K. Sauer, "The genomics and proteomics of biofilm formation.," *Genome biology*, vol. 4, p. 219, Jan. 2003.

[2] L. Hall-Stoodley, J. W. Costerton, and P. Stoodley, "Bacterial biofilms: from the natural environment to infectious diseases.," *Nature reviews. Microbiology*, vol. 2, pp. 95–108, Feb. 2004.

[3] J. W. Costerton, P. S. Stewart, and E. P. Greenberg, "Bacterial biofilms: a common cause of persistent infections.," *Science (New York, N.Y.)*, vol. 284, pp. 1318–22, May 1999.

[4] R. Daniels, J. Vanderleyden, and J. Michiels, "Quorum sensing and swarming migration in bacteria," *FEMS Microbiology Reviews*, vol. 28, no. 3, pp. 261–289, 2004.

[5] J. W. Costerton, "Introduction to biofilm.," *International journal of antimicrobial agents*, vol. 11, pp. 217–21; discussion 237–9, May 1999.

[6] I. W. Sutherland, "The biofilm matrix–an immobilized but dynamic microbial environment.," *Trends in microbiology*, vol. 9, pp. 222–7, May 2001.

[7] J. D. Bryers, "Medical biofilms," *Biotechnology and bioengineering*, vol. 100, no. 1, pp. 1–18, 2008.

[8] European Centre for Disease Prevention and Control, "Annual epidemiological report 2014," 2015.

[9] B. Kunze, M. Reck, A. Dötsch, A. Lemme, D. Schummer, H. Irschik, H. Steinmetz, and I. Wagner-Döbler, "Damage of Streptococcus mutans biofilms by carolacton, a secondary metabolite from the myxobacterium Sorangium cellulosum.," *BMC microbiology*, vol. 10, p. 199, Jan. 2010.

[10] M. E. Davey, A. O. George, and G. A. O'Toole, "Microbial Biofilms: from Ecology to Molecular Genetics Microbial Biofilms," *Microbiology and Molecular Biology Reviews*, vol. 64, no. 4, pp. 847–867, 2000.

[11] M. Moreau, N. Orange, and M. G. J. Feuilloley, "Non-thermal plasma technologies: new tools for bio-decontamination.," *Biotechnology advances*, vol. 26, no. 6, pp. 610–7, 2008.

[12] G. E. Morfill, M. G. Kong, and J. L. Zimmermann, "Focus on Plasma Medicine," *New Journal of Physics*, vol. 11, p. 115011, nov 2009.

[13] M. Dang Van Sung Mussard, O. Guaitella, and A. Rousseau, "Propagation of plasma bullets in helium within a dielectric capillary-influence of the interaction with surfaces," *Journal of Physics D: Applied Physics*, vol. 46, p. 302001, jul 2013.

[14] Z. Kovalova, M. Leroy, C. Jacobs, M. J. Kirkpatrick, Z. Machala, F. Lopes, C. O. Laux, M. S. DuBow, and E. Odic, "Atmospheric pressure argon surface discharges propagated in long tubes: physical characterization and application to bio-decontamination," *Journal of Physics D: Applied Physics*, vol. 48, no. 46, p. 464003, 2015.

[15] S. Ermolaeva, A. F. Varfolomeev, M. Y. Chernukha, D. S. Yurov, M. M. Vasiliev, A. a. Kaminskaya, M. M. Moisenovich, J. M. Romanova, A. N. Murashev, I. I. Selezneva, T. Shimizu, E. V. Sysolyatina, I. a. Shaginyan, O. F. Petrov, E. I. Mayevsky, V. E. Fortov, G. E. Morfill, B. S. Naroditsky, and A. L. Gintsburg, "Bactericidal effects of non-thermal argon plasma in vitro, in biofilms and in the animal model of infected wounds.," *Journal of medical microbiology*, vol. 60, pp. 75–83, jan 2011.

[16] J. Winter, K. Wende, K. Masur, S. Iseni, M. Dünnbier, M. U. Hammer, H. Tresp, K.-D. Weltmann, and S. Reuter, "Feed gas humidity: a vital parameter affecting a cold atmospheric-pressure plasma jet and plasma-treated human skin cells," *Journal of Physics D: Applied Physics*, vol. 46, p. 295401, jul 2013.

[17] J. P. Lim, H. S. Uhm, and S. Z. Li, "Influence of oxygen in atmospheric-pressure argon plasma jet on sterilization of Bacillus atrophaeous spores," *Physics of Plasmas*, vol. 14, no. 9, 2007.

[18] Z. Kovalová, M. Zahoran, A. Zahoranová, and Z. Machala, "Streptococci biofilm decontamination on teeth by low-temperature air plasma of dc corona discharges," *Journal of Physics D: Applied Physics*, vol. 47, no. 22, p. 224014, 2014.

[19] R. Matthes, C. Bender, R. Schlüter, I. Koban, R. Bussiahn, S. Reuter, J. Lademann, K.-D. Weltmann, and A. Kramer, "Antimicrobial efficacy of two surface barrier discharges with air plasma against in vitro biofilms.," *PloS one*, vol. 8, p. e70462, jan 2013.

[20] Z. Machala, B. Tarabová, K. Hensel, E. Špetliková, L. Šikurová, and P. Lukeš, "Formation of ROS and RNS in Water Electro-Sprayed through Transient Spark Discharge in Air and their Bactericidal Effects," *Plasma Processes and Polymers*, vol. 10, pp. 649–659, apr 2013.

[21] E. Sysolyatina, A. Mukhachev, M. Yurova, M. Grushin, V. Karalnik, A. Petryakov, N. Trushkin, S. Ermolaeva, and Y. Akishev, "Role of the Charged Particles in Bacteria Inactivation by Plasma of a Positive and Negative Corona in Ambient Air," *Plasma Processes and Polymers*, vol. 11, pp. 315–334, jan 2014.

[22] T. von Woedtke, S. Reuter, K. Masur, and K.-D. Weltmann, "Plasmas for medicine," *Physics Reports*, vol. 530, pp. 291–320, sep 2013.

[23] Z. Šipoldová and Z. Machala, "Biodecontamination of plastic and dental surfaces with atmospheric pressure air DC discharges," *IEEE Transactions on Plasma Science*, vol. 39, pp. 2970–2971, 2011.

[24] Z. Kovaľová, K. Tarabová, K. Hensel, and Z. Machala, "Decontamination of streptococci biofilms and Bacillus cereus spores on plastic surfaces with DC and pulsed corona discharges," *The European Physical Journal - Applied Physics*, vol. 61, p. 24306, 2013.

[25] C. Jiang, C. Schaudinn, D. E. Jaramillo, M. A. Gundersen, and J. W. Costerton, "A submicrosecond pulsed plasma jet for endodontic biofilm disinfection," in *NATO Science for Peace and Security Series A: Chemistry and Biology* (Z. Machala *et al.*, eds.), pp. 179–190, Springer, 2012.

[26] M. G. Kong, G. Kroesen, G. Morfill, T. Nosenko, T. Shimizu, J. Van Dijk, and J. Zimmermann, "Plasma medicine: an introductory review," *New Journal of Physics*, vol. 11, no. 11, p. 115012, 2009.

[27] M. Laroussi, "Nonthermal decontamination of biological media by atmospheric-pressure plas-

mas: review, analysis, and prospects," *Plasma Science, IEEE Transactions on*, vol. 30, no. 4, pp. 1409–1415, 2002.

[28] S. Lerouge, A. Fozza, M. Wertheimer, R. Marchand, and L. Yahia, "Sterilization by low-pressure plasma: the role of vacuum-ultraviolet radiation," *Plasmas and Polymers*, vol. 5, no. 1, pp. 31–46, 2000.

[29] M. Moisan, J. Barbeau, M.-C. Crevier, J. Pelletier, N. Philip, and B. Saoudi, "Plasma sterilization. methods and mechanisms," *Pure and applied chemistry*, vol. 74, no. 3, pp. 349–358, 2002.

[30] S. Villeger, S. Cousty, A. Ricard, and M. Sixou, "Sterilization of e. coli bacterium in a flowing n2–o2 post-discharge reactor," *Journal of Physics D: Applied Physics*, vol. 36, no. 13, p. L60, 2003.

[31] M. Boudam, B. Saoudi, M. Moisan, and A. Ricard, "Characterization of the flowing afterglows of an n2–o2 reduced-pressure discharge: setting the operating conditions to achieve a dominant late afterglow and correlating the noβ uv intensity variation with the n and o atom densities," *Journal of Physics D: Applied Physics*, vol. 40, no. 6, p. 1694, 2007.

[32] F. Fumagalli, O. Kylián, L. Amato, J. Hanuš, and F. Rossi, "Low-pressure water vapour plasma treatment of surfaces for biomolecules decontamination," *Journal of Physics D: Applied Physics*, vol. 45, no. 13, p. 135203, 2012.

[33] M. Polak, J. Winter, U. Schnabel, J. Ehlbeck, and K.-D. Weltmann, "Innovative plasma generation in flexible biopsy channels for inner-tube decontamination and medical applications," *Plasma Processes and Polymers*, vol. 9, no. 1, pp. 67–76, 2012.

[34] E. Odic, S. Limam, M. Kirkpatrick, B. Dodet, S. Salamitou, and M. DuBow, "Investigations of bacterial inactivation and dna fragmentation induced by flowing humid argon post-discharge," in *Plasma for Bio-Decontamination, Medicine and Food Security*, pp. 93–106, Springer, 2012.

[35] S. Limam, E. Odic, M. J. Kirkpatrick, and A.-M. Pointu, "Bacterial decontamination of the inner wall of narrow tubes by a nitrogen afterglow at atmospheric pressure and its relation to local atomic nitrogen concentration," *Plasma Processes and Polymers*, vol. 10, no. 8, pp. 679–685, 2013.

[36] Z. Šipoldová, "Bio-decontamination of teeth and plastic surfaces by cold plasma of corona discharge," Master's thesis, Faculty of Mathematics, Physics and Informatics, Comenius university in Bratislava, 2012.

[37] R. M. Donlan and J. W. Costerton, "Biofilms : Survival Mechanisms of Clinically Relevant Microorganisms," *Clinical Microbiology Reviews*, vol. 15, no. 2, pp. 167–193, 2002.

[38] K. Jefferson, "What drives bacteria to produce a biofilm?," *FEMS Microbiology Letters*, vol. 236, no. 2, pp. 163–173, 2004.

[39] P. Stoodley, K. Sauer, D. G. Davies, and J. W. Costerton, "Biofilms as complex differentiated communities.," *Annual review of microbiology*, vol. 56, pp. 187–209, Jan. 2002.

[40] P. Watnick and R. Kolter, "Biofilm , City of Microbes," *Journal of Bacteriology*, vol. 182, no. 10, pp. 2675–2679, 2000.

[41] M. Wilson and D. Devide, eds., *Medical Implications of Biofilms*. Cambridge, UK: Cambridge University Press, 2003.

[42] V. Martišovitš, *Základy fyziky plazmy.* Bratislava: Univerzita Komenského, 2004.

[43] Y. P. Raizer, *Gas Discharge Physic.* Berlin: Springer - Verlag, 1991.

[44] M. Goldman, A. Goldman, and R. Sigmond, "The corona discharge, its properties and specific uses," *Pure and Applied Chemistry*, vol. 57, no. 9, pp. 1353–1362, 1985.

[45] K. Becker, U. Kogelschatz, K. Schoenbach, and R. Barker, *Medical Implications of Biofilms.* Cambridge, UK: Cambridge University Press, 2003.

[46] G. W. Trichel, "The mechanism of the negative point to plane corona near onset," *Physical Review*, vol. 54, no. 12, pp. 1078–1084, 1938.

[47] H.-H. Kim, J.-H. Kim, and A. Ogata, "Time-resolved high-speed camera observation of electrospray," *Journal of Aerosol Science*, vol. 42, no. 4, pp. 249–263, 2011.

[48] H. Kim, Y. Teramoto, N. Negishi, a. Ogata, J. Kim, B. Pongrác, Z. Machala, and A. M. Gañán-Calvo, "Polarity effect on the electrohydrodynamic (EHD) spray of water," *Journal of Aerosol Science*, vol. 76, pp. 98–114, oct 2014.

[49] B. Pongrác, H.-H. Kim, N. Negishi, and Z. Machala, "Influence of water conductivity on particular electrospray modes with dc corona discharge — optical visualization approach," *The European Physical Journal D*, vol. 68, no. 8, p. 224, 2014.

[50] B. Pongrác, H. H. Kim, M. Janda, V. Martišovitš, and Z. Machala, "Fast imaging of intermittent electrospraying of water with positive corona discharge," *Journal of Physics D: Applied Physics*, vol. 47, p. 315202, aug 2014.

[51] A. Jaworek, A. Sobczyk, T. Czech, and A. Krupa, "Corona discharge in electrospraying," *Journal of Electrostatics*, vol. 72, no. 2, pp. 166–178, 2014.

[52] J. P. Borra, Y. Tombette, and P. Ehouarn, "Influence of electric field profile and polarity on the mode of EHDA related to electric discharge regimes," *Journal of Aerosol Science*, vol. 30, no. 7, pp. 913–925, 1999.

[53] J.-P. Borra, P. Ehouarn, and D. Boulaud, "Electrohydrodynamic atomisation of water stabilised by glow discharge-operating range and droplet properties," *Journal of Aerosol Science*, vol. 35, pp. 1313–1332, nov 2004.

[54] R. Burlica, R. Grim, K.-Y. Shih, D. Balkwill, and B. R. Locke, "Bacteria Inactivation Using Low Power Pulsed Gliding Arc Discharges with Water Spray," *Plasma Processes and Polymers*, vol. 7, no. 8, pp. 640–649, 2010.

[55] K. Hensel, K. Kučerová, B. Tarabová, M. Janda, Z. Machala, K. Sano, C. T. Mihai, M. Ciorpac, L. D. Gorgan, R. Jijie, *et al.*, "Effects of air transient spark discharge and helium plasma jet on water, bacteria, cells, and biomolecules," *Biointerphases*, vol. 10, no. 2, p. 029515, 2015.

[56] J. Ehlbeck, U. Schnabel, M. Polak, J. Winter, T. von Woedtke, R. Brandenburg, T. von dem Hagen, and K.-D. Weltmann, "Low temperature atmospheric pressure plasma sources for microbial decontamination," *Journal of Physics D: Applied Physics*, vol. 44, p. 013002, jan 2011.

[57] X. Lu, M. Laroussi, and V. Puech, "On atmospheric-pressure non-equilibrium plasma jets and plasma bullets," *Plasma Sources Science and Technology*, vol. 21, p. 034005, jun 2012.

[58] G. M. Wang, P. P. Sun, H. Pan, G. P. Ye, K. Sun, J. Zhang, J. Pan, and J. Fang, "Inactivation of Candida albicans Biofilms on Polymethyl Methacrylate and Enhancement of the Drug Susceptibility by Cold Ar/O2 Plasma Jet," *Plasma Chemistry and Plasma Processing*, pp. 1–14,

2015.

[59] N. Allen and A. Ghaffar, "Propagation of positive streamers over insulating surfaces in air," in *Conference on Electrical Insulation and Dielectric Phenomena, Annual Report.*, pp. 447–450, 1995.

[60] M. Akyuz, L. Gao, V. Cooray, T. G. Gustavsson, S. M. Gubanski, and A. Larsson, "Positive streamer discharges along insulating surfaces," *IEEE Transactions on Dielectrics and Electrical Insulation*, vol. 8, no. 6, pp. 902–910, 2001.

[61] A. Sobota, A. Lebouvier, N. Kramer, E. van Veldhuizen, W. Stoffels, F. Manders, and M. Haverlag, "Speed of streamers in argon over a flat surface of a dielectric," *Journal of Physics D: Applied Physics*, vol. 42, no. 1, p. 015211, 2008.

[62] X. Lu, G. V. Naidis, M. Laroussi, and K. Ostrikov, "Guided ionization waves : Theory and experiments," *Physics Reports*, vol. 540, pp. 123–166, 2014.

[63] M. Laroussi and F. Leipold, "Evaluation of the roles of reactive species , heat , and UV radiation in the inactivation of bacterial cells by air plasmas at atmospheric pressure," *International Journal of Mass Spectrometry*, vol. 233, pp. 81–86, 2004.

[64] D. B. Graves, "Low temperature plasma biomedicine: A tutorial review," *Physics of Plasmas*, vol. 21, p. 080901, aug 2014.

[65] M. Laroussi, "Low-temperature plasmas for medicine?," *Plasma Science, IEEE Transactions on*, vol. 37, no. 6, pp. 714–725, 2009.

[66] B. R. Locke, P. Lukeš, and J.-L. Brisset, *Elementary Chemical and Physical Phenomena in Electrical Discharge Plasma in Gas-Liquid Environments and in Liquids*, pp. 183–242. Wiley-VCH Verlag GmbH & Co. KGaA, first ed., 2012.

[67] M. J. Pavlovich, T. Ono, C. Galleher, B. Curtis, D. S. Clark, Z. Machala, and D. B. Graves, "Air spark-like plasma source for antimicrobial NO x generation," *Journal of Physics D: Applied Physics*, vol. 47, p. 505202, dec 2014.

[68] D. A. Mendis, M. Rosenberg, and F. Azam, "A note on the possible electrostatic disruption of bacteria," *IEEE Transactions on Plasma Science*, vol. 28, no. 4, pp. 1304–1306, 2000.

[69] M. Laroussi, D. A. Mendis, and M. Rosenberg, "Plasma interaction with microbes," *New Journal of Physics*, vol. 5, no. 03, pp. 1–10, 2003.

[70] B. M. Chassy, A. Mercenier, and J. Flickinger, "Transformation bacteria by electroporation," *Trends in Biotechnology*, vol. 6, no. 12, pp. 303–309, 1988.

[71] T. Y. Tsong, "Electroporation of cell membranes," *Biophysical Journal*, vol. 60, no. 2, pp. 297–306, 1991.

[72] J. C. Weaver and Y. A. Chizmadzhev, "Theory of electroporation: A review," *Bioelectrochemistry and Bioenergetics*, vol. 41, no. 2, pp. 135–160, 1996.

[73] J. Teissie, M. Golzio, and M. P. Rols, "Mechanisms of cell membrane electropermeabilization: A minireview of our present (lack of ?) knowledge," *Biochimica et Biophysica Acta - General Subjects*, vol. 1724, no. 3, pp. 270–280, 2005.

[74] A. Pareilleux and N. Sicard, "Lethal effects of electric current on Escherichia coli.," *Applied microbiology*, vol. 19, no. 3, pp. 421–424, 1970.

[75] W. K. Liu, M. R. W. Brown, and T. S. J. Elliott, "Mechanisms of the bactericidal activity of

low amperage electric current (DC)," *Journal of Antimicrobial Chemotherapy*, vol. 39, no. 6, pp. 687–695, 1997.

[76] J. W. Costerton, B. Ellis, K. Lam, F. Johnson, and A. E. Khoury, "Mechanism of electrical enhancement of efficacy of antibiotics in killing biofilm bacteria," *Antimicrobial Agents and Chemotherapy*, vol. 38, no. 12, pp. 2803–2809, 1994.

[77] Z. Machala, L. Chládeková, and M. Pelach, "Plasma agents in bio-decontamination by DC discharges in atmospheric air," *Journal of Physics D: Applied Physics*, vol. 43, no. 22, p. 222001, 2010.

[78] G. Brelles-mariño, "Challenges in Biofilm Inactivation : The Use of Cold Plasma as a New Approach," *Journal of Bioprocessing & Biotechniques*, vol. 2, no. 4, pp. 2–5, 2012.

[79] P. Wood, M. Jones, M. Bhakoo, and P. Gilbert, "A novel strategy for control of microbial biofilms through generation of biocide at the biofilm-surface interface," *Applied and Environmental Microbiology*, vol. 62, no. 7, pp. 2598–2602, 1996.

[80] G. Rajagopal, S. Maruthamuthu, S. Mohanan, and N. Palaniswamy, "Biocidal effects of photocatalytic semiconductor tio 2," *Colloids and Surfaces B: Biointerfaces*, vol. 51, no. 2, pp. 107–111, 2006.

[81] A. Zelaya, K. Vandervoort, and G. B.-M. no, "Battling bacterial biofilms with gas discharge plasma," in *NATO Science for Peace and Security Series A: Chemistry and Biology* (Z. Machala *et al.*, eds.), pp. 135–148, Springer, 2012.

[82] V. Arora, V. Nikhil, N. Suri, and P. Aurora, "Cold Atmospheric Plasma (CAP) In Dentistry," *Dentistry*, vol. 4, no. 1, pp. 1–5, 2014.

[83] S. Cha and Y.-S. Park, "Plasma in dentistry," *Clinical Plasma Medicine*, vol. 2, pp. 4–10, jul 2014.

[84] S. Rupf, A. Lehmann, M. Hannig, B. Schafer, A. Schubert, U. Feldmann, and A. Schindler, "Killing of adherent oral microbes by a non-thermal atmospheric plasma jet," *Journal of Medical Microbiology*, vol. 59, pp. 206–212, 2010.

[85] Z. Xiong, Y. Cao, X. Lu, and T. Du, "Plasmas in Tooth Root Canal," *IEEE Transactions on Plasma Science*, vol. 39, no. 11, pp. 2968–2969, 2011.

[86] L. van den Bedem, R. Sladek, M. Steinbuch, and E. Stoffels-Adamowicz, "Plasma treatment of S. mutans biofilms cultured in a simulated dental cavity model," (Eindhoven, the Netherlands), XXVIIth ICPIG, 18 - 22 July 2005.

[87] T. Du, J. Ma, P. Yang, Z. Xiong, X. Lu, and Y. Cao, "Evaluation of antibacterial effects by atmospheric pressure nonequilibrium plasmas against Enterococcus faecalis biofilms in vitro.," *Journal of endodontics*, vol. 38, pp. 545–9, Apr. 2012.

[88] J. Pan, K. Sun, Y. Liang, P. Sun, X. Yang, J. Wang, J. Zhang, W. Zhu, J. Fang, and K. H. Becker, "Cold plasma therapy of a tooth root canal infected with Enterococcus faecalis biofilms in vitro.," *Journal of endodontics*, vol. 39, pp. 105–10, Jan. 2013.

[89] Y. Liang, Y. Li, K. Sun, Q. Zhang, W. Li, and W. Zhu, "Plasma Thorns : Atmospheric Pressure Non-Thermal Plasma Source for Dentistry Applications," *Plasma Processes and Polymers*, vol. 12, no. 10, pp. 1186–1187, 2015.

[90] C. Schaudinn, D. Jarmillo, M. Freire, P. Sedghizadeh, A. Nguyen, P. Webster, J. W. Costerton,

and C. Jiang, "Evaluation of a non-thermal plasma needle to eliminate ex vivo biofilms in root canals of extracted human teeth," *International endodontic journal*, vol. 46, no. 20, pp. 930–937, 2013.

[91] I. Koban, A. Kramer, K.-D. Weltmann, and T. Kocher, "Medical plasma in dentistry: A future therapy for peri-implantitis," in *NATO Science for Peace and Security Series A: Chemistry and Biology* (Z. Machala *et al.*, eds.), pp. 191–200, Springer, 2012.

[92] I. Koban, R. Matthes, N.-O. Hübner, A. Welk, P. Meisel, B. Holtfreter, R. Sietmann, E. Kindel, K.-D. Weltmann, A. Kramer, and T. Kocher, "Treatment of Candida albicans biofilms with low-temperature plasma induced by dielectric barrier discharge and atmospheric pressure plasma jet," *New Journal of Physics*, vol. 12, p. 073039, 2010.

[93] I. Koban, B. Holtfreter, N.-O. Hübner, R. Matthes, R. Sietmann, E. Kindel, K.-D. Weltmann, A. Welk, A. Kramer, and T. Kocher, "Antimicrobial efficacy of non-thermal plasma in comparison to chlorhexidine against dental biofilms on titanium discs in vitro - proof of principle experiment.," *Journal of clinical periodontology*, vol. 38, pp. 956–65, Oct. 2011.

[94] S. Rupf, A. N. Idlibi, F. A. Marrawi, M. Hannig, A. Schubert, L. Von Mueller, W. Spitzer, H. Holtmann, A. Lehmann, A. Rueppell, and A. Schindler, "Removing biofilms from microstructured titanium ex vivo: a novel approach using atmospheric plasma technology.," *PLoS ONE*, vol. 6, p. e25893, Jan. 2011.

[95] T. Maisch, T. Shimizu, Y.-F. Li, J. Heinlin, S. Karrer, G. Morfill, and J. L. Zimmermann, "Decolonisation of MRSA, S. aureus and E. coli by cold-atmospheric plasma using a porcine skin model in vitro.," *PloS one*, vol. 7, p. e34610, Jan. 2012.

[96] W.-D. Zhu, P. Sun, S. Yu, H. Wu, J. Zhang, J. Fang, Y. Sun, and W. Liu, "Inactivation of candida strains in planktonic and biofilm forms using a direct current, atmospheric-pressure cold plasma micro-jet," in *NATO Science for Peace and Security Series A: Chemistry and Biology* (Z. Machala *et al.*, eds.), pp. 201–214, Springer, 2012.

[97] G. C. Kim, H. W. Lee, J. H. Byun, J. Chung, Y. C.Jeon, and J. K. Lee, "Dental applications of low-temperature nonthermal plasmas," *Plasma Processes and Polymers*, vol. 10, pp. 199–206, 2013.

[98] G. Fridman, M. Peddinghaus, H. Ayan, A. Fridman, M. Balasubramanian, A. Gutsol, A. Brooks, and G. Friedman, "Blood coagulation and living tissue sterilization by floating-electrode dielectric barrier discharge in air," *Plasma Chem Plasma Process*, vol. 26, pp. 425–442, 2006.

[99] G. Isbary, "Cold atmospheric plasma for clinical purposes: Promising results in patients and future applications," in *Plasma for Bio-Decontamination, Medicine and Food Security* (Z. Machala *et al.*, eds.), NATO Science for Peace and Security Series A: Chemistry and Biology, pp. 311–319, Springer, 2012.

[100] J. Pan, X. Yang, K. Sun, J. Wang, P. Sun, H. Wu, K. H. Becker, W. Zhu, J. Zhang, and J. Fang, "Tooth Bleaching Using Low Concentrations of Hydrogen Peroxide in the Presence of a Nonthermal Plasma Jet," *IEEE Transactions on Plasma Science*, vol. 41, no. 2, pp. 325–329, 2012.

[101] H. W. Lee, G. J. Kim, J. M. Kim, J. K. Park, J. K. Lee, and G. C. Kim, "Tooth bleaching with nonthermal atmospheric pressure plasma.," *Journal of endodontics*, vol. 35, pp. 587–91,

apr 2009.

[102] J. Wang, X. Yang, K. Sun, P. Sun, J. Pan, W. Zhu, K. H. Becker, J. Zhang, and J. Fang, "Tooth Enamel Evaluation After Tooth Bleaching With Hydrogen Peroxide Assisted by a DC Nonthermal Atmospheric-Pressure Plasma Jet," *IEEE Transactions on Plasma Science*, vol. 40, no. 9, pp. 2157–2162, 2012.

[103] Q. S. Yu, H. L. nad A.C. Ritts, B. Yang, M. Chen, L. Hong, C. Xu, X. Yao, and Y. Wang, "Non-thermal atmospheric plasma treatment for deactivation of oral bacteria and improvement of dental composite restoration," in *NATO Science for Peace and Security Series A: Chemistry and Biology* (Z. Machala *et al.*, eds.), pp. 215–228, Springer, 2012.

[104] A. Lehmann, A. Rueppell, A. Schindler, I.-M. Zylla, H. J. Seifert, F. Nothdurft, M. Hannig, and S. Rupf, "Modification of enamel and dentin surfaces by non-thermal atmospheric plasma," *Plasma Processes and Polymers*, vol. 10, pp. 262–270, 2013.

[105] R. Sladek, S. Filoche, C. Sissons, and E. Stoffels, "Treatment of streptococcus mutans biofilms with a nonthermal atmospheric plasma," *Letters in Applied Microbiology*, vol. 45, pp. 318–323, 2007.

[106] R. Matthes, L. Jablonowski, I. Koban, A. Quade, N.-O. Hübner, R. Schlueter, K.-D. Weltmann, T. von Woedtke, A. Kramer, and T. Kocher, "In vitro treatment of candida albicans biofilms on denture base material with volume dielectric barrier discharge plasma (vdbd) compared with common chemical antiseptics," *Clinical oral investigations*, vol. 19, no. 9, pp. 2319–2326, 2015.

[107] K. Fricke, I. Koban, H. Tresp, L. Jablonowski, K. Schröder, A. Kramer, K.-D. Weltmann, T. Von Woedtke, and T. Kocher, "Atmospheric Pressure Plasma: A High-Performance Tool for the Efficient Removal of Biofilms," *PLoS ONE*, vol. 7, p. e42539, Jan. 2012.

[108] R. Matthes, I. Koban, C. Bender, K. Masur, E. Kindel, K.-D. Weltmann, T. Kocher, A. Kramer, and N.-O. Hubner, "Antimicrobial efficacy of an atmospheric pressure plasma jet against biofilms of Pseudomonas aeruginosa and Staphylococcus epidermidis," *Plasma Processes and Polymers*, vol. 10, pp. 161–166, 2013.

[109] N.-O. Hübner, R. Matthes, I. Koban, C. Rändler, G. Müller, C. Bender, E. Kindel, T. Kocher, and A. Kramer, "Efficacy of chlorhexidine, polihexanide and tissue-tolerable plasma against Pseudomonas aeruginosa biofilms grown on polystyrene and silicone materials.," *Skin Pharmacology and Physiology*, vol. 23, pp. 28–34, Jan. 2010.

[110] J. Kamgang, R. Briandet, J. Herry, J. Brisset, and M. Naïtali, "Destruction of planktonic, adherent and biofilm cells of staphylococcus epidermidis using a gliding discharge in humid air," *Journal of Applied Microbiology*, vol. 103, pp. 621–628, 2007.

[111] S. Ermolaeva, O. Petrov, N. Zigangirova, M. Vasiliev, E. Sysolyatina, S. Antipov, M. Alyapyshev, N. Kolkova, A. Mukhachev, B. Naroditsky, T. Shimizu, A. Grigoriev, G. Morfill, V. Fortov, and A. Gintsburg, "Low temperature atmospheric argon plasma: Diagnostics and medical applications," in *NATO Science for Peace and Security Series A: Chemistry and Biology* (Z. Machala *et al.*, eds.), pp. 163–177, Springer, 2012.

[112] S. Salehi, A. Shokri, M. R. Khani, M. Bigdeli, and B. Shokri, "Investigating effects of atmospheric-pressure plasma on the process of wound healing," *Biointerphases*, vol. 10, p. 029504, 2015.

[113] B. A. Niemira, "Cold plasma decontamination of foods," *Annual Review of Food Science and Technology*, vol. 3, no. 1, pp. 125–142, 2012.

[114] M. Vleugels, G. Shama, X. Deng, E. Greenacre, T. Brocklehurst, and M. Kong, "Atmospheric plasma inactivation of biofilm-forming bacteria for food safety control," *IEEE Transactions on Plasma Science*, vol. 33, pp. 824–828, apr 2005.

[115] D. Ziuzina, S. Patil, P. J. Cullen, K. M. Keener, and P. Bourke, "Atmospheric cold plasma inactivation of Escherichia coli in liquid media inside a sealed package.," *Journal of applied microbiology*, vol. 114, pp. 778–87, Mar. 2013.

[116] N. N. Misra, B. K. Tiwari, K. S. M. S. Raghavarao, and P. J. Cullen, "Nonthermal Plasma Inactivation of Food-Borne Pathogens," *Food Engineering Reviews*, vol. 3, no. 3-4, pp. 159–170, 2011.

[117] G. Shama and M. G. Kong, "Prospects for treating foods with cold atmospheric gas plasmas," in *NATO Science for Peace and Security Series A: Chemistry and Biology* (Z. Machala *et al.*, eds.), pp. 433–444, Springer, 2012.

[118] S. Choi, P. Puligundla, and C. Mok, "Corona discharge plasma jet for inactivation of Escherichia coli O157:H7 and Listeria monocytogenes on inoculated pork and its impact on meat quality attributes," *Annals of Microbiology*, 2015.

[119] B. a. Niemira, G. Boyd, and J. Sites, "Cold Plasma Rapid Decontamination of Food Contact Surfaces Contaminated with Salmonella Biofilms," *Journal of Food Science*, pp. n/a–n/a, apr 2014.

[120] N. Abramzon, J. C. Joaquin, J. Bray, and G. Brelles-Mariño, "Biofilm Destruction by RF High-Pressure Cold Plasma Jet," *IEEE Transactions on Plasma Science*, vol. 34, no. 4, pp. 1304–1309, 2006.

[121] M. H. Lee, B. J. Park, S. C. Jin, D. Kim, I. Han, J. Kim, S. O. Hyun, K.-H. Chung, and J.-C. Park, "Removal and sterilization of biofilms and planktonic bacteria by microwave-induced argon plasma at atmospheric pressure," *New Journal of Physics*, vol. 11, p. 115022, 2009.

[122] J. C. Joaquin, C. Kwan, N. Abramzon, K. Vandervoort, and G. Brelles-Marino, "Is gas-discharge plasma a new solution to the old problem of biofilm inactivation?," *Microbiology*, vol. 155, pp. 724–732, 2009.

[123] M. Salamitou, S.and Kirkpatrick, H. Ly, G. Leblon, E. Odic, and M. DuBow, "Augmented survival of bacteria within biofilms to exposure to an atmospheric pressure non-thermal plasma source," *Biotechnology*, vol. 8, pp. 228–234, 2009.

[124] S. G. Joshi, M. Paff, G. Friedman, G. Fridman, A. Fridman, and A. D. Brooks, "Control of methicillin-resistant staphylococcus aureus in planktonic form and biofilms: A biocidal efficacy study of nonthermal dielectric-barrier discharge plasma," *American Journal of Infection Control*, vol. 38, pp. 293–301, 2010.

[125] A. J. Zelaya, G. Stough, N. Rad, K. Vandervoort, and G. Brelles-Mariño, "Pseudomonas aeruginosa Biofilm Inactivation: Decreased Cell Culturability, Adhesiveness to Surfaces, and Biofilm Thickness Upon High-Pressure Nonthermal Plasma Treatment.," *IEEE transactions on plasma science. IEEE Nuclear and Plasma Sciences Society*, vol. 38, no. 12, pp. 3398–3403, 2010.

[126] L. Xu, Y. Tu, Y. Yu, M. Tan, J. Li, and H. Chen, "Augmented survival of Neisseria gonorrhoeae

within biofilms : exposure to atmospheric pressure non-thermal plasmas," *European Journal of Clinical Microbiology & Infectious Diseases*, vol. 30, pp. 25–31, 2011.

[127] Y. Akishev, N. Trushkin, M. Grushin, A. Petryakov, V. Karaľnik, E. Kobzev, V. Kholodenko, V. Chugunov, G. Kireev, Y. Rakitsky, and I. Irkhina, "Inactivation of microorganisms in model biofilms by an atmospheric pressure pulsed non-thermal plasma," in *NATO Science for Peace and Security Series A: Chemistry and Biology* (Z. Machala *et al.*, eds.), pp. 149–161, Springer, 2012.

[128] F. Marchal, H. Robert, N. Merbahi, C. Fontagné-Faucher, M. Yousfi, C. E. Romain, O. Eichwald, C. Rondel, and B. Gabriel, "Inactivation of gram-positive biofilms by low-temperature plasma jet at atmospheric pressure," *Journal of Physics D: Applied Physics*, vol. 45, p. 345202, 2012.

[129] X. Pei, X. Lu, J. Liu, D. Liu, Y. Yang, K. Ostrikov, and P. K. Chu, "Inactivation of a 25.5 μm Enterococcus faecalis biofilm by a room-temperature, battery-operated, handheld air plasma jet," *Journal of Physics D: Applied Physics*, vol. 45, p. 165205, 2012.

[130] M. Y. Alkawareek, Q. T. Algwari, S. P. Gorman, W. G. Graham, D.O'Connell, and B. F. Gilmore, "Application of atmospheric pressure nonthermal plasma for the in vitro eradication of bacterial biofilms," *FEMS Immunol Med Microbiol*, vol. 65, pp. 381–384, 2012.

[131] M. Y. Alkawareek, Q. T. Algwari, G. Laverty, S. P. Gorman, W. G. Graham, D.O'Connell, and B. F. Gilmore, "Eradication of pseudomonas aeruginosa biofilms by atmospheric pressure non-thermal plasma," *PLoS ONE*, vol. 7, p. e44289, 2012.

[132] M. Y. Alkawareek, S. P. Gorman, W. G. Graham, and B. F. Gilmore, "Eradication of marine biofilms by atmospheric pressure non-thermal plasma: A potential approach to control biofouling?," *International Biodeterioration & Biodegradation*, vol. 86, pp. 14–18, aug 2014.

[133] K. G. Vandervoort and G. Brelles-Mariño, "Plasma-Mediated Inactivation of Pseudomonas aeruginosa Biofilms Grown on Borosilicate Surfaces under Continuous Culture System.," *PloS one*, vol. 9, p. e108512, jan 2014.

[134] L. Taghizadeh, G. Brackman, A. Nikiforov, J. V. D. Mullen, C. Leys, and T. Coenye, "Inactivation of Biofilms Using a Low Power Atmospheric Pressure Argon Plasma Jet ; the Role of Entrained Nitrogen," *Plasma Processes and Polymers*, vol. 12, pp. 75–81, 2015.

[135] Z. Xu, J. Shen, Z. Zhang, J. Ma, R. Ma, Y. Zhao, Q. Sun, S. Qian, H. Zhang, L. Ding, C. Cheng, P. K. Chu, and W. Xia, "Inactivation Effects of Non-Thermal Atmospheric-Pressure Helium Plasma Jet on Staphylococcus aureus Biofilms," *Plasma Processes and Polymers*, vol. 12, no. 8, pp. 827–835, 2015.

[136] A. C. O. C. Doria, C. D. P. C. Sorge, T. B. Santos, J. Brandão, P. A. R. Gonçalves, H. S. Maciel, S. Khouri, and R. S. Pessoa, "Application of post-discharge region of atmospheric pressure argon and air plasma jet in the contamination control of Candida albicans biofilms," *Research on Biomedical Engineering*, no. Atcc 10231, pp. 0–0, 2015.

[137] Z. Ben Belgacem, G. Carré, M. Boudifa, E. Charpentier, B. Cawe, and M. Gellé, "Effectiveness of Non-Thermal O2–N2 Plasma on P. aeruginosa Multilayer Biofilms Cultured on Hydroxyapatite," *Irbm*, vol. 1, pp. 1–7, 2016.

[138] A. Mai-Prochnow, M. Bradbury, K. Ostrikov, and A. B. Murphy, "Pseudomonas aeruginosa

Biofilm Response and Resistance to Cold Atmospheric Pressure Plasma Is Linked to the Redox-Active Molecule Phenazine.," *PloS one*, vol. 10, p. e0130373, jan 2015.

[139] B. F. Gilmore, "The matrix revisited : understanding the role of extracellular matrix components in biofilm tolerance to atmospheric pressure non-thermal plasma exposure," in *22nd International symposium on Plasma Chemistry 5-10 July*, (Antwerp (Belgium)), pp. 5–7, 2015.

[140] P. B. Flynn, A. Busetti, N. H. Alshraiedeh, W. G. Graham, S. P. Gorman, and B. F. Gilmore, "Atmospheric pressure non-thermal plasma-mediated attenuation of acyl homoserine lactone-dependent bacterial cell-cell communication (quorum sensing): a possible anti-virulence approach in chronic infection," in *22nd International symposium on Plasma Chemistry 5-10 July*, (Antwerp (Belgium)), pp. 1–4, 2015.

[141] M. Du, J. Chen, X. Zhang, A. Li, Y. Li, and Y. Wang, "Retention of virulence in a viable but nonculturable Edwardsiella tarda isolate," *Applied and Environmental Microbiology*, vol. 73, no. 4, pp. 1349–1354, 2007.

[142] R. R. Colwell, "Viable but nonculturable bacteria: a survival strategy.," *Journal of infection and chemotherapy : official journal of the Japan Society of Chemotherapy*, vol. 6, pp. 121–5, June 2000.

[143] J. Oliver, "Formation of viable but nonculturable cells," *Springer US*, pp. 239–272, 1993.

[144] M. probes, "FilmTracer LIVE/DEAD Biofilm Viability Kit," 2009.

[145] E. Peeters, H. J. Nelis, and T. Coenye, "Comparison of multiple methods for quantification of microbial biofilms grown in microtiter plates," *Journal of Microbiological Methods*, vol. 72, no. 2, pp. 157–165, 2008.

[146] N. W. Roehm, G. H. Rodgers, S. M. Hatfield, and A. L. Glasebrook, "An improved colorimetric assay for cell proliferation and viability utilizing the tetrazolium salt xtt," *Journal of immunological methods*, vol. 142, no. 2, pp. 257–265, 1991.

[147] J. G. Davis, *The Resazurin Test: A Review of Recent Work*. NIRD, 1940.

[148] J. O'Brien, I. Wilson, T. Orton, and F. Pognan, "Investigation of the alamar blue (resazurin) fluorescent dye for the assessment of mammalian cell cytotoxicity," *European Journal of Biochemistry*, vol. 267, no. 17, pp. 5421–5426, 2000.

[149] Promega, "BacTiter-Glo Microbial Cell Viability Assay Technical Bulletin," 2009.

[150] K. G. Vandervoort, "Plasma Interactions With Bacterial Biofilms as Visualized Through Atomic Force Microscopy.pdf," *IEEE Transactions on Plasma Science*, vol. 36, no. 4, pp. 1296–1297, 2008.

[151] Z. Machala, I. Jedlovský, L. Chládeková, B. Pongrác, D. Giertl, M. Janda, L. Šikurová, and P. Polčic, "DC discharges in atmospheric air for bio-decontamination – spectroscopic methods for mechanism identification," *The European Physical Journal D*, vol. 54, pp. 195–204, feb 2009.

[152] V. Fantova, K. Bujaček, V. Kříha, and J. Julák, "Inactivation of Candida albicans by corona discharge: The increase of inhibition zones area after far subsequent exposition," *Acta Polytechnica*, vol. 53, no. 2, pp. 148–151, 2013.

[153] V. Scholtz and J. Julak, "Plasma Jetlike Point-to-Point Electrical Discharge in Air and Its Bactericidal Properties," *IEEE Transactions on Plasma Science*, vol. 38, no. 8, pp. 1978–1980, 2010.

[154] C. Mok, T. Lee, and P. Puligundla, "Afterglow corona discharge air plasma (ACDAP) for inactivation of common food-borne pathogens," *Food Research International*, vol. 69, pp. 418–423, mar 2015.

[155] R. Bussiahn, R. Brandenburg, T. Gerling, E. Kindel, H. Lange, N. Lembke, K. D. Weltmann, T. Von Woedtke, and T. Kocher, "The hairline plasma: An intermittent negative dc-corona discharge at atmospheric pressure for plasma medical applications," *Applied Physics Letters*, vol. 96, no. 14, pp. 1–3, 2010.

[156] V. Joubert, C. Cheype, J. Bonnet, D. Packan, J.-P. Garnier, J. Teissié, and V. Blanckaert, "Inactivation of Bacillus subtilis var. niger of both spore and vegetative forms by means of corona discharges applied in water.," *Water research*, vol. 47, pp. 1381–9, Mar. 2013.

[157] J. Julák, V. Scholtz, S. Kotúčová, and O. Janoušková, "The persistent microbicidal effect in water exposed to the corona discharge," *Physica Medica*, vol. 28, no. 3, pp. 230–239, 2012.

[158] B. Pongrác and Z. Machala, "Electrospraying of water with streamer corona discharge," *Plasma Science, IEEE Transactions on*, vol. 39, no. 11, pp. 2664–2665, 2011.

[159] C. N. Satterfield and A. H. Bonnell, "Interferences in titanium sulfate method for hydrogen peroxide," *Analytical Chemistry*, vol. 27, no. 7, pp. 1174–1175, 1955.

[160] G. Alsterberg, "Methods for the determination of elementary oxygen dissolved in water in the presence of nitrite," *Biochem. Z*, vol. 159, p. 36, 1925.

[161] J. Hoigné and H. Bader, "Bestimmung von ozon und chlordioxid in wasser mit der indigo-methode," *vom Wasser*, vol. 55, pp. 261–279, 1980.

[162] B. Tarabová, P. Lukeš, K. Tarabová, K. Hensel, L. Šikurová, and Z. Machala, "Detection of ROS/RNS in water activated by air transient spark discharge," in *20th Symposium on Applications of Plasma Processes SAPP XX and COST TD1208 Workshop on Application of Gaseous Plasma with Liquids, Tatranská Lomnica (Slovakia), January 17-22*, pp. 27–31, 2015.

[163] T. Shimizu, Y. Sakiyama, D. B. Graves, J. L. Zimmermann, and G. E. Morfill, "The dynamics of ozone generation and mode transition in air surface micro-discharge plasma at atmospheric pressure," *New Journal of Physics*, vol. 14, p. 103028, 2012.

[164] M. Meselson and R. Yuan, "Dna restriction enzyme from e. coli.," *Nature*, vol. 217, no. 5134, p. 1110, 1968.

[165] T. Baba, T. Ara, M. Hasegawa, Y. Takai, Y. Okumura, M. Baba, K. A. Datsenko, M. Tomita, B. L. Wanner, and H. Mori, "Construction of escherichia coli k-12 in-frame, single-gene knockout mutants: the keio collection," *Molecular systems biology*, vol. 2, no. 1, 2006.

[166] J. B. Matsen, "E. coli genotypes," march 2013.

[167] F. De Chaumont, S. Dallongeville, N. Chenouard, N. Hervé, S. Pop, T. Provoost, V. Meas-Yedid, P. Pankajakshan, T. Lecomte, Y. Le Montagner, *et al.*, "Icy: an open bioimage informatics platform for extended reproducible research," *Nature methods*, vol. 9, no. 7, pp. 690–696, 2012.

[168] J. H. Merritt, D. E. Kadouri, and G. A. O'Toole, "Growing and analyzing static biofilms," *Current protocols in microbiology*, pp. 1B–1, 2005.

[169] K. Hensel, Z. Machala, and P. Tardiveau, "Capillary microplasmas for ozone generation," *The European Physical Journal Applied Physics*, vol. 47, no. 02, p. 22813, 2009.

[170] J. C. Morris, "Chlorination and disinfection—state of the art," *Journal (American Water Works Association)*, pp. 769–774, 1971.

[171] W. T. Broadwater, R. C. Hoehn, and P. H. King, "Sensitivity of three selected bacterial species to ozone.," *Applied microbiology*, vol. 26, pp. 391–3, sep 1973.

[172] P. A. Hyslop, D. B. Hinshaw, I. U. Scraufstatter, C. G. Cochrane, S. Kunz, and K. Vosbeck, "Hydrogen peroxide as a potent bacteriostatic antibiotic: implications for host defense," *Free Radical Biology and Medicine*, vol. 19, no. I, pp. 31–37, 1995.

[173] R. S. Dykhuizen, R. Frazer, C. Duncan, C. C. Smith, M. Golden, B. N., and C. Leifert, "Antimicrobial effect of acidified nitrite on gut pathogens: importance of dietary nitrate in host defense.," *Antimicrobial Agents and Chemotherapy*, vol. 40, no. 6, pp. 1422–1425, 1996.

[174] P. Lukes, E. Dolezalova, I. Sisrova, and M. Clupek, "Aqueous-phase chemistry and bactericidal effects from an air discharge plasma in contact with water: evidence for the formation of peroxynitrite through a pseudo-second-order post-discharge reaction of H 2 O 2 and HNO 2," *Plasma Sources Science and Technology*, vol. 23, p. 015019, feb 2014.

[175] J. Xu, X. Xu, and W. Verstraete, "The bactericidal effect and chemical reactions of acidified nitrite under conditions simulating the stomach," *Journal of applied microbiology*, vol. 90, pp. 523–529, 2001.

[176] D. B. Graves, "The emerging role of reactive oxygen and nitrogen species in redox biology and some implications for plasma applications to medicine and biology," *Journal of Physics D: Applied Physics*, vol. 45, no. 26, p. 263001, 2012.

[177] G. Fridman, A. D. Brooks, M. Balasubramanian, A. Fridman, A. Gutsol, V. N. Vasilets, H. Ayan, and G. Friedman, "Comparison of direct and indirect effects of non-thermal atmospheric-pressure plasma on bacteria," *Plasma Processes and Polymers*, vol. 4, no. 4, pp. 370–375, 2007.

[178] B. Pongrác, *Study of the Electrospraying Effect of Water in Combination with Atmospheric Pressure Corona Discharge*. Phd thesis, Fakulta matematiky, fyziky a informatiky Univerzity Komenského v Bratislave, 2014.

[179] S. Perni, G. Shama, J. L. Hobman, P. a. Lund, C. J. Kershaw, G. a. Hidalgo-Arroyo, C. W. Penn, X. T. Deng, J. L. Walsh, and M. G. Kong, "Probing bactericidal mechanisms induced by cold atmospheric plasmas with Escherichia coli mutants," *Applied Physics Letters*, vol. 90, no. 7, p. 073902, 2007.

[180] A. Muela, C. Seco, E. Camafeita, I. Arana, M. Orruño, J. A. López, and I. Barcina, "Changes in Escherichia coli outer membrane subproteome under environmental conditions inducing the viable but nonculturable state," *FEMS Microbiology Ecology*, vol. 64, no. 1, pp. 28–36, 2008.

[181] N. J. Rowan, S. Espie, J. Harrower, H. Farrell, L. Marsili, J. G. Anderson, and S. J. MacGregor, "Evidence of lethal and sublethal injury in food-borne bacterial pathogens exposed to high-intensity pulsed-plasma gas discharges," *Letters in applied microbiology*, vol. 46, no. 1, pp. 80–86, 2008.

[182] E. Dolezalova and P. Lukes, "Membrane damage and active but nonculturable state in liquid cultures of Escherichia coli treated with an atmospheric pressure plasma jet," *Bioelectrochemistry*, vol. 103, pp. 7–14, 2015.

[183] R. R. Colwell, "Viable but Not Cultivable Bacteria," in *Uncultivated Microorganisms* (S. S. Epstein, ed.), vol. 10, pp. 121–129, Springer Berlin Heidelberg, 2009.

[184] E. Robert, E. Barbosa, S. Dozias, M. Vandamme, C. Cachoncinlle, R. Viladrosa, and J. M. Pouvesle, "Experimental Study of a Compact Nanosecond Plasma Gun," *Plasma Processes and Polymers*, vol. 6, pp. 795–802, nov 2009.

[185] S. Park, W. Choe, H. Kim, and J. Y. Park, "Continuum emission-based electron diagnostics for atmospheric pressure plasmas and characteristics of nanosecond-pulsed argon plasma jets," *Plasma Sources Science and Technology*, vol. 24, no. 3, p. 034003, 2015.

[186] D. Maletić, N. Puač, N. Selaković, S. Lazović, G. Malović, A. Dordević, and Z. L. Petrović, "Time-resolved optical emission imaging of an atmospheric plasma jet for different electrode positions with a constant electrode gap," *Plasma Sources Science and Technology*, vol. 24, no. 2, p. 025006, 2015.

[187] K.-D. Weltmann, J. Winter, M. Polak, and T. Ehlbeck, J. andVon Woedtke, "Atmospheric pressure plasmas for decontamination of complex medical devices," in *NATO Science for Peace and Security Series A: Chemistry and Biology* (Z. Machala *et al.*, eds.), pp. 3–16, Springer, 2012.

[188] J. Pollak, M. Moisan, D. Kéroack, J. Séguin, and J. Barbeau, "Plasma Sterilisation within Long and Narrow Bore Dielectric Tubes Contaminated with Stacked Bacterial Spores," *Plasma Processes and Polymers*, vol. 5, pp. 14–25, Jan. 2008.

[189] A.-M. Pointu, A. Ricard, E. Odic, and M. Ganciu, "Nitrogen Atmospheric Pressure Post Discharges for Surface Biological Decontamination inside Small Diameter Tubes," *Plasma Processes and Polymers*, vol. 5, pp. 559–568, Aug. 2008.

[190] J. Lefebvre and A. Ricard, "Excitation de n2, o2 eh2 en impuretés dans des décharges de gaz rares he, ne et ar," *Revue de Physique Appliquée*, vol. 10, no. 3, pp. 137–142, 1975.

[191] C. Laux, T. Spence, C. Kruger, and R. Zare, "Optical diagnostics of atmospheric pressure air plasmas," *Plasma Sources Science and Technology*, vol. 12, no. 2, p. 125, 2003.

[192] D. Hanahan, "Techniques for transformation of e. coli," *DNA cloning*, vol. 1, pp. 109–135, 1985.

[193] B. Dodet, E. Odic, A. Goldman, M. Goldman, and D. Renard, "Hydrogen peroxide formation by discharges in argon/water vapor mixtures at atmospheric pressure," *Journal of Advanced Oxidation Technologies*, vol. 8, no. 1, pp. 91–97, 2005.

[194] E. Van Veldhuizen and W. Rutgers, "Pulsed positive corona streamer propagation and branching," *Journal of Physics D: Applied Physics*, vol. 35, no. 17, p. 2169, 2002.

[195] K. Kozlov, E. Odic, P. Tatarenko, B. Dodet, G. Fedoseev, M. Kirkpatrick, V. Samoilovich, and M. Ganciu, "Radiation kinetics and chemical reactivity of barrier discharges in humid argon," in *10th International Symp. on High Pres. Low Temp. Plasma*, pp. 124–127, 2006.

[196] C. Hibert, I. Gaurand, O. Motret, and J. Pouvesle, "[oh (x)] measurements by resonant absorption spectroscopy in a pulsed dielectric barrier discharge," *Journal of applied physics*, vol. 85, no. 10, pp. 7070–7075, 1999.

[197] X. Lu and M. Laroussi, "Dynamics of an atmospheric pressure plasma plume generated by submicrosecond voltage pulses," *Journal of Applied Physics*, vol. 100, no. 6, p. 063302, 2006.

[198] G. Naidis, "Modelling of streamer propagation in atmospheric-pressure helium plasma jets,"

Journal of Physics D: Applied Physics, vol. 43, no. 40, p. 402001, 2010.

[199] M. Potts, "Desiccation tolerance of prokaryotes.," *Microbiological reviews*, vol. 58, no. 4, pp. 755–805, 1994.

[200] D. Billi and M. Potts, "Life without water: responses of prokaryotes to desiccation," *Environmental stressors and gene responses*, vol. 1, pp. 181–192, 2000.

[201] K. P. Arjunan, V. K. Sharma, and S. Ptasinska, "Effects of atmospheric pressure plasmas on isolated and cellular dna—a review," *International journal of molecular sciences*, vol. 16, no. 2, pp. 2971–3016, 2015.

[202] K. J. Davies, "Oxidative stress, antioxidant defenses, and damage removal, repair, and replacement systems," *IUBMB life*, vol. 50, no. 4-5, pp. 279–289, 2000.

[203] W. Rutala, J. Weber, and The Healthcare Infection Control Practices Advisory Committee, "Guideline for disinfection and sterilization in healthcare facilities," *Centers for Disease Control and Prevention (CDC), Department of Health and Human Services USA, Chapel Hill, NC.*, pp. 1–158, 2008.

[204] M. Finnegan, E. Linley, S. P. Denyer, G. McDonnell, C. Simons, and J.-Y. Maillard, "Mode of action of hydrogen peroxide and other oxidizing agents: differences between liquid and gas forms," *Journal of Antimicrobial Chemotherapy*, p. dkq308, 2010.

[205] J. H. Crowe, L. M. Crowe, J. E. Carpenter, S. Petrelski, F. A. Hoekstra, P. D. Araujo, and A. D. Panek, *Anhydrobiosis: cellular adaptation to extreme dehydration*, vol. vol. II, pp. 1445–1478. Oxford University Press, 1997.

[206] M. Peak and J. Peak, "Single-strand breaks iduced in bacillus subtilis dna by ultraviolet light: Action spectrum and properties," *Photochemistry and Photobiology*, vol. 35, no. 5, pp. 675–680, 1982.

[207] M. Peak, J. Peak, M. Moehring, and R. Webs, "Ultraviolet action spectra for dna dimer induction, lethality, and mutagenesis in escherichia coli with emphasis on the uvb region," *Photochemistry and photobiology*, vol. 40, no. 5, pp. 613–620, 1984.

[208] R. G. Alscher, J. L. Donahue, and C. L. Cramer, "Reactive oxygen species and antioxidants: relationships in green cells," *Physiologia Plantarum*, vol. 100, no. 2, pp. 224–233, 1997.

[209] S.-H. Mackerness, B. Jordan, and B. Thomas, "Reactive oxygen species in the regulation of photosynthetic genes by ultraviolet-b radiation (uv-b: 280–320 nm) in green and etiolated buds of pea (pisum sativum l.)," *Journal of Photochemistry and Photobiology B: Biology*, vol. 48, no. 2, pp. 180–188, 1999.

[210] R. P. Sinha and D.-P. Häder, "Uv-induced dna damage and repair: a review," *Photochemical & Photobiological Sciences*, vol. 1, no. 4, pp. 225–236, 2002.

[211] T. Lindahl and R. D. Wood, "Quality control by dna repair," *Science*, vol. 286, no. 5446, pp. 1897–1905, 1999.

[212] A. B. Britt, "Repair of dna damage induced by ultraviolet radiation.," *Plant Physiology*, vol. 108, no. 3, p. 891, 1995.

[213] T. Lindahl, "Instability and decay of the primary structure of dna," *nature*, vol. 362, no. 6422, pp. 709–715, 1993.

[214] M. Clauß and N. Grotjohann, "Comparative mutagenesis of escherichia coli strains with different

repair deficiencies irradiated with 222-nm and 254-nm ultraviolet light," *Mutation Research/-Genetic Toxicology and Environmental Mutagenesis*, vol. 673, no. 2, pp. 83–86, 2009.

[215] M. Moisan, J. Barbeau, S. Moreau, J. Pelletier, M. Tabrizian, and L. Yahia, "Low-temperature sterilization using gas plasmas: a review of the experiments and an analysis of the inactivation mechanisms," *International journal of Pharmaceutics*, vol. 226, no. 1, pp. 1–21, 2001.

[216] D. O'Connell, L. Cox, W. Hyland, S. McMahon, S. Reuter, W. Graham, T. Gans, and F. Currell, "Cold atmospheric pressure plasma jet interactions with plasmid dna," *Applied Physics Letters*, vol. 98, no. 4, p. 043701, 2011.

[217] S. Lazović, D. Maletić, A. Leskovac, J. Filipović, N. Puač, G. Malović, G. Joksić, and Z. L. Petrović, "Plasma induced dna damage: Comparison with the effects of ionizing radiation," *Applied Physics Letters*, vol. 105, no. 12, p. 124101, 2014.

[218] M. Heise, W. Neff, O. Franken, P. Muranyi, and J. Wunderlich, "Sterilization of polymer foils with dielectric barrier discharges at atmospheric pressure," *Plasmas and polymers*, vol. 9, no. 1, pp. 23–33, 2004.

[219] N. Masoud, K. Martus, and K. Becker, "Vuv emission from a cylindrical dielectric barrier discharge in ar and in ar/n2 and ar/air mixtures," *Journal of Physics D: Applied Physics*, vol. 38, no. 11, p. 1674, 2005.

[220] J. C. Crittenden, S. Hu, D. W. Hand, and S. A. Green, "A kinetic model for h 2 o 2/uv process in a completely mixed batch reactor," *Water research*, vol. 33, no. 10, pp. 2315–2328, 1999.

[221] E. Robert, T. Darny, S. Dozias, S. Iseni, and J. M. Pouvesle, "New insights on the propagation of pulsed atmospheric plasma streams: From single jet to multi jet arrays," *Physics of Plasmas*, vol. 22, no. 12, p. 122007, 2015.

[222] J. Schindelin, I. Arganda-Carreras, E. Frise, V. Kaynig, M. Longair, T. Pietzsch, S. Preibisch, C. Rueden, S. Saalfeld, B. Schmid, *et al.*, "Fiji: an open-source platform for biological-image analysis," *Nature methods*, vol. 9, no. 7, pp. 676–682, 2012.

[223] J. Bang, A. Hong, H. Kim, L. R. Beuchat, M. S. Rhee, Y. Kim, and J.-H. Ryu, "Inactivation of escherichia coli o157: H7 in biofilm on food-contact surfaces by sequential treatments of aqueous chlorine dioxide and drying," *International journal of food microbiology*, vol. 191, pp. 129–134, 2014.

[224] R. Iibuchi, Y. Hara-Kudo, A. Hasegawa, and S. Kumagai, "Survival of salmonella on a polypropylene surface under dry conditions in relation to biofilm-formation capability," *Journal of Food Protection®*, vol. 73, no. 8, pp. 1506–1510, 2010.

[225] D. A. Hufnagel, W. H. Depas, and M. R. Chapman, "The biology of the escherichia coli extracellular matrix.," *Microbiology spectrum*, vol. 3, no. 3, 2015.

[226] A. Schmidt, K. Wende, S. Bekeschus, L. Bundscherer, A. Barton, K. Ottmüller, K.-D. Weltmann, and K. Masur, "Non-thermal plasma treatment is associated with changes in transcriptome of human epithelial skin cells," *Free radical research*, vol. 47, no. 8, pp. 577–592, 2013.

[227] D. Dobrynin, G. Fridman, G. Friedman, and A. Fridman, "Physical and biological mechanisms of direct plasma interaction with living tissue," *New Journal of Physics*, vol. 11, no. 11, p. 115020, 2009.

[228] K. Wende, K. Landsberg, U. Lindequist, K.-D. Weltmann, and T. von Woedtke, "Distinc-

tive activity of a nonthermal atmospheric-pressure plasma jet on eukaryotic and prokaryotic cells in a cocultivation approach of keratinocytes and microorganisms," *Plasma Science, IEEE Transactions on*, vol. 38, no. 9, pp. 2479–2485, 2010.

[229] B. B. Lopes, M. B. D. P. L. Kraft, J. Rehder, F. R. X. Batista, and M. B. Puzzi, "The Interactions between Non-thermal Atmospheric Pressure Plasma and Ex-vivo Dermal Fibroblasts," *Procedia Engineering*, vol. 59, pp. 92–100, jan 2013.

[230] Z. Machala, M. Janda, K. Hensel, I. Jedlovský, L. Leštinská, V. Foltin, V. Martišovitš, and M. Morvova, "Emission spectroscopy of atmospheric pressure plasmas for bio-medical and environmental applications," *Journal of Molecular Spectroscopy*, vol. 243, no. 2, pp. 194–201, 2007.

8 Appendices

Author's publications

Publications in journals

- Z. Kovalova, M. Leroy, M.J. Kirkpatrick, E. Odic, and Zdenko Machala: "Corona discharges with water electrospray for *Escherichia coli* biofilm eradication on a surface.," *Bioelectrochemistry* **112**, 91–99 (2016).
- Z. Tučeková, Z. Kovaľová, A. Zahoranová, Z. Machala, and M. Černák: "Inactivation of *Escherichia coli* on PTFE surfaces by Diffuse Coplanar Surface Barrier Discharge.," *Eur. Phys. J. Appl. Phys.*, **75**(2) 24711 (2016).
- Z. Kovalova, M. Leroy, C. Jacobs, M.J. Kirkpatrick, Z. Machala, F. Lopes, C.O. Laux, M. DuBow, and E. Odic: "Atmospheric pressure argon surface discharges propagated in long tubes: physical characterization and application to bio-decontamination.," *J. Phys. D: Appl. Phys.* **48**, 464003 (2015).
- Z. Kovaľová, M. Zahoran, A. Zahoranová, and Z. Machala: "*Streptococci* biofilm decontamination on teeth by low-temperature air plasma of DC corona discharges.," *J. Phys. D: Appl. Phys.,* **47** (22), 224014 (2014).
- Z. Kovaľová, K. Tarabová, K. Hensel, and Z. Machala: "Decontamination of *Streptococci* biofilms and Bacillus cereus spores on plastic surfaces with DC and pulsed corona discharges.," *Eur. Phys. J. Appl. Phys.,* **61**, 24306 (2013).
- Z. Machala, B. Tarabová, M. Pelach, Z. Šipoldová, K. Hensel, M. Janda, and L. Šikurová: "Bio-Decontamination of Water and Surfaces by DC Discharges in Atmospheric Air.," *Chapter 3 in: Plasma for Bio-decontamination, Medicine and Food Security,* Dordrecht: Springer (2012). - ISBN 978-94-007-28561-6.
- Z. Šipoldová and Z. Machala: "Bio-decontamination of plastic and dental surfaces with atmospheric pressure air DC discharges.," *IEEE Trans. Plasma Sci.,* **39**, 2970-2971 (2011).

Publications at conferences

- Z. Machala, B. Tarabová, K. Kučerová, Z. Kovaľová, A. Žilková, M. Janda, and K. Hensel: "Cold air Plasma Activated Water for bio-decontamination, food pasteurization, and seed germination.," *Workshop on Application of Advanced Plasma Technologies in CE Agriculture*, Ljubljana (Slovenia), April 17–21 (2016).
- Z. Machala, B. Tarabová, Z. Kovaľová, K. Kučerová, M. Janda, K. Hensel: "Water activated by non-thermal air plasma discharges for bio-decontamination and bio-medical effects.," *8th International Symposium on Advanced Plasma Science and Its Applications for Nitrides and Nanomaterials (ISPlasma) + 9th International Conference on Plasma-Nano Technology and*

Science (IC-PLANTS), Nagoya (Japan), March 6–10, (2016)

- Z. Kovaľová, M. Leroy, E. Odic, and Z. Machala: "Decontamination of *Escherichia coli* biofilm by positive and negative DC corona discharge in air.," *4th Young Professionals Workshop on Plasma-Medicine*, Rostock (Germany), September 21–24, (2015)
- Z. Kovaľová, M. Leroy, E. Odic, and Z. Machala: "*Escherichia coli* biofilm decontamination by air DC corona discharges.," *Joint Conference of COST ACTIONS TD1208 Electrical discharges with liquids for future applications and MP1101 Biomedical Applications of Atmospheric Pressure Plasma Technology*, Bertinoro (Italy), September 13–16 (2015).
- Z. Kovaľová, B. Tarabová, M. Leroy, E. Odic, M.J. Kirkpatrick, and Z. Machala: "DC corona discharges in air for bio-decontamination of glass surface from *Escherichia coli.*," *22nd International Symposium on Plasma Chemistry*, Antwerp (Belgium), July 5–10 (2015).
- Z. Kovaľová, K. Tarabová, K. Hensel, Z. Machala: "Decontamination of *Bacillus cereus* Spores and *Streptococci* Biofilms on Plastic Surfaces with DC and Pulsed Corona Discharges.," *Electroporation Workshop 2015: From basics knowledge to industry, co-organized by COST TD1104 EP4Bio2Med and LEA-EBAM*, Toulouse (France), April 14–15 (2015).
- Z. Kovaľová, M. Leroy, M. Kirkpatrick, Z. Machala, and E. Odic: "Decontamination of *Escherichia coli* biofilm by DBD argon jet.," *3rd Young Professionals Workshop on Plasma-Medicine*, Zinnowitz (Germany), September 18–20 (2014).
- Z. Kovaľová, M. Leroy, M. Kirkpatrick, M.S. DuBow, Z. Machala, and E. Odic: "Decontamination of the inner walls of a narrow tube at atmospheric pressure using long distance propagation discharge in argon.," *5th International Conference on Plasma Medicine ICPM-5*, Nara (Japan), May 18–23 (2014).
- Z. Kovaľová, M. Leroy, M.J. Kirkpatrick, Z. Machala, M.S. Dubow, C.O. Laux,F.P. Sainct, F. Lopes, and E. Odic: "Décontamination de surface par plasma froid d'argon à pression atmosphérique-cas du traitement des parois internes de tubes.," *Journées GDR ABioPlas*, November 13–15 (2013).
- Z. Kovaľová, M. Leroy, M.J. Kirkpatrick, M.S. DuBow, and E. Odic: "Decontamination of *E. coli* on Inner Wall of Quartz Tube by Pulsed Corona Discharge and Streptococci Biofilm by DC Corona Discharge.," *2nd Young Professionals Workshop on Plasma-Medicine,* Koelpinsee (Germany), September 16–18 (2013).
- Z. Kovaľová, M. Leroy, M.J. Kirkpatrick, M.S. DuBow, and E. Odic: "Bio-decontamination of *E. coli* on Inner Wall of a Thin Tube Using Pulsed Corona Discharge.," *6th Central European Symposium on Plasma Chemistry CESPC,* Balaton (Hungary), August 25–29, (2013).

université PARIS-SACLAY
ÉCOLE DOCTORALE
Physique et ingénierie : électrons, photons, sciences du vivant (EOBE)

Titre : Etude de traitement par plasma froid de surfaces contaminés par biofilms

Mots clefs : décharge couronne, jet de plasma d'argon, *E. coli*, bactéries planctoniques, biofilm bactérien

Résumé : Dans cette thèse, les applications des plasmas à basse température à la pression atmosphérique sont discutées. En particulier, la bio-décontamination des bactéries planctoniques et biofilms bactériens sur des surfaces planes et complexe sont réalisées par des décharges corona de l'air et de plasma d'argon.
Dans ce travail, nous caractérisons trois sources de plasma qui sont utilisées pour la décontamination d'*Escherichia coli*. CC corona décharges dans l'air - corona streamer positive et négative des impulsions Trichel ont été utilisés pour la décontamination des bactéries planctoniques et biofilms bactériens. Dans certaines expériences de l'eau a été électro-pulvérisée sur des échantillons de haute tension électrode. Bio-décontamination des biofilms bactériens a été réalisée sur des lames en verre, pendant 15 min le traitement de plasma a été rendu majorités des bactéries incultivables. Selon la microscopie confocale à balayage laser de biofilms colorées par kit de la viabilité, une partie de ces bactéries incultivables restait viables, seulement les couches les plus supérieures du biofilm ont été tuées. La deuxième source de plasma est corona décharge pulsée propagé à l'intérieur du tube de quartz longue et étroite où l'argon sec ou l'argon avec de la vapeur d'eau coulait à la pression atmosphérique. Ce type de décharge et a une application potentielle dans la décontamination des surfaces intérieures des cathéters ou d'autres dispositifs longs et tubulaires ou pourrait fournir un plasma à basse température sur des distances longues à l'intérieur du corps humain. Tout d'abord, cette source de plasma à basse température a été caractérisée par ses paramètres électriques, et ensuite, une spectroscopie d'émission optique identifiés l'émission de plasma UV-B de radical hydroxyle excité en particulier avec l'argon humide. L'effet de cette UV-B a été testé sur des bactéries planctoniques et a été découvert pour causer jusqu'à un dommage substantiel encore plus loin en aval du tube. La source de plasma d'argon dernière doit aller qui utilise l'argon saturé sec, humide ou de l'eau en tant que gaz de travail. Cette décharge a été principalement utilisée pour la décontamination biofilm, et nous avons reçu des résultats similaires comme décharges corona CC.

Title : Bio-decontamination of biofilms on surfaces by cold plasma

Keywords : Corona discharges, argon plasma jet, *Escherichia coli*, planktonic bacteria, bacterial biofilm

Abstract : In this PhD thesis, applications of low-temperature plasmas at atmospheric pressure are discussed. In particular, bio-decontamination of planktonic bacteria and bacterial biofilms on flat and complex surfaces by air corona discharges and argon plasma.
In this work, we characterize three plasma sources which are used for decontamination of *Escherichia coli*. DC corona discharges in air - positive streamer corona and negative Trichel pulses were used for decontamination of planktonic bacteria and bacterial biofilms. In some experiments water was electrosprayed onto samples from high voltage electrode. Bio-decontamination of bacterial biofilms was carried out on glass cover slides, within 15 min plasma treatment most of the bacteria were rendered uncultivable. Part from these uncultivable bacteria remained viable only top layers of the biofilm were killed, according to confocal laser scanning microscopy of biofilms stained by live/dead viability kit. The second plasma source was pulsed corona discharge propagated inside the long narrow quartz tube in which dry argon or argon with water vapor was flowing at atmospheric pressure. This type of discharge has a potential application in decontamination of inner surfaces of catheters or other long tubular devices or could able to deliver low-temperature plasma on longer distances inside the human body. Firstly, this low-temperature plasma source was characterized by its electrical parameters, then, an optical emission spectroscopy of plasma identified UV B emission form excited hydroxyl radical especially with humid argon working gas. The effect of this UV B was tested on planktonic bacteria and was found out to cause up to a substantial damage even further downstream the tube. The last plasma source has argon jet which used dry, humid or water saturated argon as a working gas. This discharge was predominantly used for biofilm decontamination, where we received similar results as with DC corona discharges.

Université Paris-Saclay
Espace Technologique / Immeuble Discovery
Route de l'Orme aux Merisiers RD 128 / 91190 Saint-Aubin, France